

For Reference

NOT TO BE TAKEN FROM THIS ROOM

Ex LIBRIS
UNIVERSITATIS
ALBERTAENSIS





Digitized by the Internet Archive
in 2020 with funding from
University of Alberta Libraries

<https://archive.org/details/Blakney1971>

THE UNIVERSITY OF ALBERTA

ELECTRONIC SPECTRA AND BONDING OF Mn AND Re METAL
CARBONYLS

by



GEORGE BARTON BLAKNEY

A THESIS

SUBMITTED TO THE FACULTY OF GRADUATE STUDIES
IN PARTIAL FULFILMENT OF THE REQUIREMENTS FOR THE
DEGREE OF DOCTOR OF PHILOSOPHY.

DEPARTMENT OF CHEMISTRY

EDMONTON, ALBERTA

SPRING, 1971

UNIVERSITY OF ALBERTA
FACULTY OF GRADUATE STUDIES

The undersigned certify that they have read, and recommend to the Faculty of Graduate Studies for acceptance, a thesis entitled
ELECTRONIC SPECTRA AND BONDING OF MN AND RE METAL
CARBONYLS
submitted by GEORGE BARTON BLAKNEY in partial fulfilment of the requirements for the degree of Doctor of Philosophy.

ABSTRACT

The electronic spectra of some 70 metal carbonyl compounds of Mn and Re are reported in the range 5000-1900 Å. The compounds are arranged in groups for convenience of discussion. LM(CO)₅ compounds of C_{4v} or related symmetry are divided into three classes. The L groups exhibit primarily a σ effect on the metal atom (Mn or Re) in Class 1 compounds; e.g. CH₃, CF₃ or H. In Class 2 compounds, the L group has a π donating ability; e.g. Cl, Br, or I. Energy level diagrams are proposed to account for the electronic spectra of Class 1 and 2 compounds and these diagrams are co-ordinated where possible with photoelectron spectral results. In Class 3 compounds the L group generally is assumed to have a varying π acceptor capacity. The general formula for Class 3 compounds is X₃M-M'(CO)₅ where X may be Cl, Br, C₆H₅, C₆F₅ or CH₃; M may be Sn, Pb, Ge, or Si and M' either Mn or Re. Band assignments are made and qualitative molecular orbital energy diagrams are given to account for changes in the position of the charge transfer bands with changes in X, M, and M'.

Spectral trends are examined within groups of tris pentacarbonyl, X-M-(M'(CO)₅)₃, and bis pentacarbonyl, X₂-M-(M'(CO)₅)₂ compounds. For these compounds X may be Cl, I, C₆H₅, CH₃, CH₂=CH or Bu; M may be Sn or Pb and M' either Mn or Re. Spectra are discussed with respect to the σ and π properties of X and M and intramolecular M'(CO)₅ group interactions. The

reactivities of tris pentacarbonyl compounds in MeOH and MeOH-HCl solutions are discussed. Isobestic points are observed in methanol and the spectral properties of the bis products obtained are investigated.

The electronic spectra of the Mn tetracarbonyl dimers of Cl, Br, and I ($X_2Mn_2(CO)_8$) are also examined. Band assignments based on a qualitative energy level diagram are given using D_{2h} symmetry orbitals. Comparisons of the spectra for the tetracarbonyl dimers are made with those of $LMn(CO)_5$ and $L_2M(CO)_4$ compounds. The I.R. and U.V. spectra of the reaction product of the Br tetracarbonyl dimer with methanol are reported and comparisons are made with the spectra of $BrMn(CO)_5$ in methanol. In addition, the spectra of the pentacarbonyl dimers of Mn and Re, ($M_2(CO)_{10}$), are examined and assignments are proposed with the aid of existing U.V. polarization and photoelectron spectral information.

ACKNOWLEDGEMENTS

The author would like to express his deep appreciation for the direction and guidance of Professor W. F. Allen throughout the course of this work.

Also, special thanks goes to Professor W. A. G. Graham and members of his group for discussions and suggestions. I am particularly grateful to Jeff Thompson, Andy Oliver, Roger Gay, Dave Cook, Wally Jetz and Jim Hoyano, who so kindly supplied many of the compounds examined.

Financial assistance from the University of Alberta and the National Research Council of Canada is gratefully acknowledged.

TABLE OF CONTENTS

	Page
Abstract	iii
Acknowledgements	v
List of Tables	ix
List of Figures	xi
Chapter 1 Introduction	1
Chapter 2 Electronic Spectra of Class 1 and Class 2	
Pentacarbonyl Compounds of Mn and Re. . .	11
Background	11
Experimental	13
Results	15
Discussion	22
Class 1 Compounds	27
Class 2 Compounds	34
Chapter 3 Electronic Spectra of Class 3 Mn and Re	
Pentacarbonyl Compounds Containing	
Group IV Metals	43
Background	43
Experimental	45
Results and Discussion	46
Comparison of Class 1 and Class 3 Compounds	55
Comparison of Class 3 Compounds with	
Varying Sn Substituents	61

	Page
Chapter 3 - Continued	
Comparison of Mn and Re Pentacarbonyls	66
Comparison of $\text{Cl}_3\text{M}-\text{Mn}(\text{CO})_5$ Compounds with Varying M	71
Comparison of $n - \sigma^*$ Transitions in $\text{I}_3\text{Sn}-\text{Y}$ Compounds	72
Chapter 4	
Spectra and Reactivities of Bis and Tris Mn and Re Pentacarbonyl Compounds	77
Background	77
Experimental	79
Results	81
Discussion	88
Spectral Trends	88
Reactivity of Tris Pentacarbonyls	90
Chapter 5	
Spectra and Reactivities of the Tetracarbonyl Dimers of Cl, Br and I	114
Background	114
Experimental	116
Results	117
Discussion	121
Chapter 6	
Electronic Spectra of the Pentacarbonyl Dimers of Mn and Re	134
Background	134

	Page
Chapter 6 Continued	
Experimental	136
Results	137
Discussion	140
Bibliography	148
Appendix I	152
Appendix II	156

LIST OF TABLES

Table		Page
2-I	U.V. Data and Assignments for Class 1 Compounds	16
2-II	U.V. Data and Assignments for Class 2 Compounds	17
2-III	Splitting of O_h Levels Under C_{4v} Symmetry	26
3-I	Summary of U.V. Data and Assignments for Selected Class 3 Compounds.	47
3-II	Summary of U.V. Data and Assignments for Metal- Metal Bonded Mn Pentacarbonyls	48
3-III	Summary of U.V. Spectra for Phenyl Tin Mn Penta- carbonyls	49
3-IV	Spectral Summary of Metal-Metal Bonded Re Penta- carbonyl Compounds	68
3-V	Summary of $n \rightarrow \sigma^*$ Transitions in Iodo Tin Compounds	73
4-I	Summary of Electronic Spectra of Tris Pentacarbonyl Compounds	81
4-II	Spectral Summary of Tris Re Pentacarbonyls	82
4-III	Spectral Summary of Bis Mn and Re Pentacarbonyls	83
4-IV	Low Energy Band Maxima Comparison for Mono, Bis and Tris Pentacarbonyls.	88
4-V	Isobestic Point Data for Tris Mn Pentacarbonyls . .	95
4-VI	Summary of I.R. Spectra of Reaction Products in MeOH-HCl	99

Table		Page
4-VII	Mass Spectral Data for $\text{Cl}_2\text{Sn} [\text{Mn}(\text{CO})_5]_2$, $\text{BuCl}_2\text{SnMn}(\text{CO})_5$ and $\text{MeCl}_2\text{SnMn}(\text{CO})_5$	101
4-VIII	Summary of NMR Data of Tris Vinyl Mn Penta- carbonyl and the Reaction Product in MeOH	104
5-I	Summary of U.V. Spectral Data for the Tetra- carbonyl Dimers	119
5-II	Summary of I.R. Data for Tetracarbonyl Dimers . .	120
5-III	Proposed U.V.-Visible Assignments for Tetra- carbonyl Dimers	129
5-IV	I.R. Comparison of BrTCD in CCl_4 and CCl_4 -2% MeOH	132
6-I	Summary of Electronic Spectra Data for Penta- carbonyl Dimer Compounds.	139
6-II	Solvent Effects on U.V. Bands of $\text{Mn}_2(\text{CO})_{10}$ and $\text{Re}_2(\text{CO})_{10}$	141
6-III	Transformation Properties of Metal and Ligand Bonding Orbitals in $\text{M}_2(\text{CO})_{10}$ Molecules	145

LIST OF FIGURES

Figure		Page
2.01	Tetracarbonyl Dimer Formation from ClMn(CO)_5 in C_6H_{12}	18
2.02	U.V. Spectra of $\text{CH}_3\text{Mn(CO)}_5$ and $\text{CF}_3\text{Mn(CO)}_5$ in C_6H_{12}	19
2.03	U.V. Vapor Spectra of HMn(CO)_5 and HRe(CO)_5 . .	20
2.04	U.V. Spectra of Cl, Br and I-Mn(CO) $_5$ in C_6H_{12} . .	21
2.05	Co-ordinate System for L-M(CO) $_5$ Compounds . . .	23
2.06	Geometric Favoring of d - π^* over p - π^* Interaction	24
2.07	Qualitative Energy Level Diagram for Class 1 L-Mn(CO) $_5$ Compounds	28
2.08	Placement of M(π) and CO(π^*) Energy Levels for Class 1 Compounds	31
2.09	Placement of M(π), X(π) and CO(π^*) Energy Levels for Class 2 Compounds	35
2.10	Solvent Study of the Low Energy $e(\pi) \longrightarrow \pi^*\text{CO(N.I)}$ Band in IMn(CO)_5	39
3.01	Spectra of $\text{Cl}_3\text{SnMn(CO)}_5$ and $\text{Cl}_3\text{SnMn(CO)}_4\text{F(Ph)}_2\text{Ph}_f$ in CH_3CN and C_6H_{12}	50
3.02	Spectra of Chloroalkyl Tin Mn Pentacarbonyl Compounds in C_6H_{12}	51
3.03	Spectra of Group IVA Chlorophenyl Derivatives of Mn Pentacarbonyl in C_6H_{12}	52

Figure	Page
3.04 Spectra of Phenyl Pentafluorophenyl Derivatives of Mn Pentacarbonyl in C_6H_{12}	53
3.05 Qualitative Energy Level Diagram for $X_3SnMn(CO)_5$ Compounds	54
3.06 Relative Placement of the Filled π Levels in $LMn(CO)_5$ compounds	56
3.07 Relative Placement of $M(\pi)$ and $\pi^*(CO)$ Levels for $Cl_3SnMn(CO)_5$ and $CF_3Mn(CO)_5$	57
3.08 Relative Placement of $M(\pi)$ and $\pi^*(CO)$ Levels for $Cl_3SnMn(CO)_5$ and $Cl_3SnMn(CO)_4PPh_2Ph_f$	60
3.09 Relative Placement of $M(\pi)$ and $\pi^*(CO)$ Levels for $Cl_3SnMn(CO)_5$ and $Me_3SnMn(CO)_5$	63
3.10 Relative Placement of $M(\pi)$ and $\pi^*(CO)$ Levels for $(Ph_f)_3SnMn(CO)_5$ and $Ph_3SnMn(CO)_5$	65
3.11 Spectra of $X_3SnRe(CO)_5$ Compounds in C_6H_{12}	69
3.12 Spectra of Group IVA Triphenyl-Re Pentacarbonyl Compounds in C_6H_{12}	70
3.13 Spectra of Tri-iodo Tin Compounds in C_6H_{12}	74
4.01 Spectra of $ISn[Mn(CO)_5]_3$, $CH_2=CHSn[Mn(CO)_5]_3$ and $CH_2=CHSn[Re(CO)_5]_3$ in C_6H_{12}	84
4.02 Spectra of $Cl_2Sn[Re(CO)_5]_2$, $Me_2Sn[Re(CO)_5]_2$, $Ph_2Pb[Mn(CO)_5]_2$ and $PhSn[Re(CO)_5]_3$ in C_6H_{12}	85
4.03 Spectra of $BuSn[Re(CO)_5]_3$, $ClSn[Re(CO)_5]_3$, $ClSn[Mn(CO)_5]_3$ and $BuSn[Mn(CO)_5]_3$ in C_6H_{12}	86

Figure	Page
4.04 Spectra of $\text{MeSn}[\text{Re}(\text{CO})_5]_3$, $\text{MeSn}[\text{Mn}(\text{CO})_5]_3$, $\text{Cl}_2\text{Sn}[\text{Mn}(\text{CO})_5]_2$ and $\text{Me}_2\text{Sn}[\text{Mn}(\text{CO})_5]_2$ in C_6H_{12}	87
4.05 Isobestic Point Spectra for $\text{CH}_2=\text{CHSn}[\text{Mn}(\text{CO})_5]_3$ in MeOH	93
4.06 Isobestic Point Spectra for $\text{BuSn}[\text{Mn}(\text{CO})_5]_3$ in MeOH	94
4.07 Spectra of $\text{BuSn}[\text{Mn}(\text{CO})_5]_3$ in MeOH and in MeOH-1% HCl	97
4.08 Isobestic Point Spectra for $\text{BuSn}[\text{Mn}(\text{CO})_5]_3$ in MeOH-1% HCl	98
4.09 I.R. Spectra of $\text{CH}_2=\text{CHSn}[\text{Mn}(\text{CO})_5]_3$ -MeOH Reaction Product	100
4.10 Isobestic Point Spectra for $\text{ClSn}[\text{Mn}(\text{CO})_5]_3$ in MeOH	106
4.11 Isobestic Point Spectra for $\text{ISn}[\text{Mn}(\text{CO})_5]_3$ in MeOH	107
4.12 I.R. Spectra in CCl_4 of the Product from the Reaction of $\text{ClSn}[\text{Mn}(\text{CO})_5]_3$ and MeOH	109
4.13 Spectra of $\text{CH}_2=\text{CHSn}[\text{Re}(\text{CO})_5]_3$ in MeOH	112
4.14 Spectra of $\text{CH}_2=\text{CHSn}[\text{Re}(\text{CO})_5]_3$ in MeOH-1% HCl	113
5.01 Spectra of the Tetracarbonyl Dimers of Cl, Br and I in C_6H_{12}	118
5.02 Structure and axes Representations for $\text{Br}_2\text{Mn}_2(\text{CO})_8$	122

Figure	Page
5.03	Representations of Carbonyl Vibrations for $ML_2(CO)_4$ Compounds 123
5.04	Axes Representations for Comparison of Bonding of $LMn(CO)_5$ and $L_2Mn(CO)_8$ 124
5.05	Placement of Filled π Levels in $XMn(CO)_5$ and $X_2Mn(CO)_4$ Based on π Interaction 125
5.06	Placement of Filled π Levels in $XMn(CO)_5$ and $X_2Mn(CO)_4$ Based on σ and π Interactions 126
5.07	Qualitative Energy Level Diagram for the Tetra- carbonyl Dimers of Cl, Br and I 128
5.08	U.V. Spectra of Products of $BrMn(CO)_5$ -MeOH and $Br_2Mn_2(CO)_8$ -MeOH Reactions. 131
5.09	I.R. Spectra of $Br_2Mn_2(CO)_8$ in CCl_4 and CCl_4 - 2% MeOH 133
6.01	Spectra of $Mn_2(CO)_{10}$, $Re_2(CO)_{10}$ and $Mn_2(CO)_9PPh_2Ph_f$ in C_6H_{12} 138
6.02	Qualitative Energy Level Diagram for the Penta- carbonyl Dimer of Mn 143

Chapter 1 - Introduction

In recent years the study of transition metal complexes in which carbon monoxide groups serve as ligands has been an active area for research. After the discovery of the first binary carbonyl compound, Ni(CO)_4 ,¹ in 1890, other carbonyls such as $\text{Co}_2(\text{CO})_8$, Mo(CO)_6 , Cr(CO)_6 , Ru(CO)_5 and $\text{Re}_2(\text{CO})_{10}$ were recognized and examined in the years from 1910 to 1941. The field was relatively dormant for some years until the discovery of ferrocene in 1951² and 1952³ and dibenzene chromium in 1955⁴ stimulated metal carbonyl research activity. The onset of more sophisticated techniques in spectroscopy and general physical methods combined with the realization that metal carbonyls and their derivatives readily lend themselves to analysis by these physical methods further stimulated interest in this field. The fact that a large number of metal carbonyls and metal-metal bonded carbonyls could be readily synthesized provided the impetus for research into the bonding and structure of a variety of these compounds. Abel and Stone have provided an extensive review on the development and synthesis of a large variety of metal carbonyls and metal-metal bonded carbonyls with the greatest emphasis on structural considerations.⁵

Metal-metal bonds were generally considered rare, but all members of the transition metal series now appear to be able to form such bonds. Detailed crystallographic analysis often gives evidence for the presence of such bonds by indicating a short

distance between the metal atoms. This is however a criterion that should be used cautiously. For purposes of discussion metal-metal bonds may be regarded as two center bonds between like or unlike metal atoms or as multicenter bonds about the transition metal atom such as occur in cluster compounds ($\text{Co}_4(\text{CO})_{12}$).

The carbonyl compounds which will form the basis for the following discussion of bonding, electronic structure and spectra are compounds with two center bonds with respect to the transition metal. Metal-metal carbonyl compounds occur both with bridging CO groups, e.g. $\text{Fe}_2(\text{CO})_9$, and without, e.g. $\text{Mn}_2(\text{CO})_{10}$. $\text{Me}_3\text{SnMn}(\text{CO})_5$, $\text{CH}_3\text{Mn}(\text{CO})_5$ and $\text{MeSn}(\text{Mn}(\text{CO})_5)_3$ are some compounds which represent various classes of metal-metal and organometallic compounds which will be discussed.

Carbon monoxide in its role as a π acceptor is known to fulfill in different compounds three structural functions; $\text{M}-\text{C}\equiv\text{O}$ terminal bonding, $\begin{array}{c} \text{O} \\ \parallel \\ \text{M}-\text{C}-\text{M} \end{array}$ bridging between two metal atoms and $\begin{array}{c} \text{O} \\ | \\ \text{M}-\text{C} \\ | \\ \text{M} \end{array}$ bridging of three metal atoms. The compounds to be discussed here generally involve only terminal CO bonding. The common mononuclear carbonyl compounds serve as a natural starting point for the discussion of substituted metal carbonyl compounds. The structures of these carbonyls; $\text{Cr}(\text{CO})_6$ - octahedral symmetry, O_h , $\text{Ni}(\text{CO})_4$ - tetrahedral, T_d , and $\text{Fe}(\text{CO})_5$ - trigonal bipyramidal, D_{3h} , are expected to form the basis for the structures of the respective substituted compounds. The structures of the compounds which will be encountered include the

distorted octahedral (C_{4v}) for $L-Mn(CO)_5$ compounds, D_{4d} for the binuclear pentacarbonyl dimers of Mn and Re, and D_{2h} for the halide tetracarbonyl dimers of Mn. Tetracarbonyl dimers ($Mn_2(CO)_8Cl_2$ and $Mn_2(CO)_8Br_2$) have no metal-metal bond but are joined by halogen bridges. C_{3v} and C_{2v} are the approximate symmetries for the tris, $XSn(Mn(CO)_5)_3$, and bis, $X_2Sn(Mn(CO)_5)_2$, carbonyl compounds that are to be discussed.

The bonding and structure of metal carbonyl compounds are generally dependent on the utilization of all nine valence orbitals on the metal (nd^5 , $(n+1)s$, $(n+1)p^3$) and the ability of the CO group to stabilize metal atoms in a zero or low positive or negative oxidation state. While a resonance approach can describe the metal to carbon bonding, a molecular orbital approach is generally considered superior due to the greater detail and the increased accuracy. The ability of the CO group to stabilize the metal d orbitals is considered to be due to a 'backbonding' or 'synergic' bonding effect. The carbon monoxide ligand first forms a σ bond with the metal atom. This dative σ bond is formed by overlap of a filled sp hybrid σ orbital on the carbon with an empty hybrid orbital on the metal: e.g. sp^3 in $Ni(CO)_4$ and d^2sp^3 in $Cr(CO)_6$. The build-up of negative charge on the metal atom as a result of the dative σ bonds formed with the CO ligands requires a means of dispersing this charge. A dative π bond is then formed by the donation of π electrons from the filled d or dp hybrid orbitals on the metal to the empty C-O antibonding π^* orbitals. The bonding

effect is called synergic since the greater the donation of σ electrons to the metal orbitals from the CO's, the greater will be the back π donation from the filled metal orbitals to the CO π^* orbitals. It is this backbonding effect which accounts for the stability of a great many metal carbonyl compounds. The stabilization of the metal d orbitals by interaction with the CO π^* levels results in the generally high energy electronic transitions from metal to ligand which are observed and described in the compounds examined here.

The physical and spectroscopic methods which have been used to gain structural information on metal carbonyls and their derivatives include mass spectrometry, electron diffraction, mossbauer spectroscopy, N.M.R., I.R. and Raman spectroscopy, dipole moment and magnetic susceptibility studies, and X-ray diffraction measurements. It is this last method which has provided the greatest amount of structural information, although it has the limitation that the structure of the metal carbonyl in the crystal may not be preserved in solution. X-ray diffraction measurements have established or confirmed the structures of the mononuclear carbonyls Ni(CO)_4 ,⁶ Fe(CO)_5 ,⁷ Cr(CO)_6 ,⁸ and V(CO)_6 .⁹ In addition X-ray diffraction studies have provided structural information for some metal carbonyl derivatives to be studied here such as $\text{Ph}_3\text{SnMn(CO)}_5$,¹⁰ and $\text{Me}_3\text{SnMn(CO)}_5$.¹¹

The structural studies of many carbonyl compounds have also been based on I.R. data because of the relative ease of observing and interpreting the CO stretching frequencies of these metal

carbonyls and their derivatives. The first step in such a structure analysis is to assign symmetries to several possible structures. A group theoretical and mathematical procedure determines the number of CO stretching bands which should appear in the spectrum for each of these structures. Experimental observations are then compared with predictions and if the predictions disagree with observation, these particular structures are eliminated. In the simple uncomplicated cases there will often be only one possible structure which remains. From the symmetry of the molecule and the positions of the CO stretching bands, values for the CO force constant may be calculated.¹² The ability of :CO to form dative σ bonds with the metal results in a build up of negative charge on the metal atom which is redistributed into the empty π^* orbitals of the C-O bond. As charge is placed in the empty π^* antibonding orbitals, the strength of the C-O bond is diminished and the force constant decreases. Values for the force constants and the CO stretching frequencies in metal carbonyl compounds give an estimate of the amount of $M(d_{\pi})-\pi^*(CO)$ interaction which takes place. In the I.R. spectrum of free carbon monoxide the CO stretching frequency is 2155 cm^{-1} . In the isoelectronic series $Mn(CO)_6^+$, $Cr(CO)_6$, and $V(CO)_6^-$, the increasing negative charge on the metal atom should result in greater $M(d_{\pi})-\pi^*(CO)$ interaction and lower CO stretching frequencies. Observed CO stretches for this series show $Mn(CO)_6^-$ 2096 cm^{-1} , $Cr(CO)_6$ 2000 cm^{-1} and $V(CO)_6$ 1859 cm^{-1} in agreement with predictions.

Cotton and Kraihanzel¹² and Orgel¹³ have pioneered work in this field of I.R. analysis of substituted metal carbonyl compounds of general formula $ML_n(CO)_{6-n}$ where $0 \leq n \leq 4$. These compounds have essentially octahedral distribution of the ligand and CO groups about the metal atom. Cotton and Kraihanzel¹² have proposed a simple model for analyzing and assigning the I.R. active CO stretching frequencies of some simple and substituted metal carbonyl compounds described above. Their model involves some qualitative and semi-quantitative assumptions based on general bonding theory. One such assumption which affects the size and magnitude of the CO stretching force constants is that the axial CO in an $LM(CO)_5$ compound will have a greater interaction with L than the equatorial CO's have. The basis for this assumption, which can also play an important role in electronic structure analysis, is as follows. If the z axis is placed along the L-M-CO bonds then the d_{xz} , d_{yz} orbitals point towards L and the axial CO. This results in L interacting with the axial CO through two different d orbitals. Each of the CO's in the xy plane however may interact with L through one d orbital, either the d_{xz} or the d_{yz} . The d_{xy} orbital in the plane perpendicular to the z axis has little or no interaction with L in the sense that the d_{xz} , d_{yz} orbitals have. Since L is usually a poorer π acceptor than CO it is expected that there will be increased interaction of the d_{π} orbitals with each of the remaining CO's. The axial CO, by virtue of its doubled interaction with L through the metal d_{π} orbitals is then expected to have a greater

$M(d_{\pi})-\pi^*(CO)$ interaction than any of the individual equatorial CO's and a weaker CO (axial) bond or smaller axial force constant value (k_1) should result. Cotton and Kraihanzel initially applied this model to Group VI metal carbonyls but other researchers have applied and modified the approach to a large number of Group VII substituted metal carbonyl compounds. Graham et al^{14, 15} have calculated force constant values for a large number of Group VII $LM(CO)_5$ compounds of essentially C_{4v} symmetry to study the trends in k values as ligand L is changed. These values and the separation in these values serve as a guide to the σ and π abilities of L ,¹⁵ which can be qualitatively useful in the construction of an electronic energy level diagram for these compounds.

A portion of this thesis deals with metal carbonyls of general formula $L-M(CO)_5$. It has been found useful to describe these $L-M(CO)_5$ compounds according to the π donating or π accepting properties of the L group. Compounds in which L has little or no π capability are designated as Class 1: $HMn(CO)_5$, $HRe(CO)_5$, $CH_3Mn(CO)_5$ and $CF_3Mn(CO)_5$. In Class 2 compounds L is a π donating group as in the Mn pentacarbonyl halides where the filled p orbitals on the halide may interact with filled d orbitals on the metal atom. Class 3 compounds are ones in which L exhibits a π accepting ability in addition to a σ inductive effect. $Cl_3SnMn(CO)_5$, $Me_3SnMn(CO)_5$ and $(C_6H_5)_3SnMn(CO)_5$ are representative of this class.

In recent years a large number of Class 1, 2 and 3 metal carbonyl compounds have been prepared and examined. For most of these, structural interpretations and assignments based on the I.R. spectra have been published.^{12, 13, 16, 17} Only a limited amount, however, of U.V. and visible spectral data has appeared and a small number of assignments and interpretations have been made.^{18, 19} Photoelectron Spectra (PES) have appeared for a number of these compounds²⁰ and recent M.O. calculations have been published for HMn(CO)_5 and the pentacarbonyl halides.²¹ The most extensive evaluation of electronic spectra and sophisticated structuring of an energy level diagram has been carried out for the Group VI hexacarbonyls of Cr, Mo and W.²²⁻²⁵ For these compounds low energy, low intensity bands are observed which are assigned as d-d transitions. Higher energy and very high intensity bands are assigned as M-L charge transfer transitions. The purpose of the present work is to give reliable U.V. and visible spectra for the L-M(CO)_5 compounds dealt with and to make reasonable assignments for the observed electronic bands. These assignments are correlated with those for the hexacarbonyls and with I.R. data for the Class 1, 2 and 3 compounds. A simple but useful bonding picture is developed based upon qualitative molecular orbital energy level diagrams.

A number of bis and tris compounds of Mn and Re have been prepared and examined.²⁶ Tris and bis carbonyls have respectively the general formulae $\text{X-M-(M'(CO)}_5)_3$ and $\text{X}_2\text{-M-(M'(CO)}_5)_2$

in which X may be Cl, I, C_6H_5 , $CH_2=CH$, or Bu, M may be Sn or Pb and M' either Mn or Re. The I.R. and mass spectra of a number of these compounds have been investigated but structure analysis by I.R. has proved difficult.²⁶ The number of bands in the I.R. spectra does not coincide with the number of bands predicted from the group theoretical treatment in which it is assumed that individual $M'(CO)_5$ groups within a molecule do not interact with each other. This assumption appears to be invalid both in the I.R. and U.V.. X-ray diffraction studies on the bis compound, $Ph_2Sn(Mn(CO)_5)_2$,²⁷ and the tris compound, $ClSn(Mn(CO)_5)_3$,²⁸ have shown essentially octahedral bonding about the Mn and tetrahedral bonding about the Sn. These studies have also indicated that the length of the Sn-Mn bond increases from the mono to the bis to the tris compounds. The electronic spectra of the bis and tris Mn and Re compounds will be discussed here in terms of the σ and π abilities of X and the interactions between the $M'(CO)_5$ groups within a molecule. The reactivities of the tris compounds are examined in polar solvents and the spectra of the products are compared with those of the reactants.

An extensive structural analysis of the Cl and Br tetracarbonyl dimers ($Cl_2Mn_2(CO)_8$ and $Br_2Mn_2(CO)_8$) has been carried out by El-Sayed and Kaesz²⁹. These I.R. studies as well as X-ray diffraction studies on the bromine tetracarbonyl dimer³⁰ show the symmetry of the molecule to be D_{2h} and suggest little interaction of the $M(CO)_4$ groups joined by the halogen bridges. I.R. data has

been used to calculate the force constants for the CO's which are axial and equatorial to the halogen bridging ligands.¹² These results suggest greater $\text{Mn}(d_{\pi}) - \pi^*(\text{CO})$ interaction and smaller CO stretching force constants for the CO's axial to the halogen bridges. The electronic structure of the compounds will be discussed here as will be the results observed in the I.R. and U.V. from the reactions of these compounds in MeOH and in solutions of CCl_4 with small quantities of MeOH added.

The I.R. bands of the pentacarbonyl dimers of Mn and Re have been examined and assigned and force constants for the axial and equatorial CO bonds have been calculated.³¹ Polarization studies in the I.R. using a nematic liquid crystal have confirmed these assignments.³² The low energy band at $29,400 \text{ cm}^{-1}$ in the U.V. for the $\text{Mn}_2(\text{CO})_{10}$ compound has also been investigated using these same polarization techniques.³² This band has been assigned as a $\text{Mn}(\sigma) - \text{Mn}(\sigma^*)$ transition on the basis of its z axis polarization. Higher energy bands in the Mn compound and all bands in the Re compound do not lend themselves to polarization studies by the nematic liquid crystal method. X-ray diffraction studies on the two dimers have been carried out and show that the Re-Re bond length is longer than the Mn-Mn bond length as expected.^{33, 34}

The complete electronic spectra of the Mn and Re pentacarbonyl dimers will be examined and discussed here. Qualitative energy level diagrams are proposed which account for the observed U.V. spectra as well as a number of general bonding characteristics observed using other spectroscopic methods.

Chapter 2 - Electronic Spectra of Class 1 and Class 2 Pentacarbonyl Compounds of Mn and Re

BACKGROUND

This chapter deals primarily with Class 1 and Class 2 compounds. U.V. spectra with band interpretations have been reported previously for Cl-Mn(CO)₅, Br-Mn(CO)₅ and I-Mn(CO)₅.¹⁸ The frequencies reported for the high energy bands do not agree with the results presented here. Since the spectra themselves were not published it is impossible to make precise comparisons, but the ready formation of the bromine and chlorine tetracarbonyl dimers may account for some of the earlier reported values. CF₃-Mn(CO)₅ and CH₃-Mn(CO)₅ are included in the spectra reported by Lundquist and Cais,¹⁹ who assigned in a general way all bands for these compounds, including the end absorption for which no $\bar{\nu}_{\text{max.}}$ is reported, to the M-CO moiety. Comprehensive spectra in the U.V. and visible range for some L-M(CO)₅ compounds are presented in this chapter. The spectra have generally been recorded for both solvent and vapor phases. Reasonable assignments of the bands are made: these are correlated with PES²⁰ and I.R.¹⁵ results and comparisons are made with the M.O. calculations where possible. Qualitative M.O. energy level diagrams based on a simple bonding picture are presented.

The correlation of the U.V. spectra with available PES affords an approximate placement of the antibonding levels which

is not generally available from ionization work, PES or quantum mechanical calculations. The examination of the spectra and assignments for some of these more common pentacarbonyl compounds will also serve as the basis for a study of Class 3 $L-M(CO)_5$ compounds involving metal-metal bonding.

Some low temperature studies have been reported.²⁴ These give additional information but restrictions in choice of solvent and in frequency range limit their usefulness for the compounds examined here.

EXPERIMENTAL PROCEDURE

The Class 1 and 2 compounds examined, with the exception of IMn(CO)_5 , were obtained in pure form from W.A.G. Graham and coworkers. Purity checks on the crystal compounds were carried out using I.R. and Mass Spectrometry. The compounds had been prepared as recommended by King.³⁵ Visible and U.V. spectra were obtained using a Cary 14 Spectrometer covering the range from 1900-5000 Å. High energy absorption bands were rechecked on a Jasco U.V. 5 ORD, CD instrument with an N_2 flushed system. Spectral grade solvents were used in all cases.

H-Mn(CO)_5 was purified by trap to trap transfer and was collected in vacuo in a 1 mm. cell. The spectrum was obtained at much less than the saturated vapor pressure of the compound. A satisfactory but unknown pressure for the compound was obtained by pumping off H-Mn(CO)_5 until this desired pressure was reached as shown by a reasonable absorbance value in the U.V. When the cell was allowed to stand for a period of 3 hrs there were no observable changes in the spectrum. This was taken as an indication of the absence of decomposition.

H-Re(CO)_5 was obtained in a similar manner to its Mn analog. However the vapor pressure at room conditions was low enough to yield a good spectrum covering the U.V. region. The spectrum of this compound was also obtained in C_6H_{12} by introducing the solvent into the evacuated cell in successive amounts until a suitable concentration was reached.

Spectra of CF_3 - and CH_3 - $\text{Mn}(\text{CO})_5$ were obtained in MeOH and C_6H_{12} . Vapor spectra were obtained in air at room temperature in 5 mm. cells above pure crystals of the compounds.

Spectra of $\text{Cl-Mn}(\text{CO})_5$ and $\text{Br-Mn}(\text{CO})_5$ were observed in CCl_4 , C_6H_{12} and MeOH. Molar absorptivity values in MeOH were calculated for the high energy bands, and in CCl_4 for the low energy bands. MeOH was used in preference to C_6H_{12} because of a smaller tendency of the monomers to form the tetracarbonyl dimers in MeOH. The solubility of these compounds in CCl_4 made possible the determinations of low energy, low ϵ bands but the formation of the tetracarbonyl dimers in some cases precluded accurate λ measurements. Gentle heating of solution of the Cl and Br pentacarbonyl compounds resulted in the rapid formation of tetracarbonyl dimers. This, combined with the fact that solubilities of these compounds are very low, made the determination of the ϵ values difficult in non-polar solvents.

$\text{IMn}(\text{CO})_5$ was prepared from $\text{Na}^+\text{Mn}(\text{CO})_5^-$ and I_2 in tetrahydrofuran solution. After the solvent was removed, the $\text{IMn}(\text{CO})_5$ was purified by sublimation at room temperature and 1 mm. pressure. The U.V. spectra of $\text{IMn}(\text{CO})_5$ were obtained in a variety of solvents, since solubility posed no problem.

RESULTS

Table 2-I and Table 2-II give the results of the U.V. and visible spectra of Class 1 and Class 2 compounds with the appropriate assignments. Figures 2.01 - 2.04 show the U.V. and visible spectra of these compounds.

TABLE 2-I

Class 1 Compounds

Summary of U.V. Data and Assignments

Compound	Type of Transition									
	1. $M \rightarrow L(C.T.)$ $e_{\pi} \rightarrow \pi^*(CO)N.I.$ Note A			2. $M \rightarrow L(C.T.)$ $e_{\pi} \rightarrow e_{\pi}^*(CO)$			3. $M \rightarrow L(C.T.)$ $e_{\pi} \rightarrow b2\pi^*(CO)$ [and $b2\pi \rightarrow e\pi^*(CO)$ for $MeMn(CO)_5$]			
	$\lambda_{max}(\text{\AA})$	$\bar{\nu}_{max}$	Note B ϵ	λ_{max}	$\bar{\nu}_{max}$	Note B ϵ	λ_{max}	$\bar{\nu}_{max}$	Note B ϵ	
$CF_3Mn(CO)_5$										
C_6H_{12} vapor	~ 2700 (sh)	$\sim 37,000$	$\sim 3,000$	2155	46,380	30,000	< 1900 (sh)	$> 52,600$	$> 12,000$	
	~ 2700 (sh)	$\sim 37,000$	(.09)	2120	47,170	(.9)	< 1900	$> 52,600$		
$CH_3Mn(CO)_5$										
C_6H_{12} vapor	~ 2800 (sh)	$\sim 35,500$	$\sim 3,000$	2220	45,050	28,000	1960	51,020	36,000	
	~ 2750 (sh)	$\sim 36,500$	(.07)	2190	45,660	(.6)	~ 1925	52,000	(.7)	
$HMn(CO)_5$ vapor	~ 2850 (sh)	34,500	(.1)	2140	46,730	(.75)	~ 1950 (sh)	51,300	(1.0)	
$HRe(CO)_5$ vapor	2700 (sh)	37,000	(.25)	2115	47,280	(1.46)	1975	50,630	(1.72)	
C_6H_{12}	2725 (sh)	36,700	(1.30)	2150	46,510	-				

A See Text

B Molar absorptivity, (in the absence of known concentrations relative intensity values are given in brackets).

TABLE 2-II

Summary of U.V. Data and Assignments for Class 2 Compounds

	C ₆ H ₁₂ Solution		MeOH Solution				Assignment [†]
	λ_{\max} (\AA)	$\bar{\nu}_{\max}$	ϵ or (Rel. Int.)	λ_{\max} (\AA)	$\bar{\nu}_{\max}$	ϵ	
ClMn(CO) ₅	3750	26,670	(.01)	3770	26,520	600 (570) ^a	A
	not observable			~2700 (sh)	37,000	~1,500	B (D hidden)
	2270	44,050	(.5)	2220	45,050	13,000	C, G (weak)
	1980	50,500	(.6)	<1900	>52,600		E (F & H out of range)
BrMn(CO) ₅	3855	25,940	(.02)	3835	26,070	420 (390) ^a	A
	~2700 (sh)	~37,000	(.07)	2700	37,000	1,700	B (D hidden)
	2325	43,010	(.45)	2275	43,950	15,000	C, G
	~2000 (sh)	~50,000	(.2)	1980	50,500	7,000	E
	1880	53,000	(.75)	beyond spect. range			H & F
IMn(CO) ₅	4250	23,530	380	4000	25,000	360 (330) ^a	A
	3050	32,800	2,310	2980	33,600	3,000	B
	not observable			2750 (sh)	36,400	1,500	D
	2380	42,000	15,300	2340	42,700	20,000	C, E
	1970	50,800	79,000	1900	52,630	88,000	F, H

^a bracketted value for CCl₄ solution[†] Letters refer to transition assigned as shown in Figure 2.09

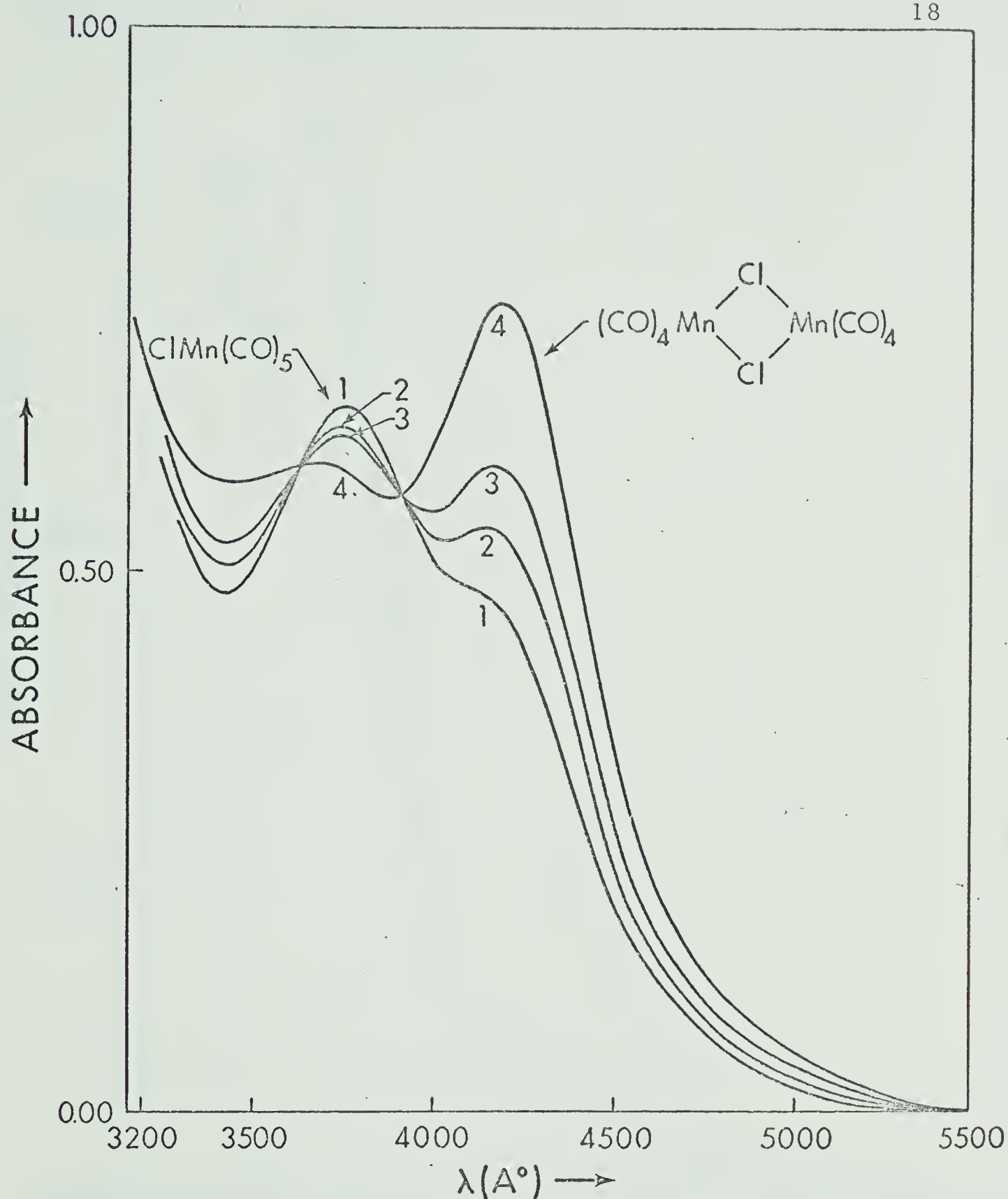


Figure 2.01 - Tetracarbonyl dimer formation from Cl-Mn(CO)_5 in cyclohexane solution at room temperature. Cell path length - 10 cm. Curve 1 obtained 10 min. after solution made up; curve 2 after 30 min.; curve 3 after 50 min.; curve 4 after 70 min.

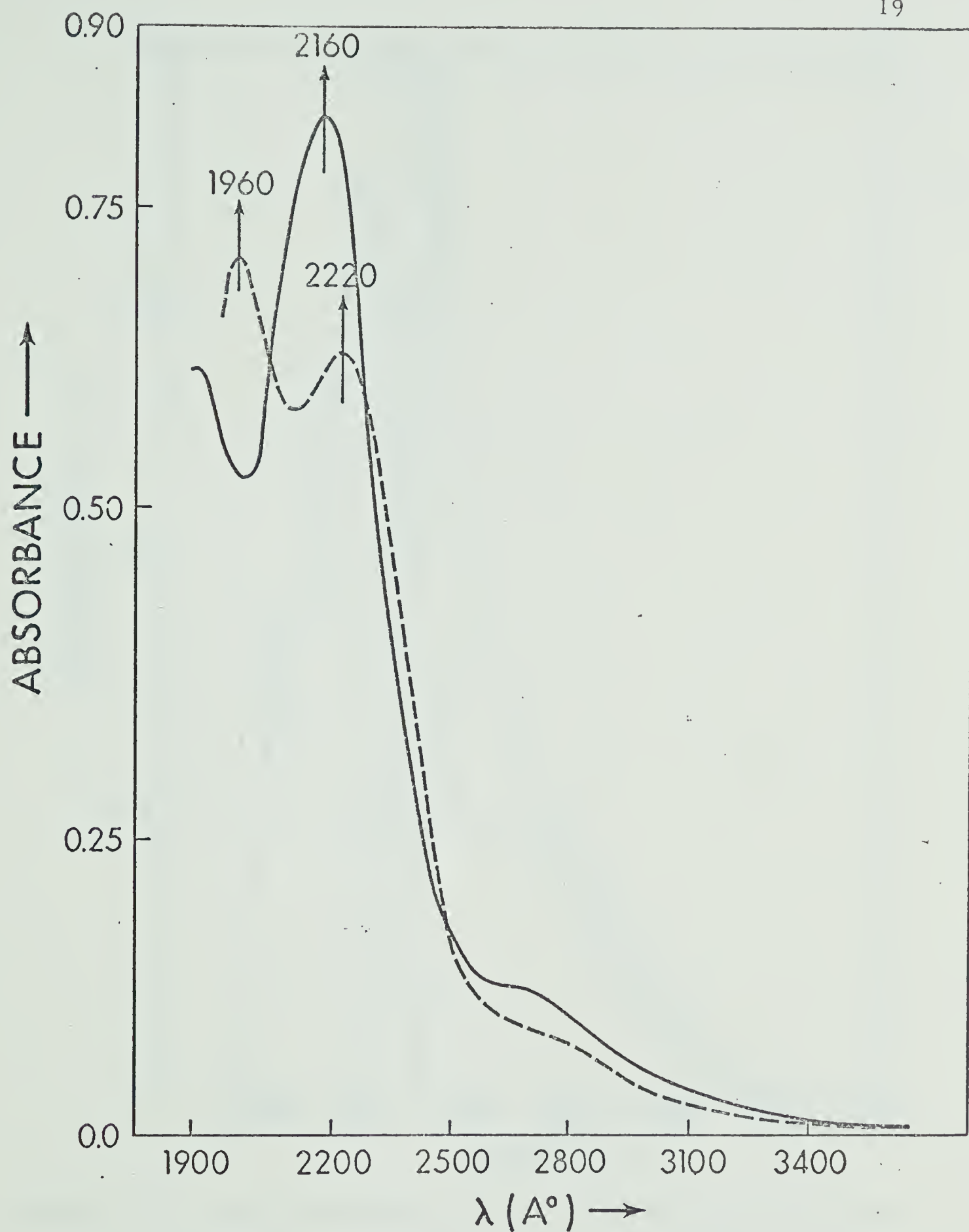


Figure 2.02 - - - - - $\text{CH}_3\text{-Mn(CO)}_5$ conc. = 1.7×10^{-4} M; ——— $\text{CF}_3\text{-Mn(CO)}_5$ conc. = 2.4×10^{-4} M. Solvent and reference - cyclohexane. Path length 1 mm.

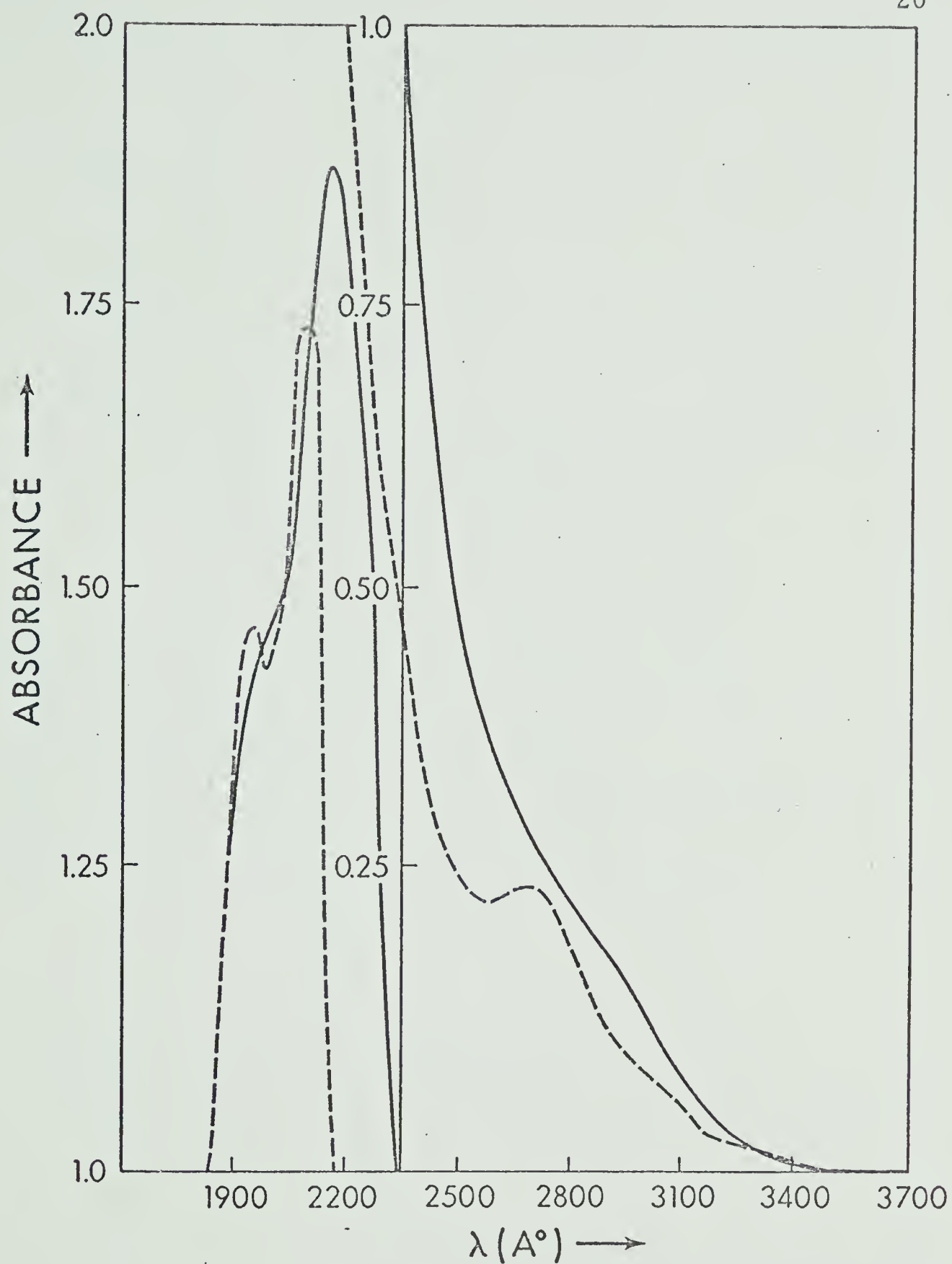


Figure 2.03 - — HMn(CO)_5 and ---- HRe(CO)_5 in vapor phase in 1 mm. cells with air as reference. Absorbance values for higher λ region of spectrum extend from 0.0 to 1.0 and in lower λ region from 1.0 to 2.0.

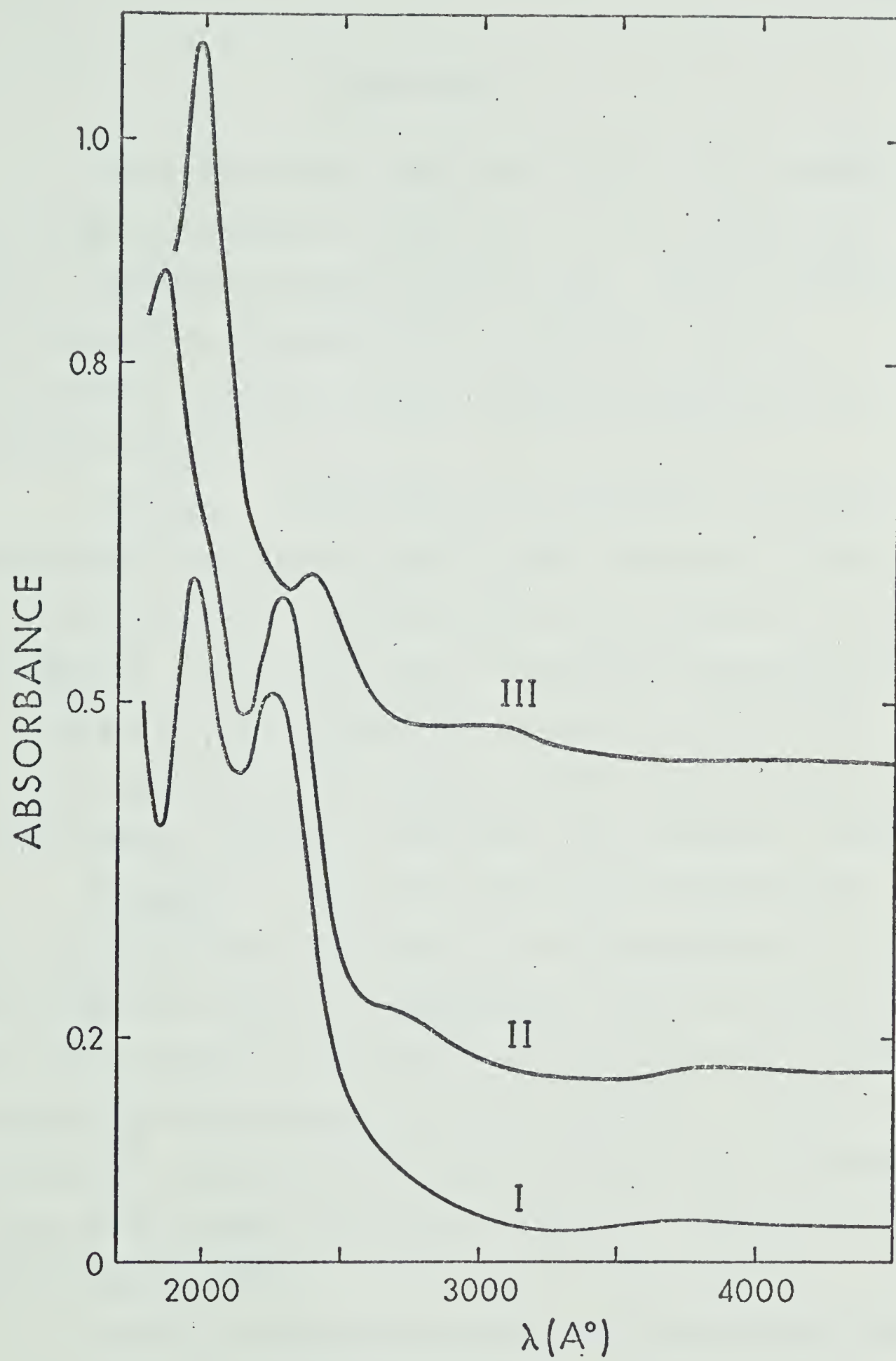
Figure 2.04 - Curve I - ClMn(CO)_5 , 3.5×10^{-4} M

Curve II - BrMn(CO)_5 , 2.0×10^{-4} M

Curve III - IMn(CO)_5 , 0.8×10^{-4} M

Path length - 1 mm

Solvent and reference - cyclohexane. The baseline has been successively displaced in going from curves I to III. Concentration for the Cl and Br penta-carbonyl halides have been estimated from more precise ϵ values determined in methanol.



DISCUSSION

A generalized model used to describe the σ and π bonding in $L\text{-Mn(CO)}_5$ compounds is given below. The co-ordinate axes for C_{4v} compounds are shown in Figure 2.05. Strictly speaking, the CF_3 and CH_3 compounds are of C_s symmetry, but it is convenient to treat them as C_{4v} , assuming little participation of the F or H atoms.¹²

σ Bonding CO bonding is accomplished by interaction of the lone pair on the carbon atom with some combination of metal s, p, and d orbitals. For Mn this involves the use of 4s, 4p, $3d_{z^2}$ and $3d_{x^2-y^2}$. It is assumed that σ bonding takes preference over π bonding in the use of orbitals where symmetry considerations would allow a choice. In σ bonding with the L atom or group s, p_z , d_{z^2} Mn orbitals are used in combination with appropriate L orbitals.

π Bonding This involves the interaction of the filled d_{xy} , d_{xz} , d_{yz} orbitals on the metal atom with the empty π^* 's on the CO groups to give d- π^* backbonding. Symmetry would allow the metal p orbitals to participate but σ bond priority over π bonding suggests that this involvement should be neglected. It is also reasonable to expect that the more favorable geometric availability of the metal d orbitals will favor d- π^* over p- π^* interaction as shown in Figure 2.06.

As the principal quantum number of the central metal atom or L increases, the introduction of extra nodal surfaces may inhibit efficient overlap as governed by size, shape and energy of

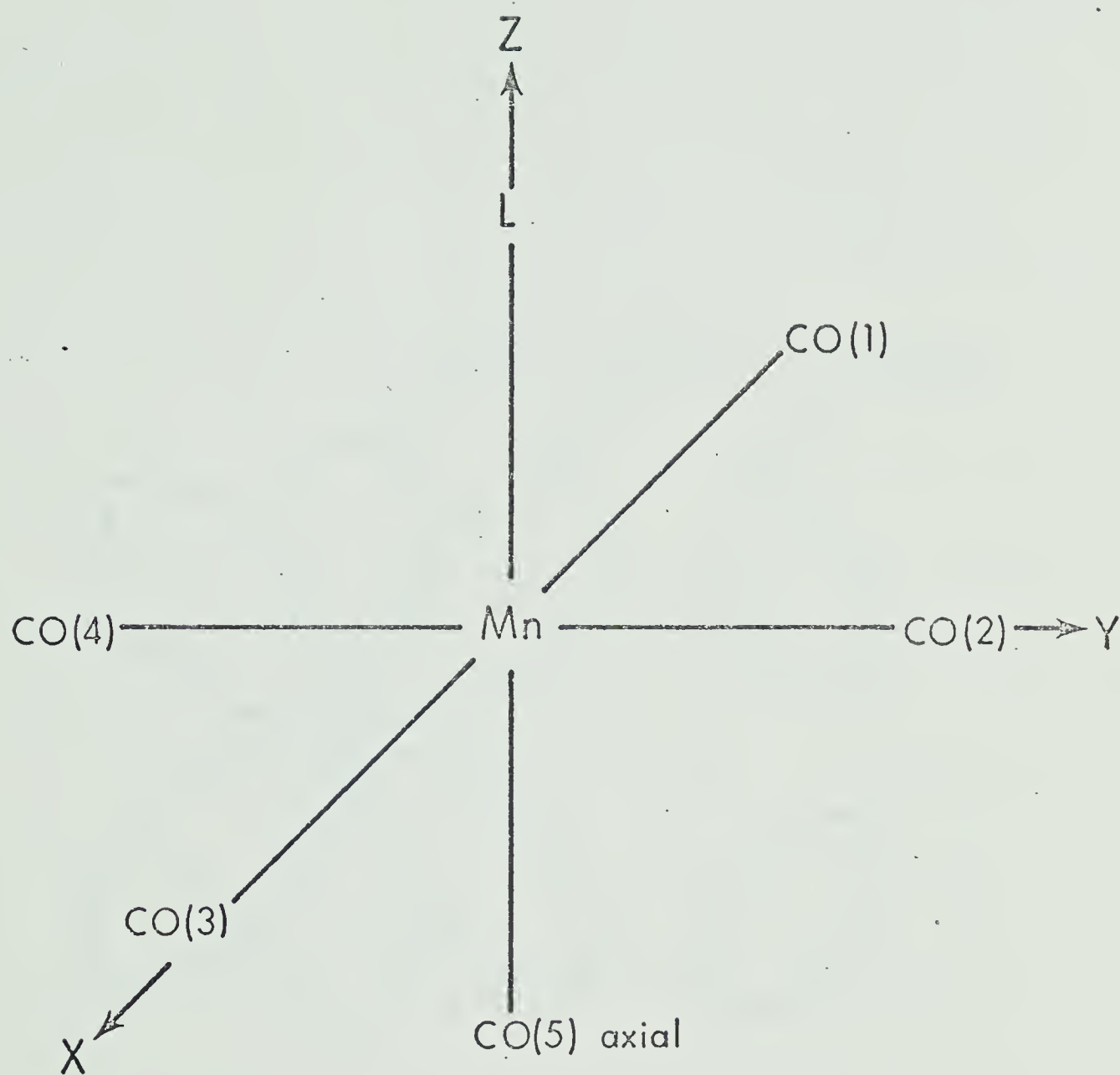


Figure 2.05 - Co-ordinate system for $L-M(CO)_5$ compounds.

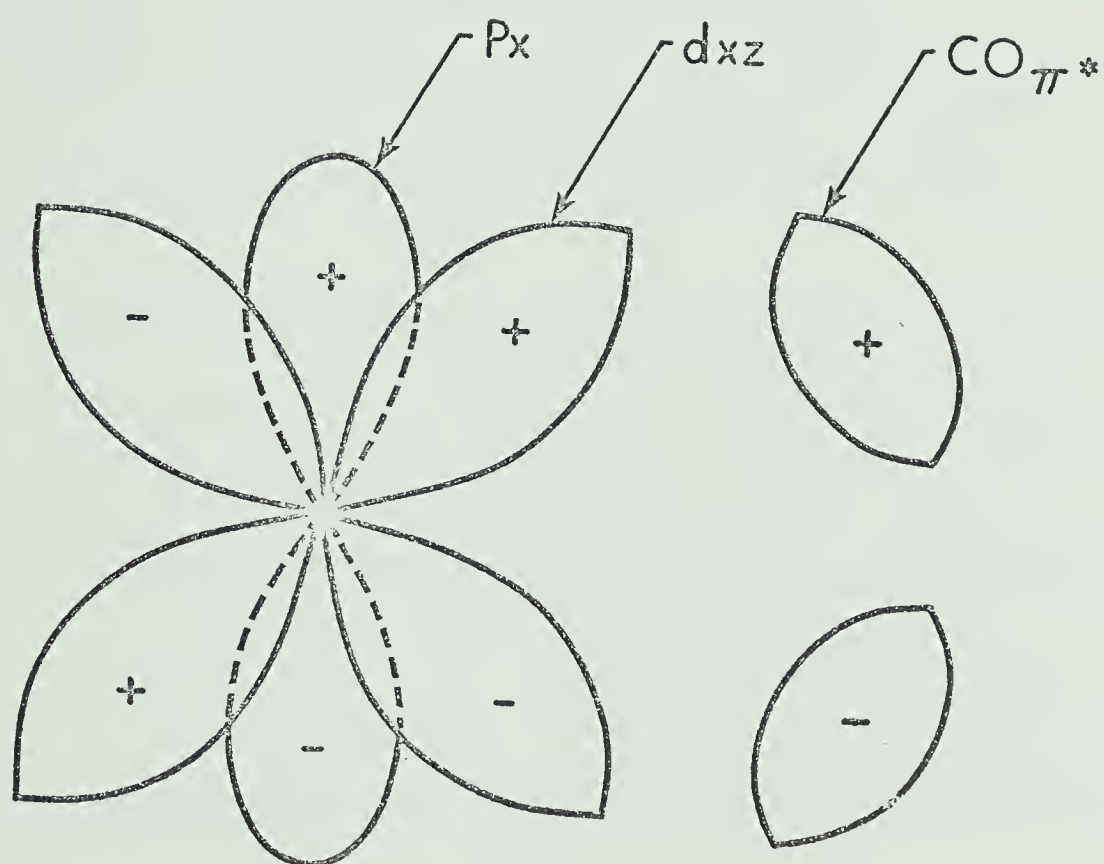


Figure 2.06 - Geometric favoring of d - π^* over p - π^* interaction.

the orbitals involved.

π interactions between filled metal d orbitals of suitable symmetry and p or d orbitals of the L atom or group may take place e.g. π repulsion between Cl 3p and Mn $3d_{xz,yz}$; π acceptance between empty Sn d orbitals in Cl_3Sn and Mn $3d_{xz}, d_{yz}$. In the absence of orbitals of suitable symmetry, size and energy no π interactions are possible as when L is H or CH_3 .

Models based on this bonding picture have accounted reasonably for changes in the CO stretching force constants as L is varied.^{12, 15}

Electronic structures and M.O. diagrams for Group VI B Metal Hexacarbonyls (O_h symmetry) have been reported with varying degrees of sophistication and some controversy.^{23, 24, 36-38}

The corresponding diagrams for $\text{LM}(\text{CO})_5$ compounds are based on C_{4v} symmetry with the axis representation given in Figure 2.05 and the O_h energy levels split as shown in Table 2-III. Changes in the levels for the C_{4v} compounds are dictated by the following:

- i) The metal core has now a charge of +1 compared to 0 in the hexacarbonyl species. This results in a lowering of all the energy levels.
- ii) One :CO group has been replaced by :L⁻. This will raise energy levels, especially those associated with the +z axis, by amounts which depend upon the size and electronegativity of the L group or atom.

TABLE 2-III

Splitting of O_h Levels Under C_{4v} Symmetry

Metal Orbitals	O_h	C_{4v}
4p	t_{1u}	$e(p_x, p_y)$ $a_1(p_z)$
4s	a_{1g}	a_1
3d	e_g	$a_1(d_z^2)$ $b_1(d_x^2 - y^2)$
	t_{2g}	$e(d_{xz}, d_{yz})$ $b_2(d_{xy})$
Ligand Orbitals		
$\pi^*(CO)$	$t_{2g}, t_{2u}, t_{1u}, t_{1g}$	$e, b_2; e, b_1; e, a_1; a_2^\dagger$
$\pi_b(CO)$	$t_{2g}, t_{2u}, t_{1u}, t_{1g}$	$e, b_2; e, b_1; e, a_1; a_2^\dagger$
$\sigma(L)$	a_{1g}, e_g, t_{1u}	$a_1; a_1, b_1; e, a_1$

[†] In the absence of the sixth CO group one of the e levels must be eliminated.

- iii) The ligand will differ from CO in its π characteristics: it may be a better or a poorer π acceptor, or it may have π donating ability.

The net effect of (i) and (ii) will be a general lowering of all levels, since (i) will predominate. Other specific interactions as cited by (ii) and (iii) may raise or lower particular levels.

Class 1 Compounds

An energy level diagram is proposed for Class 1 compounds as shown in Figure 2.07. A number of the levels are essential to the bonding in the molecule but are not expected to play a significant part in the observation of the electronic spectra. For this reason little more will be said of the strongly σ bonding orbitals, (grouped at one level for convenience), the filled π orbitals on the CO's and the strongly antibonding σ^* orbitals.

Orbitals of the $:L^-$ group (not all shown in Figure 2.07) may have either σ or π symmetry with respect to the L-Mn bond axis. In the ionic approach taken here the corresponding energy levels will be high for the $:L^-$ anion, but will drop sharply as charge is transferred to the $Mn(CO)_5^+$ group through σ bonding. For the Class 1 and Class 2 compounds considered here the resultant energy levels will be low lying σ or high energy σ^* levels and will not participate directly in U.V. transitions at less than $50,000\text{ cm}^{-1}$.

The levels that are primarily involved in the transitions observed are discussed, beginning first with the filled d_π orbitals, then the empty d_{σ^*} levels, and finally the π^* CO levels. We place

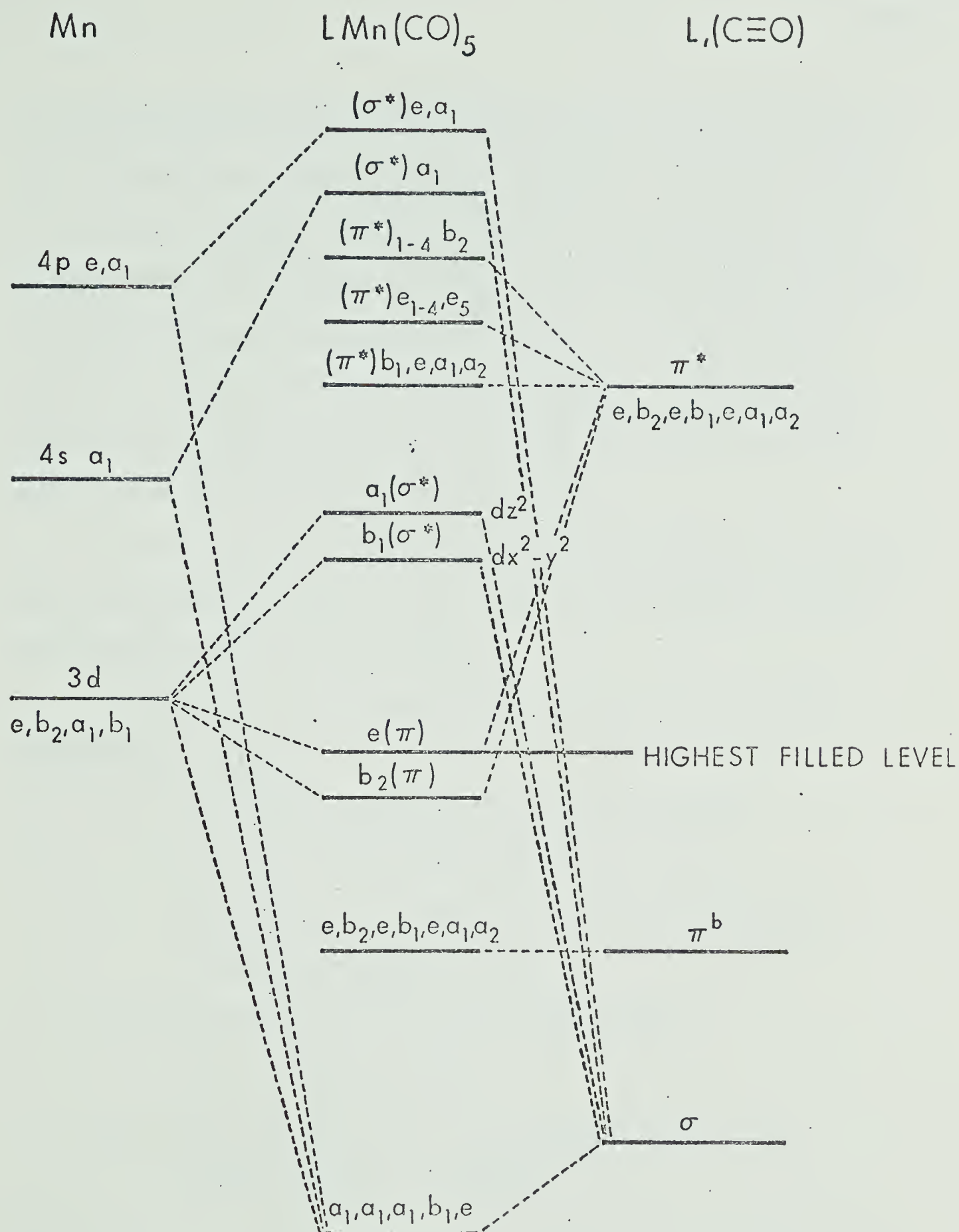


Figure 2.07 - Qualitative energy level diagram for Class 1

$L\text{-Mn(CO)}_5$ compounds. The basis of the approach to this and other energy level diagrams is taken primarily from reference 36.

the $e(d_{xz}, d_{yz})$ level above the $b_2 (d_{xy})$ level because of the lack of any π accepting properties of Class 1 ligands. This lack results in a decrease in total π backbonding with the $e(d_{xz}, d_{yz})$ orbitals, although there may well be a greater π backbonding per CO for the remaining carbonyl groups, since there are now only five such groups as compared to six in the hexacarbonyl. This distinction between total π interaction and π interaction per CO is a major difference in I.R. and U.V. interpretations.

The placement of the Mn d_{σ^*} levels (a_1 and b_1) is dependent on the nucleophilic properties of L; they are generally expected to be just below the π^* (CO) levels.

Among the π^* levels of the CO groups, there are three distinguishable types;

- i) Those whose symmetry or geometry forbids interaction with the Mn orbitals [i.e. π^* $CO_{1-4}(a_1, a_2, b_1, \text{ and } e)$] and which are labelled π^* non-interacting or π^* N.I.
- ii) Those which interact with $b_2(d_{xy})$ of Mn [i.e. $\pi^* CO_{1-4}(b_2)$]
- iii) Those which interact with $e(d_{xz}, d_{yz})$ of Mn [i.e. $\pi^* CO_{1-4}(e)$ and $\pi^* CO_5(e)]^\dagger$

[†] The $\pi^* CO_{1-4}$ orbitals combine to yield two e combinations, one of which is oriented parallel to the z axis, and one perpendicular to the z axis. Thus there are orientation limitations upon the interactions of these e levels with the four levels of the $Mn(d_{xz}, d_{yz})$; one of the $\pi^* CO(e)$ levels is non-interacting.

The final energy level diagram thus has as its highest filled levels the e and b_2 ($Mn\ 3d_{xz}, 3d_{yz}, 3d_{xy}$), and as its lowest empty levels the a_1 and b_1 ($Mn\ 3d_z^2, 3d_{x^2-y^2}$) and the various π^* (CO) levels. The lowest energy transitions possible are $d-d$, followed by the Mn to CO charge transfer transitions.

Recent PES results²⁰ allow an absolute placement of the filled metal d orbitals and, combined with the U.V. spectral results, can yield qualitative placement of the π^* (CO) levels. Because of its greater interaction, the π^* (CO) b_2 level is placed above that of the π^* (CO) e levels. The π^* (CO) N.I. levels will appear as the lowest of the antibonding π levels. The placement of the levels in this way indicates six possible C.T. transitions from the $M(\pi)$ to the CO (π^*) levels. The placement of the energy levels corresponding to the bonding σ and π electrons of the CO ligands indicates that transitions from these levels to the empty levels in Class 1 compounds should not appear within the range of our observations. Transitions from filled $M(\pi)$ orbitals to metal σ^* orbitals ($d-d$ transitions) are expected to be very weak and will often be masked by the $M \rightarrow L$ C.T. transitions. Figure 2.08 shows the placement of the $M(\pi)$ and $CO(\pi^*)$ levels on an energy scale which places the filled metal orbitals (e and b_2) at values calculated from PES.²⁰ The π^* CO levels are placed at appropriate energies based on the observed U.V. transitions and the expected ordering of these levels.

The largest splitting in the antibonding levels is shown to be between the N.I. π^* (CO) levels and the π^* (CO) e levels. It is

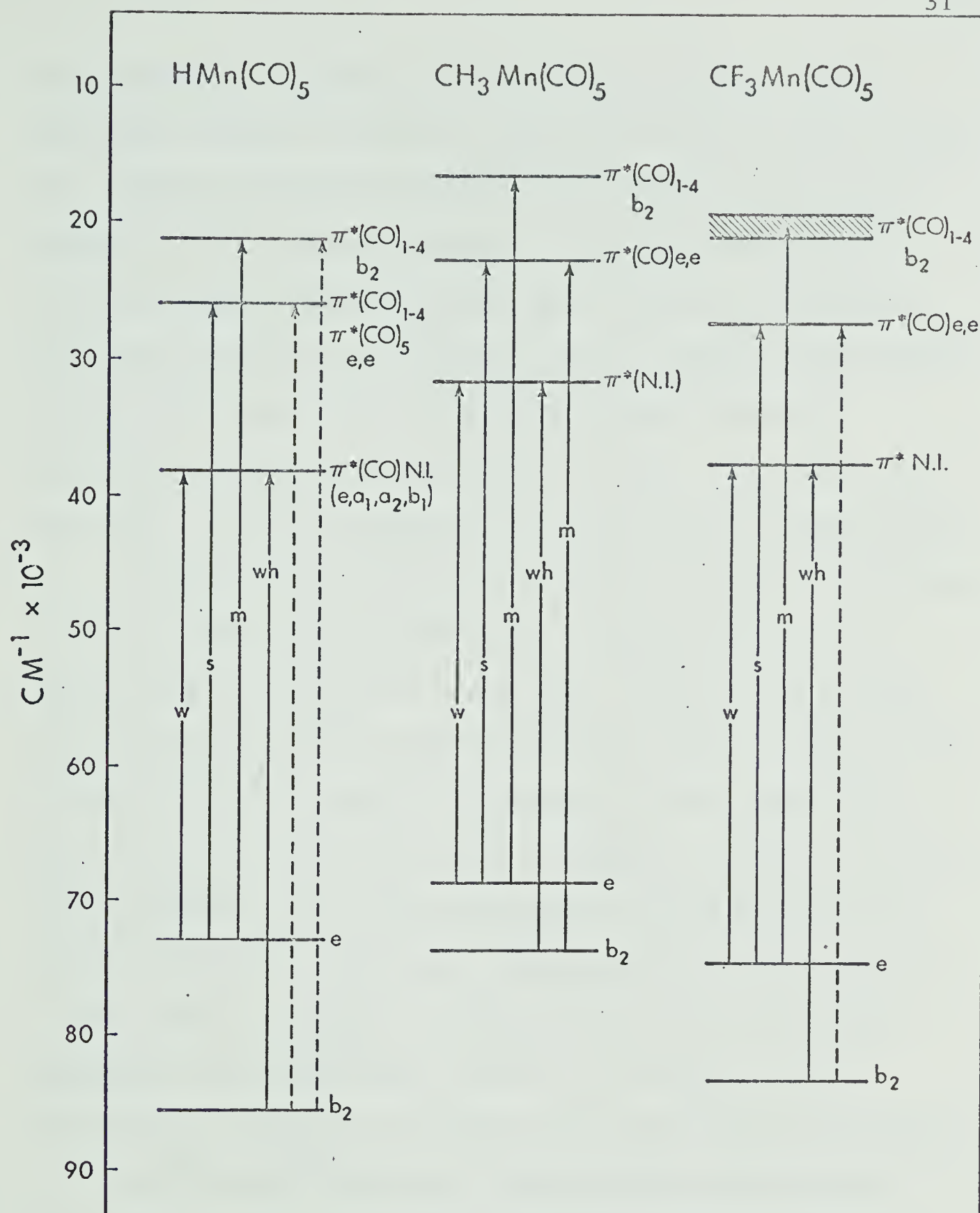


Figure 2.08 - Placement of the $\text{M}(\pi)$ and $\text{CO}(\pi^*)$ on an absolute energy axis for Class 1 compounds. Legend w = weak, s = strong, m = medium, wh = weak, hidden, and transitions denoted by dotted lines are beyond the range of the instrument.

expected that the splitting between π^* levels that interact with the metal π orbitals and levels which do not interact will be larger than splittings between two levels whose interaction differ only slightly ($\pi^*(\text{CO}) e$ and $\pi^*(\text{CO}) b_2$). Quantum mechanical calculations suggest that for $\text{Cr}(\text{CO})_6$ there is little involvement of the metal p orbitals in π bonding³⁷ and any splitting brought about by the interaction of the metal p orbitals with π^* levels of appropriate symmetry is expected to be small. For this reason the $\pi^*(\text{N.I.})$ levels are grouped at one level in the energy diagram.

Consistent with assignments in the hexacarbonyl compounds, transitions occurring from the metal π orbitals to the group of lowest lying $\pi^*(\text{CO})$ levels, in this case $\pi^*(\text{N.I.})$, are expected to be much weaker than transitions from the metal π orbitals to the $\pi^*(\text{CO})$, (e and b_2) levels. The summary of the assignments for the observed transitions for Class 1 compounds is given in Table 2-I. The assignment of the bands is internally consistent in terms of expected intensities and λ max. values of similar bands appearing in compounds of varying L. Where comparisons can be made, splittings in the filled metal π levels as calculated from the observed U.V. bands are consistent with those obtained from PES.

PES results²⁰ indicate a reversal of the e and b_2 levels associated with the Mn d orbitals in $\text{MeMn}(\text{CO})_5$ as compared to the other Class 1 compounds examined. This is contrary to expectations: there is no corresponding change in intensities of U.V. bands based on these two levels in the assignments

(see Table 2-I).

The λ max of the intense C.T. band in Class 1 compounds varies with the σ property of L as shown by the transition: CF_3^- 47,200 cm^{-1} , H-46,700 cm^{-1} , CH_3 45,700 cm^{-1} . It appears that the stronger the σ accepting ability of L the lower the d orbitals (e and b_2) will be placed and the higher will be the energy of the transition.

The reversal of the e and b_2 bands would affect the assignments of the U.V. bands only in that bands assigned as originating from the e and b_2 levels would be reversed in origin.

The comparison of CF_3^- and $\text{CH}_3\text{-Mn(CO)}_5$ (Figure 2.02) shows marked similarities. The highest energy band in the CH_3 compound appears red shifted and more intense than in the CF_3 compound. Figure 2.08 shows that the $\text{M}(b_2)\pi - \pi^*(\text{CO})$ e transition, which is out of the spectrometer range for the CF_3 compound, should appear at approximately the same energy as the assigned $\text{M}(e)\pi - \pi^*(\text{CO})$ b_2 transition in the CH_3 compound and enhance the intensity of this highest energy band.

The ability of CF_3 to accept π charge from Mn by means of d - σ^* backbonding has been suggested by Cotton and McCleverty³⁹. This should result in a lowering of the $\text{M}(\pi)$ e level for the CF_3^- as compared to the CH_3^- compound. The U.V. results are inconclusive since the recognized differences in σ inductive effects can easily explain the observed blue shift.

A comparison of the U.V. spectra of the pentacarbonyl hydrides of Mn and Re (Figure 2.03) shows blue shifts of the U.V. bands in going from H-Mn(CO)_5 to H-Re(CO)_5 . This suggests that the filled d levels of Re lie at a lower level than those of Mn, and also indicates that there is less d - π^* interaction for Re than for Mn. Reported carbonyl stretching force constants for these hydrides⁴⁰ are in agreement with this interpretation.

Although PES are not currently available for the HRe(CO)_5 compound, U.V. spectra and assignments similar to those for HMn(CO)_5 are shown in Table 2-I.

The spectrum of the Re pentacarbonyl hydride (Figure 2.03) indicates that there are two weak bands on the low energy side of the band assigned as $\text{M}(\pi) \rightarrow \pi^*(\text{CO})$ N.I. Although the origin of these bands is not certain, it is assumed that they are either d-d transitions from the filled metal π orbitals to the σ^* metal orbitals or triplet components of higher intensity bands.

Class 2 Compounds

Class 2 compounds are represented by ClMn(CO)_5 , BrMn(CO)_5 and IMn(CO)_5 whose U.V. spectra and corresponding assignments are illustrated in Figure 2.04 and Table 2-II. A level diagram is presented in Figure 2.09. The bands are lettered in this diagram for quick reference. The placement of the filled metal and halide π levels in Figure 2.09 is based on PES and their interpretation.²⁰

The energies of the $\pi(\text{X})$ levels have a direct bearing on

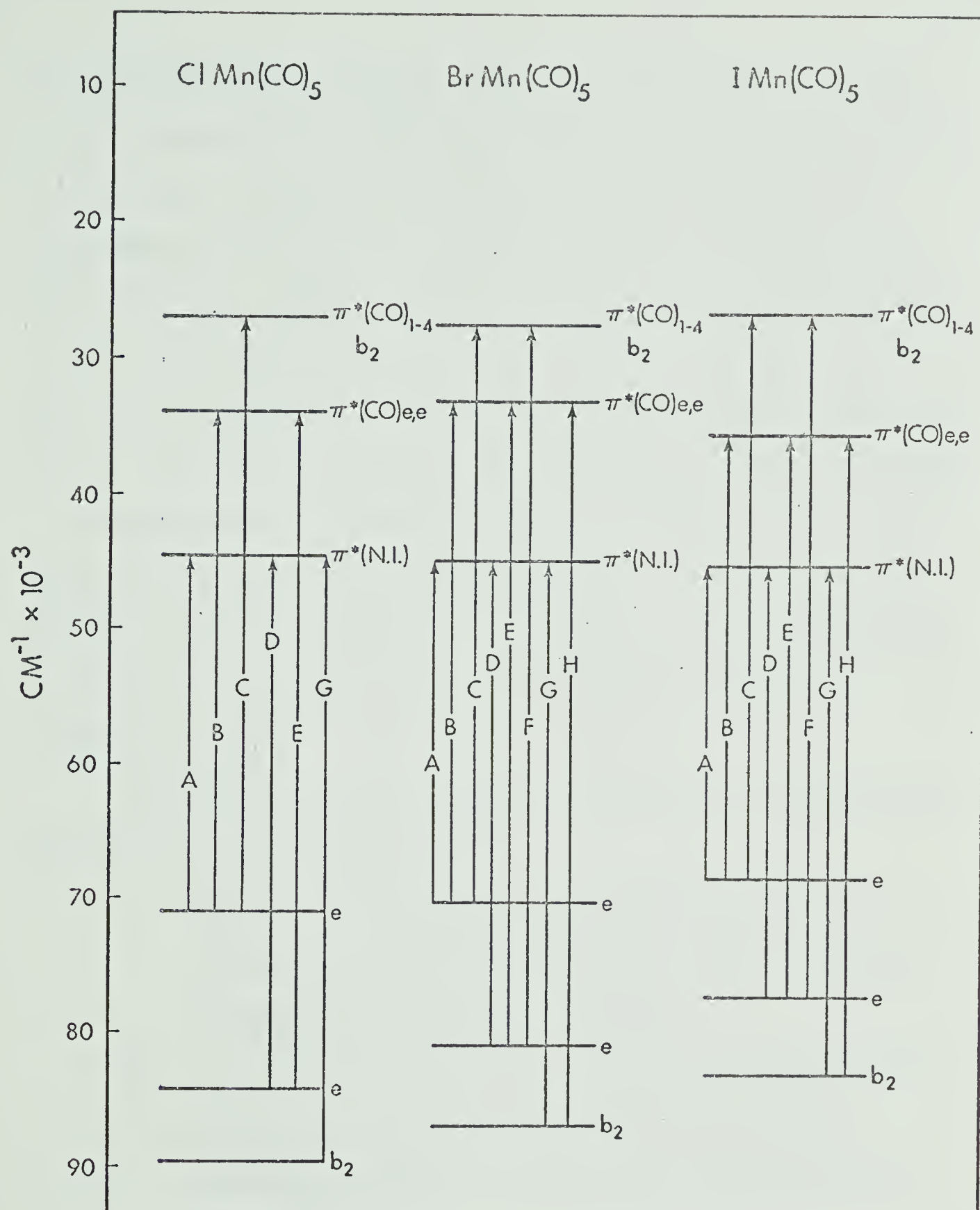


Figure 2.09 - Placement of the $M(\pi)$, $X(\pi)$ and $\pi^*\text{CO}$ levels on an absolute energy axis for Class 2 compounds.

the amount of halide character expected in the uppermost filled e level. Quantitative measures of halide character are uncertain, but the iodine compound is expected to have the largest such character because its filled orbitals are closest in energy to the Mn(π)d levels. The CO π^* (N.I.) levels are grouped at one level as for Class 1 compounds. The $b_2 \pi^*$ (CO) level is placed above that of the e π^* (CO) since the b_2 level has the greatest interaction with the filled metal orbitals. The e π^* (CO)₁₋₄ and the e π^* (CO)₅ are grouped at one level since, as later results show, bands with separations of 2500 cm^{-1} are not resolvable. It is assumed that the splitting in these levels is less than this. The π^* antibonding levels are placed in accordance with arguments developed for Class 1 compounds.

The assignments as outlined in Table 2-II are based on the following general considerations:

- i) transitions to the lower antibonding π^* (CO) levels (π^* N.I.) are generally much weaker than transitions to higher π^* (CO) interacting levels.
- ii) transitions to π^* (CO) N.I. levels from predominantly metal bonding orbitals show little solvent effect; transitions to higher π^* states show marked solvent shifts.^{24, 36}
- iii) transitions which originate from filled levels involving a large amount of halide character may be expected to exhibit a solvent effect, regardless of the π^* antibonding

level to which the transition takes place.

- iv) the antibonding states are expected to exist over a range of energies. This accounts in part for the broadness of the observed bands and the fact that weak bands may be hidden by bands of greater intensity which occur at or near the same energy.
- v) triplet states are neglected although it is possible that they may play some role in the case of iodine compounds.

Band A is expected to be a weak band since it is a transition to the π^* (CO) N.I. level from the uppermost filled e level. Solvent shifts are an indication of the amount of halide character in this level. The negligible solvent shift for the Cl compound, the small blue shift for the Br compound and the large blue shift for the I one indicate that the largest degree of halide character occurs in the upper e level of IMn(CO)_5 . PES indicates approximately 50% halide character in this e level for IMn(CO)_5 ,²⁰ although quantum mechanical calculations indicate that there is over 90% halide character in the uppermost filled e level,²¹ for even the penta-carbonyl bromide and chloride. The observed solvent shifts and changing intensities for the band originating from this e level as reported in Table 2-II suggest large decreases in the halide character from I to Br and Cl.

The width of band A for the I compound is double that for the Cl and Br compounds. This is in keeping with the spin-orbit coupling predicted by PES for IMn(CO)_5 . In addition the behaviour

of this band in polar solvents (Figure 2.10) shows distinctly that two bands are present, although not completely resolvable. In non-polar solvents the band width is large and the band is slightly asymmetric. The appearance of the spectra in polar solvents indicates not only an increased splitting of these two bands but an apparent intensity enhancement of the higher energy component. This increased splitting is in keeping with expected increased spin-orbit coupling in polar solvents.

In the Cl compound no band appears in the region of $37,000\text{ cm}^{-1}$ in cyclohexane solution, but in MeOH solution a weak shoulder appears in this region. In BrMn(CO)_5 the shoulder appears in both polar and non-polar solvents but with little observable solvent shift. For the I compound band B occurs in both solvents with a large solvent shift similar to that for band A (600 cm^{-1}). These observations and the assignment of this band as a transition from the upper filled e to the $e\pi^*(\text{CO})$ are consistent with the previous discussion of band A.

For all three pentacarbonyl halides a strong band appears in the region of $43,000\text{ cm}^{-1}$ which shows in all cases a blue shift from non-polar to polar solvents. The band is assigned as a combination of two transitions arising from the filled π levels.

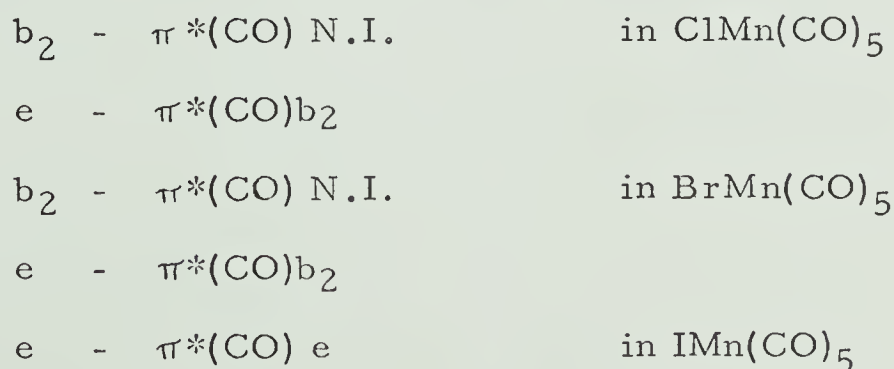


Figure 2.10 - Behaviour of the $\epsilon(\pi) \longrightarrow \pi^*\text{CO (N.I)}$ band in polar and non-polar

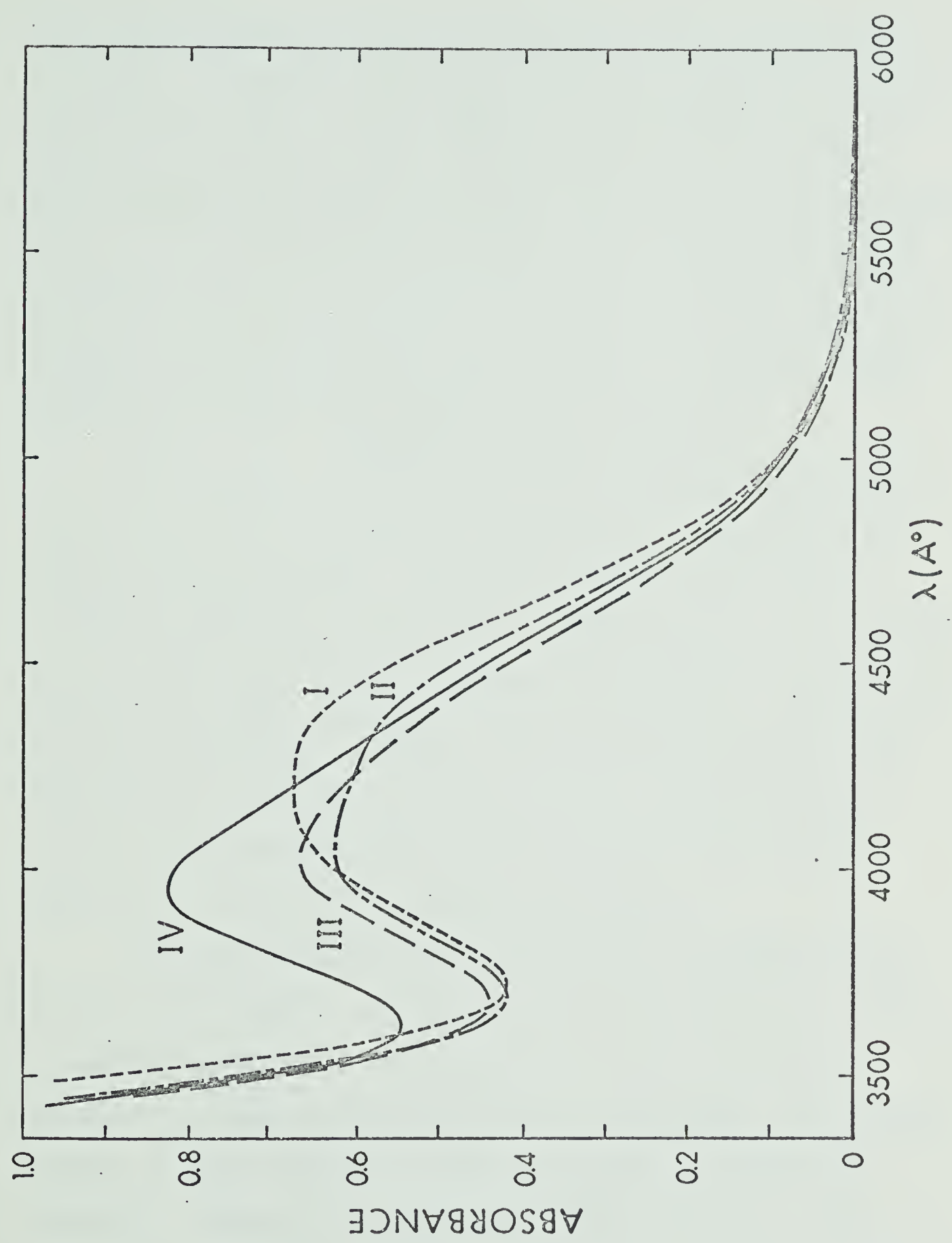
solvents for IMn(CO)_5 .

Curve I - 0.134 g/l = in CCl_4

Curve II - 0.132 g/l = in CHCl_3

Curve III - 0.120 g/l = in CH_2Cl_2

Curve IV - 0.160 g/l = in MeOH



The energy separation of these components is too small to allow resolution. In addition, one of these bands is expected to be weak since the transition is to the $\pi^*(\text{N.I.})$ levels. The intensity of this band increases slightly from the Cl to Br to the iodine compound. The increase in band intensity for the iodine compound over these for the Br and Cl compounds may well be a result of the coincidence in $\text{IMn}(\text{CO})_5$ of the main band with the $e_{\text{lower}} - \pi^*(\text{CO}) e$, a band expected to be more intense than the $b_2 - \pi^*(\text{CO}) \text{N.I.}$

The $e_{\text{lower}} - \pi^*(\text{CO}) \text{N.I.}$ band in the iodine compound is expected to be weak and also to occur at lower energies than for the Br and Cl compounds. No band is evident at the expected energy in cyclohexane solution but in MeOH solution a weak shoulder, which could be this transition, appears at $37,000 \text{ cm}^{-1}$ between the $42,000$ and $32,800 \text{ cm}^{-1}$ bands. The increasing metal character of the lower e level for the iodine compound could account for a smaller solvent shift than for the higher energy bands and the appearance of this weaker shoulder in $\text{IMn}(\text{CO})_5$.

The end absorption region of the spectrum shifts to lower energy for the I and Br compounds from that of the Cl one. This is expected on the basis of the higher lying filled π levels and relatively unchanged antibonding levels for $\text{IMn}(\text{CO})_5$. This would indicate a larger number of possible transitions of fairly high intensity. Although it is suspected that the transitions in this region are mainly $\text{M} - \pi^*(\text{CO})$ and $\text{X} - \pi^*(\text{CO})$ or a mixture of these where $\text{M}(\pi) - \text{X}(\pi)$ interaction is strong, there is a possibility of

$L(\sigma)$ to $M(\sigma^*)$ transitions contributing to the intensities. PES results do however suggest that the CO σ and π levels lie at such low energies that transitions from these levels to empty $\pi^*(CO)$ levels occur at energies much larger than $50,000\text{ cm}^{-1}$.

The placement of the energy levels for the various penta-carbonyl halides and the assignments of the bands are generally consistent internally for the series of compounds examined and indicate splittings in the ground state levels consistent with those reported for PES. However it must be borne in mind that the ground state levels were calculated from compounds in the vapor state for PES whereas the U.V. spectral results are taken from solutions in non-polar solvents.

The I.R. spectra of the halide compounds and calculated C-O force constant values (k_1 and k_2) show a small but significant trend for which no entirely satisfactory explanation has been proposed. The values of the force constants listed below are taken from reference 15.

	k_1 (axial)	k_2 (equatorial)
ClMn(CO)_5	16.22	17.50
BrMn(CO)_5	16.26	17.41
IMn(CO)_5	16.30	17.28

Since the axial k 's are more affected by π interaction than the equatorial ones, these values indicate that there is less π interaction for the iodine compound than for Cl and Br, giving a higher axial force constant¹⁵. The trend in equatorial k 's, as

expected from inductive effects, shows increasing π interaction from Cl to Br to I. The opposite trend in the axial force constants may well be the result of the increasing halide character in the $M(\pi)_e$ level from Cl through to the iodine compound, which should decrease the efficiency of the $M(\pi) - \pi^*(CO)$ interaction by distortion of the $M(\pi)_e$ orbital. This is consistent with the relatively small changes in the antibonding levels as shown in Figure 2.09.

Chapter 3 - Electronic Spectra of Class 3 Mn and Re Pentacarbonyl Compounds Containing Group IV Metals

BACKGROUND

In the previous chapter the electronic spectra and interpretations of a number of metal carbonyls of C_{4v} or related symmetry have been classified in terms of the σ and π properties of the ligand L in the complex $L-M'(CO)_5$. This chapter includes discussion of the electronic spectra of compounds which have a varying π acceptor capability in addition to a σ effect. These are called Class 3 compounds in contrast to Class 1, which have only a σ effect and Class 2 which have σ accepting but π donating capabilities. The Class 3 compounds reported and discussed here are represented by the general formula $X_3M-M'(CO)_5$ in which X may be Cl, Br, I, C_6H_5 , C_6F_5 , or CH_3 and X_3 may be some mixture of these. M may be Sn, Pb, Ge, or Si and M' either Mn or Re. An additional Class 3 compound included here is $trans\ Cl_3SnMn(CO)_4P(C_6H_5)_2C_6F_5$.

Empty d orbitals on M are assumed to accept π charge from the filled d orbitals of M'. The varying π accepting ability of X_3M is governed by the X substituents as well as the nature of M. It has been generally accepted that X_3M is a poorer π acceptor than a $:CO$ group,¹² for the compounds considered here.

A number of C_{4v} $LCr(CO)_5$ and $LMo(CO)_5$ compounds have been reported^{22, 41} with accompanying electronic spectra. I.R.

studies have resulted in the calculation of σ and π parameters for a number of L groups in C_{4v} compounds of Cr, Mo, Mn and Re^{15, 41}. The electronic spectra of these and similar compounds indicate that the position of the bands is sensitive to the nature of the L group and the M' atom. For this reason electronic spectra offer a means of comparing the σ and π abilities of the L group with those calculated from I.R. and their effect on a qualitative energy level diagram.

EXPERIMENTAL PROCEDURE

The compounds, with the exceptions noted below, were obtained in pure form from W.A.G. Graham and coworkers and had been prepared as outlined by Graham et al. or by the references noted therein.¹⁴ Purity and identity rechecks on the compounds were carried out using I.R. and Mass Spectrometry. Compounds were recrystallized, if necessary, from n-hexane. Visible and U.V. spectra were obtained using a Cary 14 Spectrometer covering the range from 1900-5000 Å. High energy absorption bands were rechecked on a Jasco U.V. 5 ORD-CD instrument with an N₂ flushed system. Spectral grade solvents were used in all cases.

$\text{MeCl}_2\text{SnMn(CO)}_5$ and $\text{BuCl}_2\text{SnMn(CO)}_5$ were prepared by reaction of the corresponding $\text{R-Sn(Mn(CO)}_5)_3$ compound in methanol solution acidified with a few drops of conc. HCl. These reactions are described more completely in the following chapter.

RESULTS AND DISCUSSION

A summary of the λ max. values and band assignments for the $X_3M-Mn(CO)_5$ compounds is given in Tables 3-I, 3-II, 3-III and the spectra are shown in Figures 3.01-3.04. The spectra are of similar form, most showing three bands: one near 2000 \AA , the others near 2200 \AA and 2700 \AA . For certain compounds there is also a very weak band observed in the region $3000-3500 \text{ \AA}$. The observed variations in intensity and λ max. are discussed in terms of the general model and energy level diagram developed in the previous chapter for Classes 1 and 2. The $Cl_3SnMn(CO)_5$ compound is used as a standard for comparison. To link Class 3 with Class 1 and 2 compounds, $Cl_3SnMn(CO)_5$ is first compared to $CF_3Mn(CO)_5$.

Figure 3.05 shows a qualitative one electron energy level diagram for Class 3 compounds. This has as its highest filled levels the e and b_2 ($Mn d_{xz, yz, xy}$) and as its lowest empty levels the a_1 and b_1 , $Mn(d_z^2, d_{x^2-y^2}^2)$ and the various $\pi^*(CO)$ levels.

The relative placement of the e and b_2 levels depends primarily on the π accepting properties of $L(X_3M)$. If L is equivalent to CO in π accepting properties, then the filled d orbitals of M' should be equivalent and the e and b_2 levels should be degenerate. If L is a poorer π acceptor then the decreased total L (e) and M (e) π interaction should result in the e level being raised relative to the b_2 . If however, L is a better π acceptor than :CO then the e level should be lowered relative to

TABLE 3-I

Summary of U.V. Data and Assignments

Type of Transition

Compound A	Type of Transition											
	1. M \rightarrow L (C.T.) $e_{\pi} \rightarrow \pi^*(CO)$ N.I.	2. M \rightarrow L (C.T.) $e_{\pi} \rightarrow e\pi^*(CO)$ and $b_2\pi \rightarrow \pi^*(CO)$ N.I.	3. M \rightarrow L (C.T.) $e_{\pi} \rightarrow b_2\pi^*(CO)$ and $b_2\pi \rightarrow e\pi^*(CO)$	4. M(π) \rightarrow M(σ^*) $e_{\pi} \rightarrow a_1(\sigma^*)$ or $b_1(\sigma^*)$								
	λ max. (Å) $\bar{\nu}_{cm^{-1}}$ ϵ B	λ max. (Å) $\bar{\nu}_{cm^{-1}}$ ϵ	λ max. (Å) $\bar{\nu}_{cm^{-1}}$ ϵ	λ max. (Å) $\bar{\nu}_{cm^{-1}}$ ϵ								
$Cl_3SnMn(CO)_5$	2660 37,600 17,000	~ 2250 (sh) $\sim 44,500$ ~ 9000	2000 50,000 58,000	~ 3200 (sh) $\sim 31,200$ ~ 400								
$Cl_3SnMn(CO)_4PPh_2Ph_2$	2750 36,400 32,000	~ 2300 (sh) 45,500 $\sim 20,000$	1950 $\sim 51,300$ $\sim 80,000$	3450 29,000 600								
$Cl_3SnRe(CO)_5$	2480 40,300 12,500 ~ 2700 (sh) $\sim 37,000$ $\sim 3,000$	2100 (sh) 47,600 $\sim 10,000$	1930 51,800 50,000	3675 27,200 ~ 200 3200 31,200 ~ 700								
$CF_3Mn(CO)_5$	~ 2700 $\sim 37,000$ $\sim 3,000$	2155 46,380 30000	< 1900 (sh) $> 52,500$ $> 12,000$	not observable								

A All above spectra recorded in cyclohexane solution.

B Molar absorptivity

TABLE 3-II

Summary of U. V. Data and Assignments for Metal-Metal Bonded Mn Pentacarbonyls

Type of Transition

Compound A	Type of Transition							
	1. M+L (C.T.) $e_{\pi} \rightarrow \pi^*(CO)$ N.I.	2. M+L (C.T.) $e_{\pi} \rightarrow e_{\pi^*}(CO)$ and $b_2 \pi \rightarrow \pi^*(CO)$ N.I.	3. M+L (C.T.) $e_{\pi} \rightarrow b_2 \pi^*(CO)$ and $b_2 \pi \rightarrow e_{\pi^*}(CO)$	4. M(π) \rightarrow M(σ^*) $e_{\pi} \rightarrow a_1 \sigma^*$ or $e_{\pi} \rightarrow b_1 \sigma^*$				
	$\lambda_{max.}(\text{\AA})$ $\bar{\nu}cm^{-1}$ ϵ	λ max. (Å) $\bar{\nu}cm^{-1}$ ϵ	λ max. (Å) $\bar{\nu}cm^{-1}$ ϵ	$\lambda_{max.}(\text{\AA})$ $\bar{\nu}cm^{-1}$ ϵ				
$Me_2ClSnMn(CO)_5$	~ 2600 $\sim 38,500$ ~ 7000	Hidden	2070 48,300 60,000	not observable				
$MeCl_2SnMn(CO)_5$	2625 38,100 12,000	Hidden	2045 48,900 50,000	$\sim 31,250$ ~ 500				
$BuCl_2SnMn(CO)_5$	2650 37,700 12,000	Hidden	2065 48,400 50,000	not observable				
$Me_3SnMn(CO)_5$	not observable	~ 2200 (sh) 45,400 $\sim 20,000$	1970 50,700 50,000	not observable				
$Cl_3SiMn(CO)_5$	not observable	2250 (sh) 44,500 $\sim 17,000$	1970 50,700 60,000	34,500 ~ 500				
$Ph_3GeMn(CO)_5$	~ 2650 37,700 ~ 9000	2250 (sh) 44,500 $\sim 8,000$	1950 51,300 85,000	not observable				
$Cl_3GeMn(CO)_5$	2520 39,700 11,000	2220 (sh) 45,000 $\sim 7,000$	1950 51,300 50,000	not observable				
$Ph_3SiMn(CO)_5$	~ 2600 38,500 $\sim 10,000$	Hidden	~ 1950 51,300 $\sim 60,000$	not observable				

A All above spectra recorded in cyclohexane solution.

TABLE 3-III

Summary of Spectra of Phenyl Tin Mn Pentacarbonyls

Type of Transition

Compound A	1. M \rightarrow L (C.T.) $e_{\pi} \rightarrow \pi^* \text{CO (N.I.)}$		2. M \rightarrow L (C.T.) $e_{\pi} \rightarrow e\pi^*(\text{CO})$ and $b_2\pi \rightarrow \pi^*(\text{CO})$ N.I.		3. M \rightarrow L (C.T.) + Ph transitions $e_{\pi} \rightarrow b_2\pi^*(\text{CO})$ and $b_2\pi \rightarrow e\pi^*(\text{CO})$	
	$\lambda_{\text{max.}} (\text{\AA})$	$\bar{\nu} \text{ cm}^{-1}$	ϵ	$\lambda_{\text{max.}} (\text{\AA})$	$\bar{\nu} \text{ cm}^{-1}$	ϵ
$\text{Ph}_3\text{SnMn}(\text{CO})_5$	~ 2700 (sh)	$\sim 37,000$	$\sim 15,000$	hidden by end absorptions	1960 51,100	150,000
$\text{Ph}_2\text{Ph}_f\text{SnMn}(\text{CO})_5$	~ 2670 (sh)	$\sim 37,400$	$\sim 17,000$	hidden by end absorptions	~ 1950 $\sim 51,300$	$\sim 125,000$
$\text{Ph}(\text{Ph}_f)_2\text{SnMn}(\text{CO})_5$	2620	38,100	17,000	2100 (sh) 47,600 \approx 20,000	< 1920 $> 52,300$	$> 90,000$
$(\text{Ph}_f)_3\text{SnMn}(\text{CO})_5$	2605	38,400	18,000	~ 2100 (sh) 47,600 \sim 20,000	< 1900 $> 52,000$	$> 100,000$
$\text{Ph}_2\text{ClSnMn}(\text{CO})_5$	~ 2700	$\sim 37,000$	$\sim 12,000$	~ 2200 (sh) 45,400 \approx 15,000	1950 50,500	100,000
$\text{PhCl}_2\text{SnMn}(\text{CO})_5$	2675	37,500	15,000	hidden by end absorptions	1980 50,500	75,000

A All spectra recorded above in cyclohexane solution.

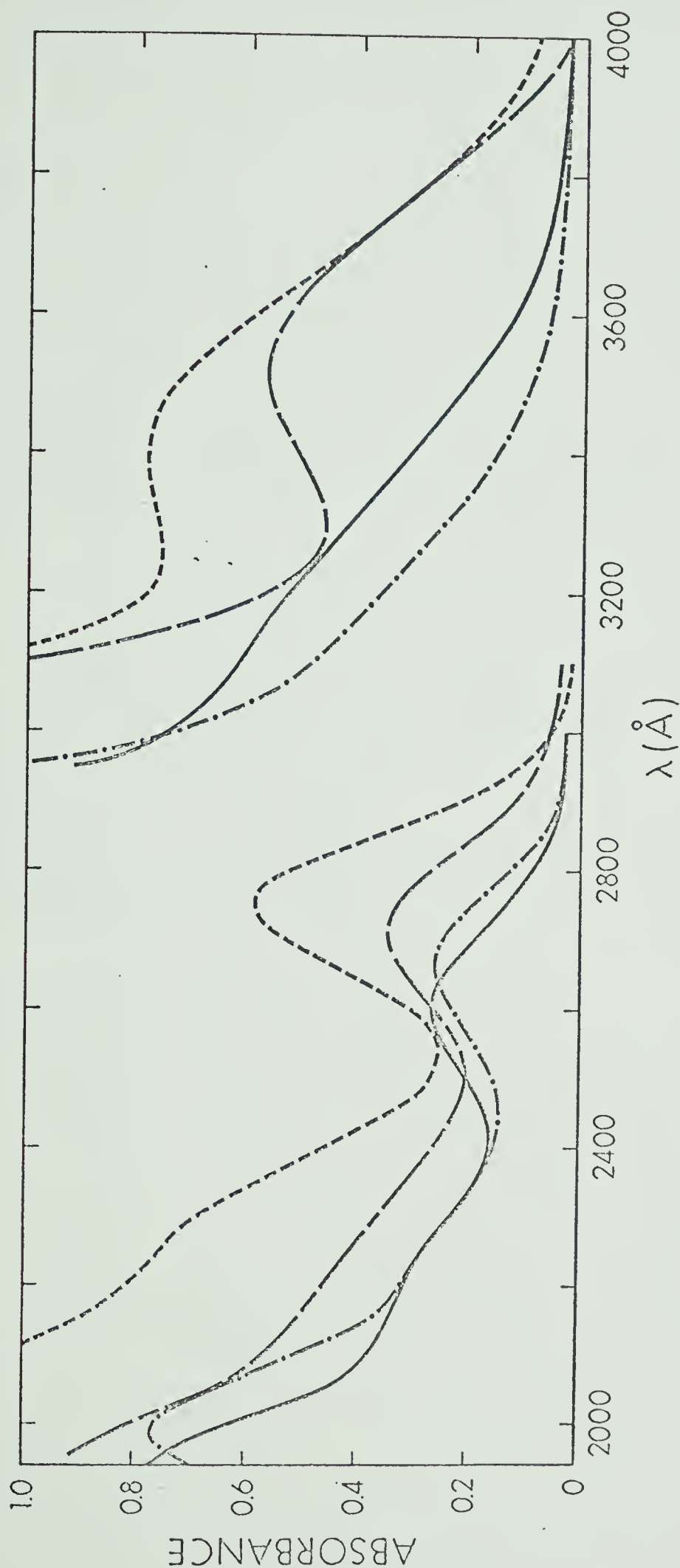


Figure 3.01 - Spectra of $\text{Cl}_3\text{SnMn}(\text{CO})_5$ and $\text{tr Cl}_3\text{SnMn}(\text{CO})_4\text{P}(\text{Ph})_2\text{Ph}_f$ in CH_3CN and C_6H_{12} .

— $\text{Cl}_3\text{SnMn}(\text{CO})_5$ in CH_3CN , 1.4×10^{-4} M

— · — $\text{Cl}_3\text{SnMn}(\text{CO})_5$ in C_6H_{12} , 1.2×10^{-4} M

--- $\text{Cl}_3\text{SnMn}(\text{CO})_4\text{P}(\text{Ph})_2\text{Ph}_f$ in CH_3CN , 1.0×10^{-4} M

----- $\text{Cl}_3\text{SnMn}(\text{CO})_4\text{P}(\text{Ph})_2\text{Ph}_f$ in C_6H_{12} , 1.5×10^{-4} M

For the region from 2000 Å to 3000 Å cell path lengths of 1 mm were used; from 3000 Å to 4000 Å cell path lengths of 5 cm were used for all compounds except $\text{Cl}_3\text{SnMn}(\text{CO})_4\text{P}(\text{Ph})_2\text{Ph}_f$ where a 10 cm cell was used.

Figure 3.02 - Spectra of chloroalkyl tin Mn pentacarbonyl compounds.

Solvent - C_6H_{12} ; Path length 1 mm vs 1 mm C_6H_{12} reference cell.

- Curve I - Cl_3SnMe - 3.3×10^{-4} M
- Curve II - $Me_3SnMn(CO)_5$ - 1.2×10^{-4} M
- Curve III - $Me_2ClSnMn(CO)_5$ - 1.0×10^{-4} M
- Curve IV - $BuCl_2SnMn(CO)_5$ - 1.2×10^{-4} M
- Curve V - $Cl_3SnMn(CO)_5$ - 1.2×10^{-4} M
- Curve VI - $MeCl_2SnMn(CO)_5$ - 1.7×10^{-4} M

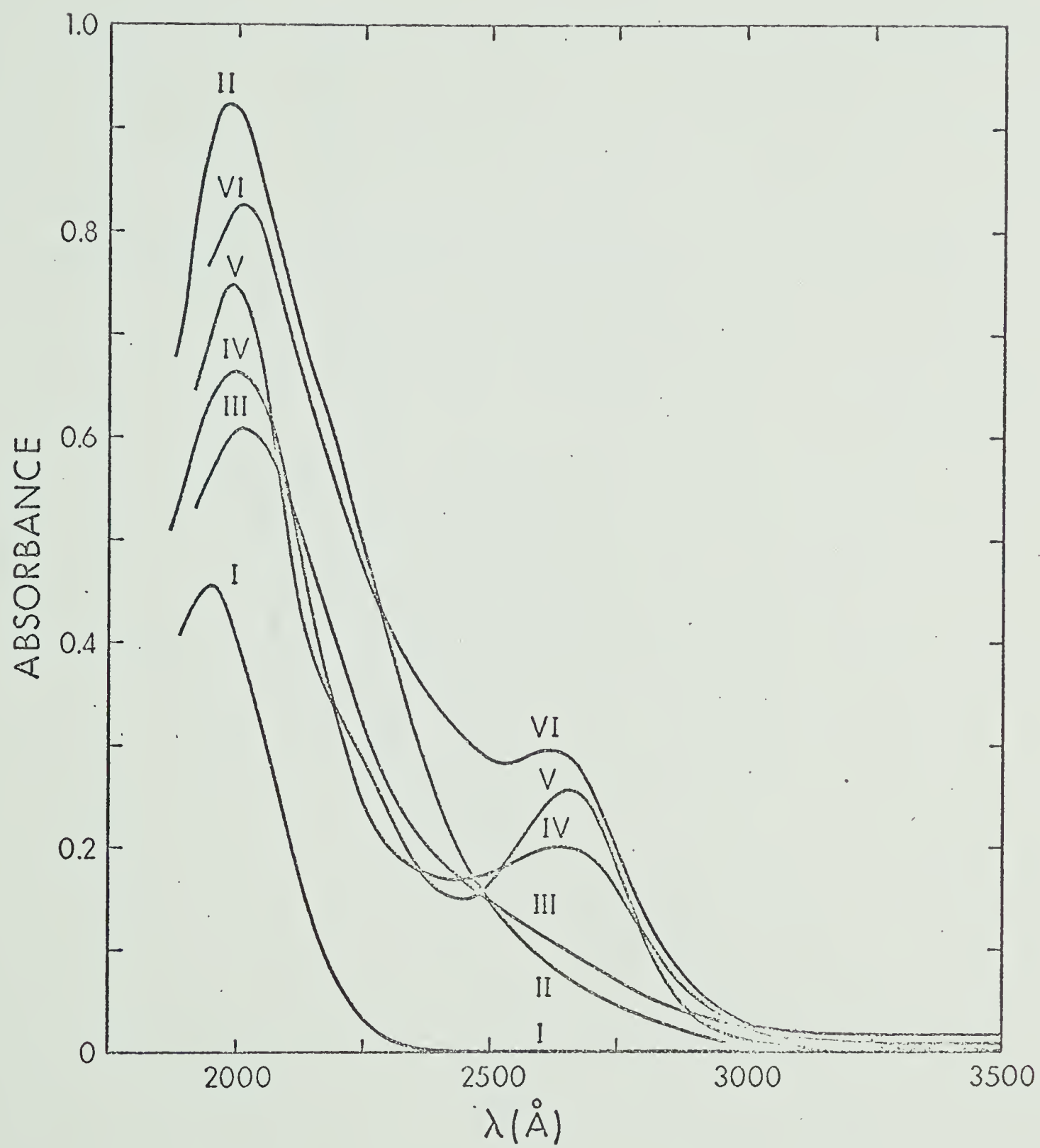


Figure 3.03 - Spectra of Group IV A chlorophenyl derivatives of Mn pentacarbonyl.

Solvent - C_6H_{12} . Path length 1 mm vs 1 mm reference.

- Curve I - $Cl_3SiMn(CO)_5$ - 1.0×10^{-4} M
Curve II - $Cl(Ph)_2SnMn(CO)_5$ - 0.7×10^{-4} M
Curve III - $Cl_3GeMn(CO)_5$ - 1.6×10^{-4} M
Curve IV - $PhCl_2SnMn(CO)_5$ - 1.3×10^{-4} M
Curve V - $Ph_3GeMn(CO)_5$ - 1.3×10^{-4} M
Curve VI - $Ph_3SiMn(CO)_5$ - 1.6×10^{-4} M

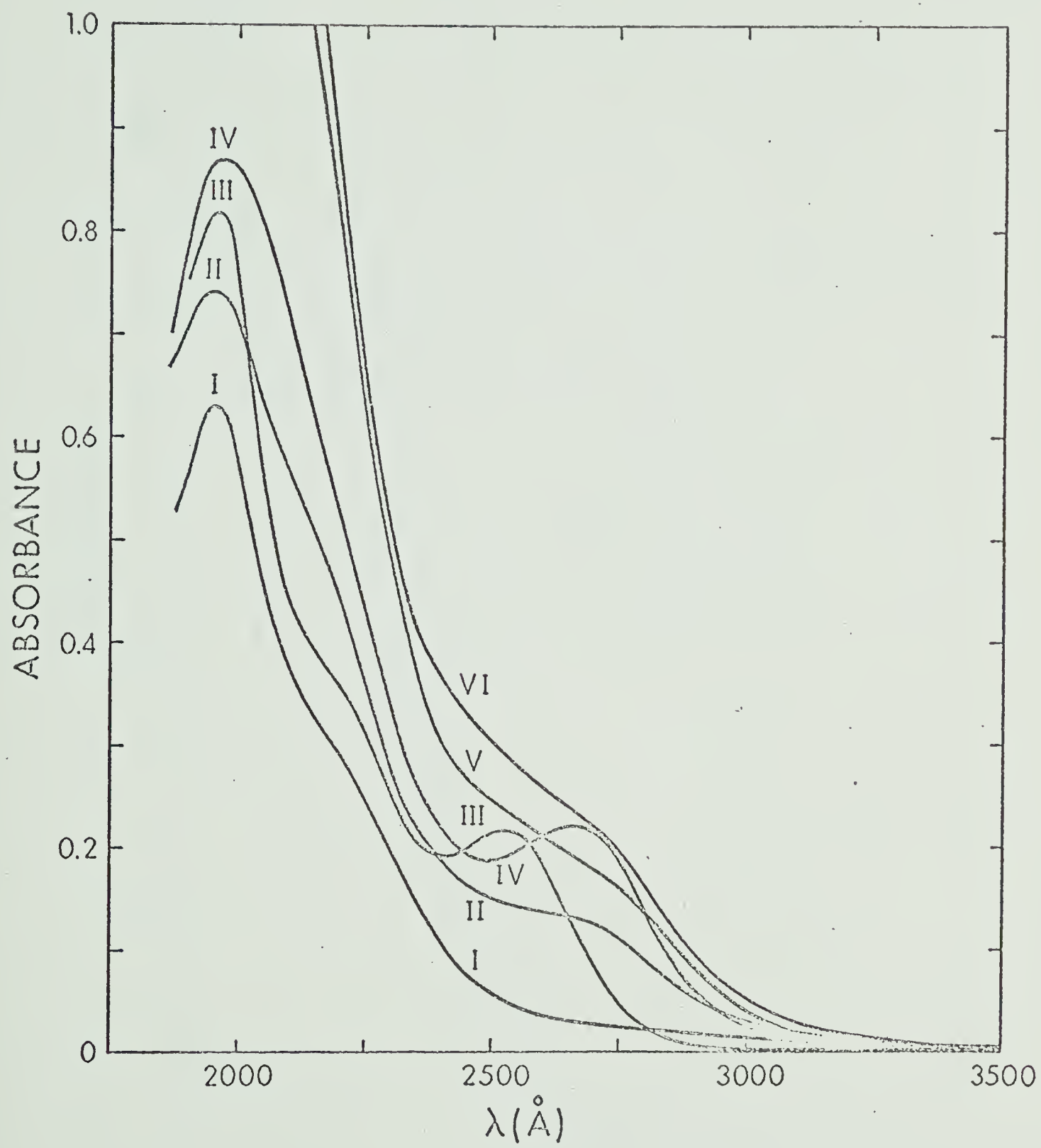
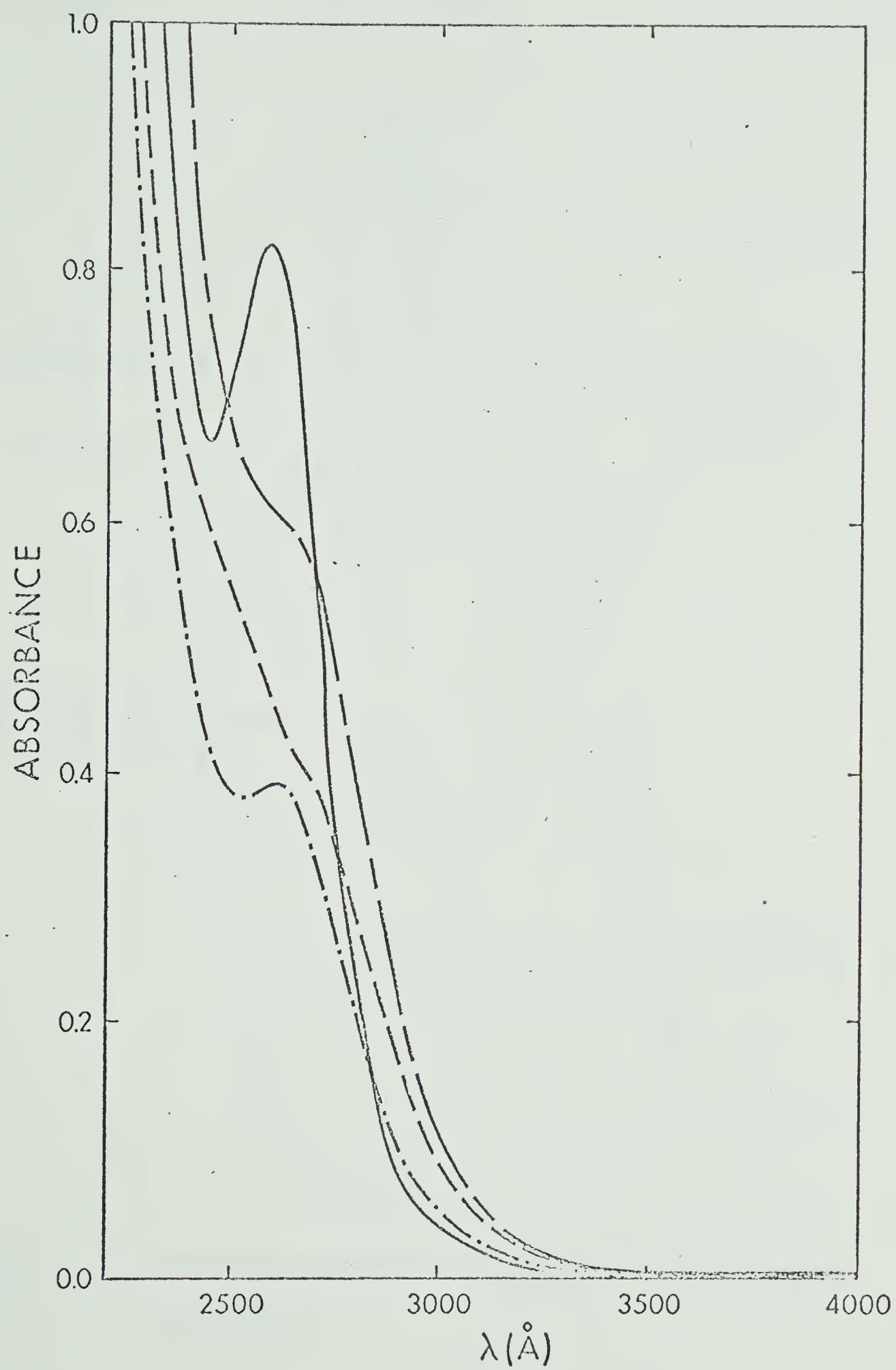


Figure 3.04 - Spectra of phenyl pentafluorophenyl derivatives of

Mn pentacarbonyl. Solvent - C_6H_{12} .

Path length 1 mm vs 1 mm reference.

————— $(Ph_f)_3SnMn(CO)_5$ - 3.5×10^{-4} M
— · — · — $(Ph_f)_2PhSnMn(CO)_5$ - 2.0×10^{-4} M
— - — $Ph_fPh_2SnMn(CO)_5$ - 2.9×10^{-4} M
- - - - - $Ph_3SnMn(CO)_5$ - 2.2×10^{-4} M



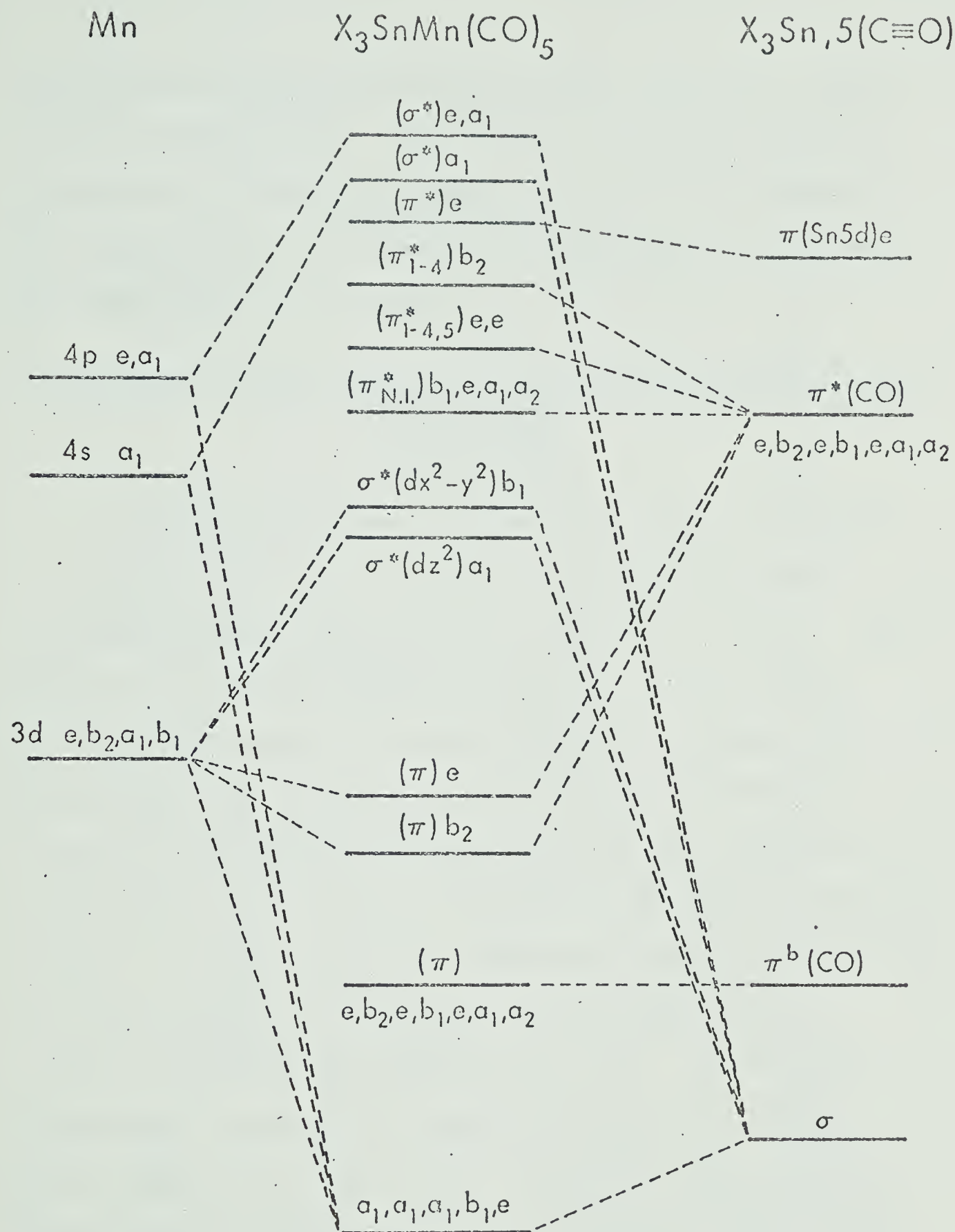


Figure 3.05 - Qualitative energy level diagram for $X_3\text{SnMn}(\text{CO})_5$ compounds.

the b_2 and the ordering of the levels will be reversed. This is pictured in Figure 3.06. The raising or lowering of levels as brought about by the σ properties of L should effect changes in the electronic spectrum through a general raising or lowering of the filled metal e and b_2 levels.

Comparison of Class 1 and Class 3 Compounds ($CF_3Mn(CO)_5$ and $Cl_3SnMn(CO)_5$)

Although both ligands are σ acceptors, CF_3 is a stronger σ acceptor than Cl_3Sn . In addition, the Cl_3Sn group has π accepting abilities whereas CF_3 has virtually no π effect. The superior σ accepting ability of CF_3 should result in a lower placement of the Mn d levels than in the corresponding Cl_3Sn compound. The π accepting ability of Cl_3Sn will result in a lowering of the Mn (e) level compared to the CF_3 compound as a result of the greater total π interaction for the Class 3 compound. Figure 3.07 shows the relative raising and lowering of the d levels by σ and π effects. The t_{2g} and e and b_2 levels serve as reference points for the shifting of the levels. The t_{2g} level represents a hypothetical compound in which L has σ and π effects identical to those of :CO. The first e and b_2 splitting illustrates the effect for a ligand with identical σ ability to that of :CO, but with no π capability. Relative σ and π effects are then introduced with respect to these reference levels for the Cl_3Sn and CF_3 compounds. Due to greater σ withdrawal effects,

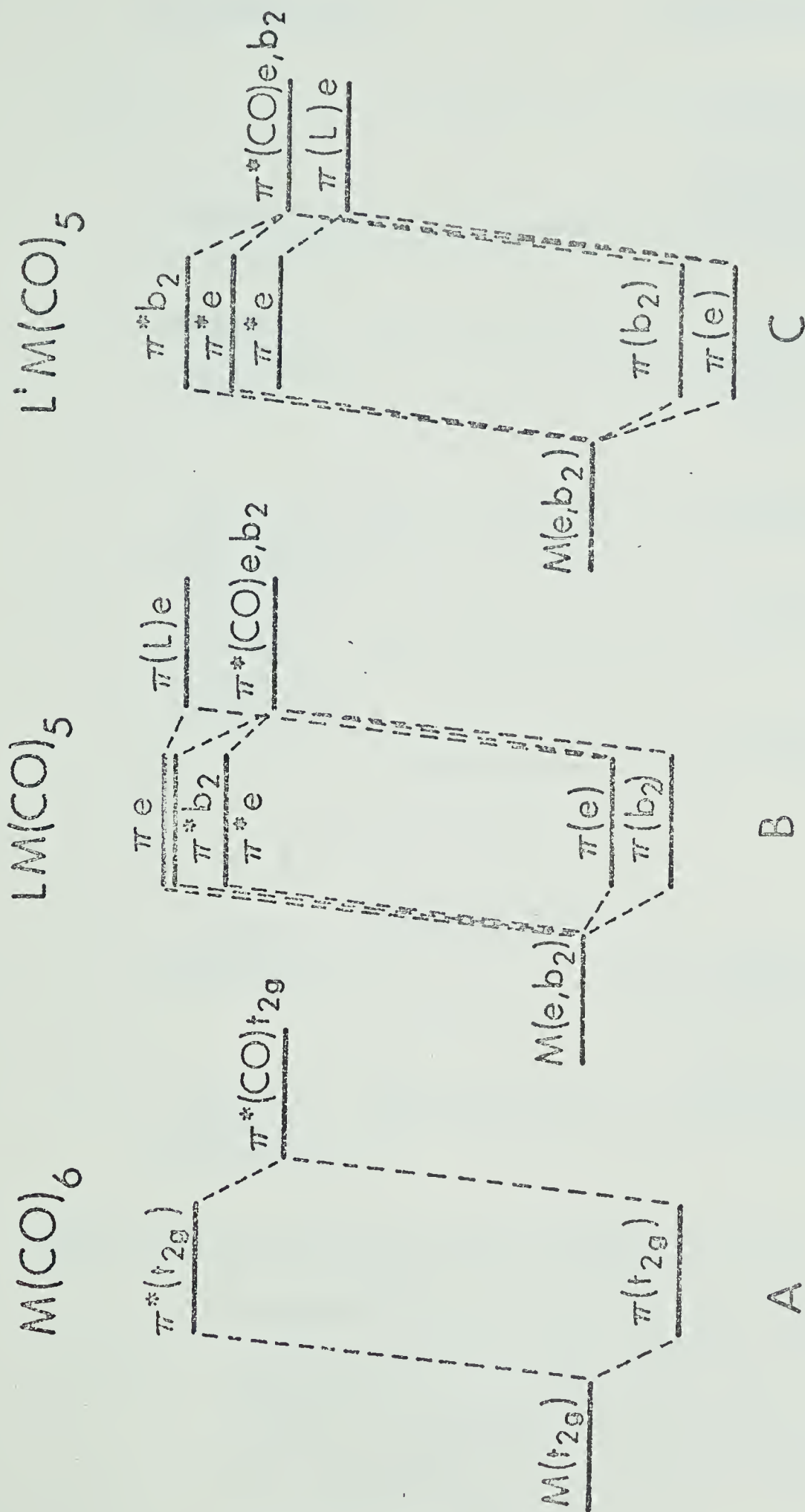


Figure 3.06 - Relative placement of metal e and b_2 levels with varying π acceptor properties of L in $LMn(CO)_5$ compounds. For simplicity the diagram shows a constant σ property throughout.

- A - L has identical π accepting capacity as CO;
- B - L has a poorer π accepting capacity than CO;
- C - L has a better π accepting capacity than CO.

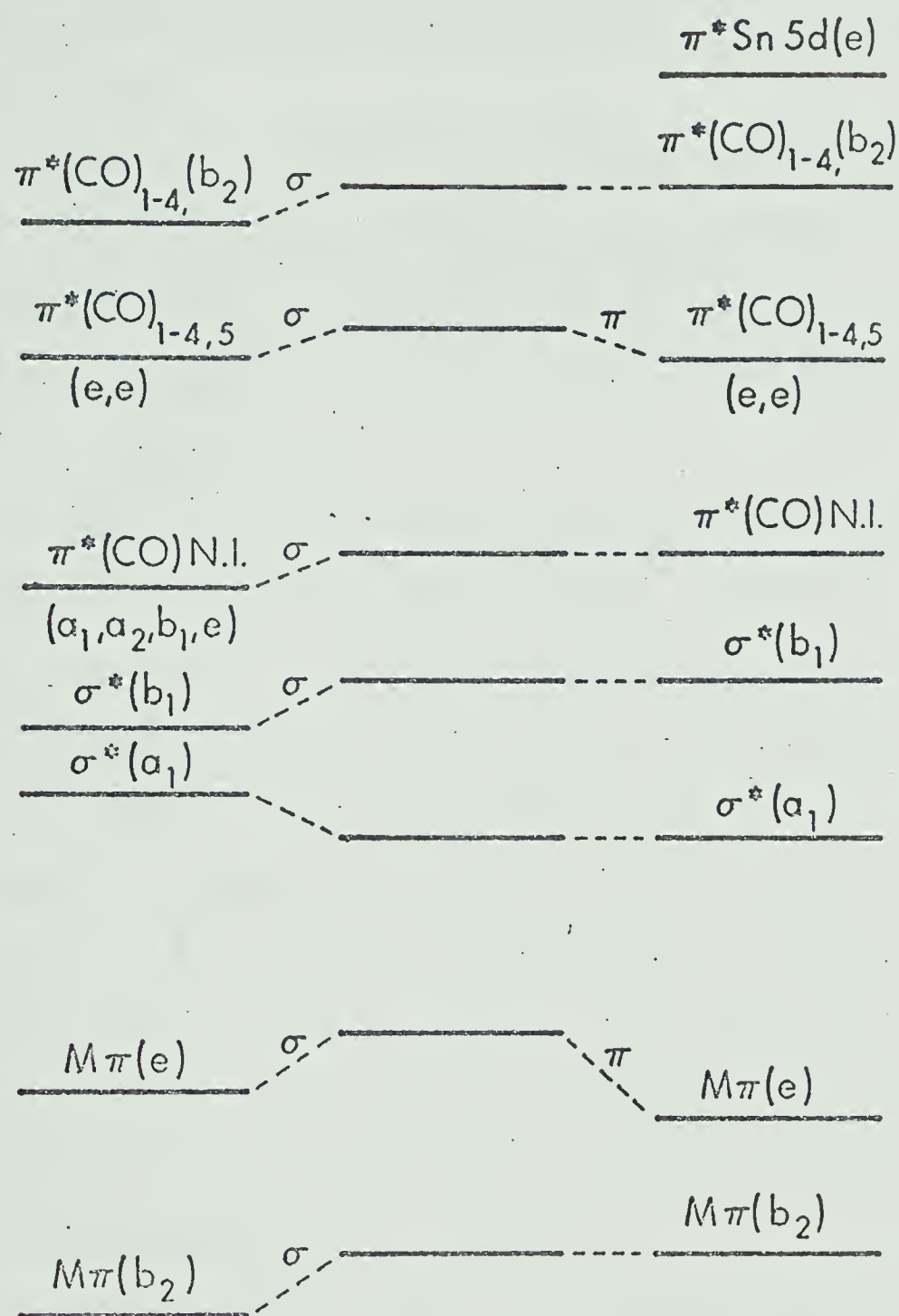
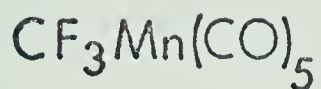


Figure 3.07 - Relative placement of $M(\pi)$ and $\pi^*(\text{CO})$ levels for $\text{Cl}_3\text{SnMn}(\text{CO})_5$ and $\text{CF}_3\text{Mn}(\text{CO})_5$. The placement is dependent on the σ and π properties of L. The $a_1(\sigma^*)$ level for $\text{Cl}_3\text{SnMn}(\text{CO})_5$ is placed lower than this level for $\text{CF}_3\text{Mn}(\text{CO})_5$ since a weaker L-Mn σ bond is expected for the former.

the upper levels may be slightly lower in the CF_3 compound than in the Cl_3Sn one.

Competitive π (e) interaction of the Sn 5d (e) level and the π^* (CO) 1-4,5 levels with the Mn(e) level should lower the π^* (CO) levels in the Cl_3Sn compound as compared to the CF_3 compound. Figure 3.05 shows the expected placement of the levels involved in the U.V. transitions.

The observed bands as summarized in Table 3-I match the qualitative diagram. The weak shoulder at $\sim 3200 \text{ \AA}$ in $\text{Cl}_3\text{SnMn}(\text{CO})_5$ may be a $M(\pi) \rightarrow \sigma^*$ (d-d) transition, or possibly a singlet-triplet transition appearing as a result of the Cl and Sn heavy atom effects. The single electron diagrams here are inadequate to represent triplet levels, and the low intensity of the band, combined with the limited number of compounds where it appears makes assignment difficult. The absence of any bands in Cl_3SnCH_3 above 1975 \AA (Figure 3.02) makes it unlikely that Cl to Sn or Sn to Cl transitions are involved in the lower energy transitions in the $\text{Cl}_3\text{SnMn}(\text{CO})_5$ compound.

Charge distribution within the molecular orbitals used in the energy level diagrams can be related to the bonding of Mn to L and various CO groups and leads to predictions of σ and π abilities of L which are qualitatively in agreement with those reported by Graham from I.R. studies.¹⁵

Comparison of $\text{Cl}_3\text{SnMn}(\text{CO})_5$ and trans $\text{Cl}_3\text{SnMn}(\text{CO})_4 \text{P}(\text{C}_6\text{H}_5)_2\text{C}_6\text{F}_5$.

In this case the :CO in the position trans to the Cl_3Sn group is replaced by diphenylpentafluorophenyl phosphine, a slightly better σ donor and a poorer π acceptor than the :CO¹⁵. Although the empty 3d orbitals on the P atom are available for back π bonding, there will be a net decrease in total π interaction of the Mn(e) orbitals and a consequent raising of the Mn(e) level. The effect of the σ property of the phosphine group will be to raise both the e and b_2 levels. The combination of σ and π effects accounts for the red shifts observed in the bands that have been assigned to the Mn(e) - $\pi^*(\text{CO})$ and Mn(b_2) - $\pi^*(\text{CO})$ transitions (Figure 3.01 and Table 3-I).

The fact that substitution of the axial CO by this phosphine affects the shape of the spectrum very little strongly suggests little involvement of the e $\pi^*(\text{CO})_5$ antibonding level in the observed transitions. The phosphorus 3d level of $\text{P}(\text{Ph})_2\text{Ph}_f$ is expected to be higher and less available for Mn d(π) - p (3d) backbonding than the CO's and not to contribute significantly to the observed spectrum. A comparison of the qualitative energy level diagrams for these two compounds is given in Figure 3.08.

Figure 3.01 shows a distinct weak band at $3450 \text{ } \overset{\circ}{\text{A}}$ for the phosphine substituted compound but only a weak shoulder ($\sim 3200 \text{ } \overset{\circ}{\text{A}}$) for the $\text{Cl}_3\text{SnMn}(\text{CO})_5$ compound. For the phosphine compound the band which appears at $3450 \text{ } \overset{\circ}{\text{A}}$ in C_6H_{12} shifts to $3500 \text{ } \overset{\circ}{\text{A}}$ in CH_3CN . In contrast higher energy bands in these two compounds

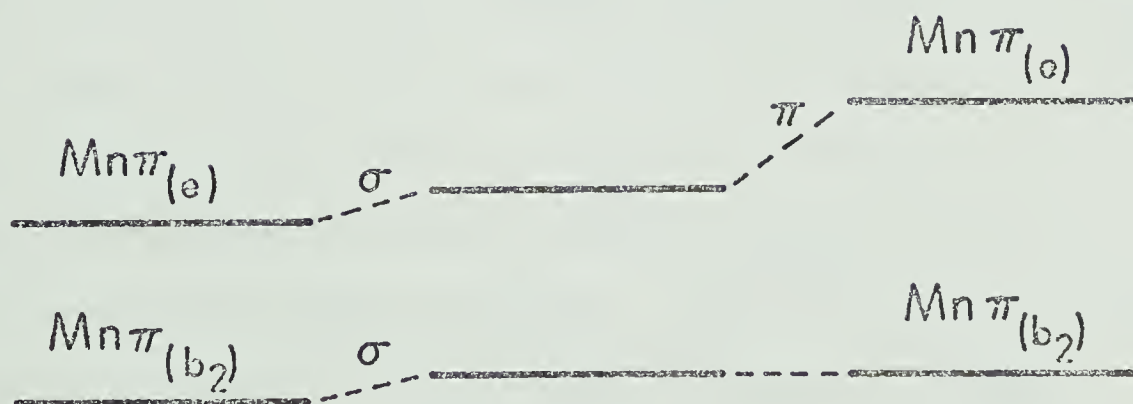
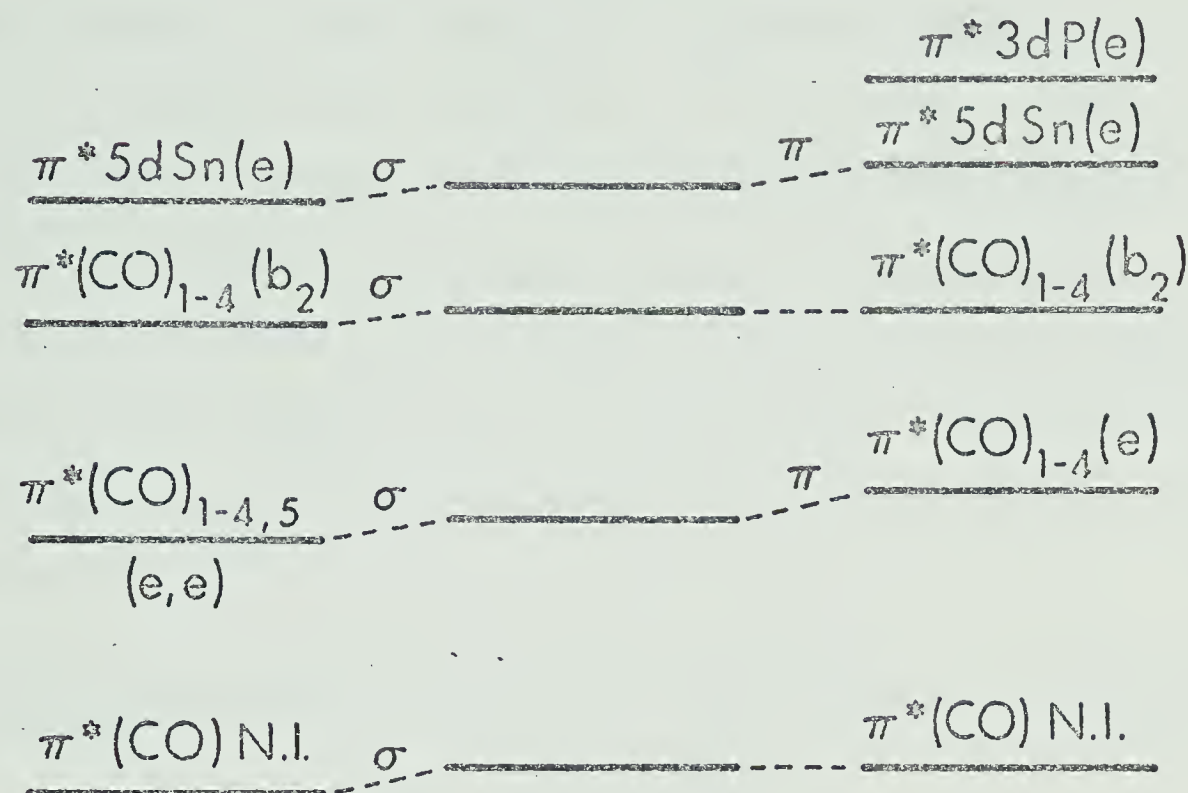
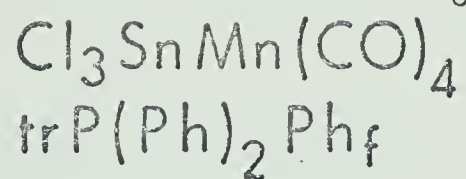


Figure 3.08 - Relative placement of $\text{M}(\pi)$ and $\pi^*(\text{CO})$ levels for $\text{Cl}_3\text{SnMn(CO)}_5$ and $\text{Cl}_3\text{SnMn(CO)}_4\text{trP(Ph)}_2\text{Ph}_f$.

show a large blue shift from C_6H_{12} to CH_3CN : $Cl_3SnMn(CO)_5$ 2660 Å (C_6H_{12}), 2600 Å (CH_3CN); $Cl_3SnMn(CO)_4PPh_fPh_2$ 2750 Å (C_6H_{12}), 2700 Å (CH_3CN), indicating different types of transitions. The low ϵ value of the 3500 Å band and the fact that the red shift in going from the parent compound to the phosphine substituted one is larger for this band than for higher energy bands suggest a $M(\pi) - \sigma^*$ transition. Transitions of this type are expected to lie at lower energies than $M(\pi) - \pi^* CO$ transitions.²⁴

Comparisons of Class 3 compounds with varying Sn substituents

1) $Cl_nMe_{3-n}SnMn(CO)_5$, $Cl_2BuSnMn(CO)_5$

The spectra for this group of compounds appear in Figure 3.02 and the assignments are summarized in Tables 3-I and 3-II. Figure 3.02 shows the absence of the 2700 Å band in the Me_3Sn compound, a band which is well defined in the Cl_3Sn compound. From the same figure, it is obvious that for equimolar concentrations, the end absorptions strongly shift to the red for the Me_3Sn compound. This in part accounts for the disappearance of the expected high λ transition. In addition, band positions for the alkyl dichloro tin derivatives indicate that this band is successively blue shifted with alkyl substitution. These blue shifts indicate stabilization of the $Mn(\pi_d)$ e level with increasing alkyl substitution and suggest that Me_3Sn is a better π acceptor than Cl_3Sn . The red shifts of the higher energy bands result from an

elevation in the b_2 level due to increasing donor properties of the alkyl groups. The placement of the b_2 level should be relatively unaffected by ligand π effects.

The monosubstituted compounds, $\text{MeCl}_2\text{SnMn}(\text{CO})_5$ and $\text{C}_4\text{H}_9\text{Cl}_2\text{SnMn}(\text{CO})_5$, give spectra very similar to that for $\text{Cl}_3\text{SnMn}(\text{CO})_5$ while the $\text{Me}_2\text{ClSnMn}(\text{CO})_5$ spectrum is very close to that for $\text{Me}_3\text{SnMn}(\text{CO})_5$. This is interpreted to mean that a single Cl can be accommodated on the Sn offering little competition with the Mn for π donation to the Sn. With two Cl's such competition is unavoidable, while the addition of a third does not increase it markedly. Figure 3.09 gives a comparison of the expected σ and π abilities of Me_3Sn and Cl_3Sn and their effect on an energy diagram. Qualitatively they are in agreement with those parameters calculated by Graham.¹⁵

2) $\text{Ph}_n(\text{Cl})_{3-n}\text{SnMn}(\text{CO})_5$ Compounds

Table 3-III gives the λ max. values for the transitions in this group of compounds as shown in Figures 3.01, 3.03 and 3.04. As Cl is replaced by Ph there is a continual red shift of the high λ band ($\text{Mn } e - \pi^*(\text{CO})$) which is apparently a result of the large σ donating property of the Ph ligand. The λ maximum values of the end absorption do not change with any regularity but introduction of Ph groups may be expected to complicate interpretation of this region. A number of transitions contribute to the end absorption and a blue shift in λ maximum of the broad main band around 2000 \AA for Ph substituted compounds does not necessarily indicate

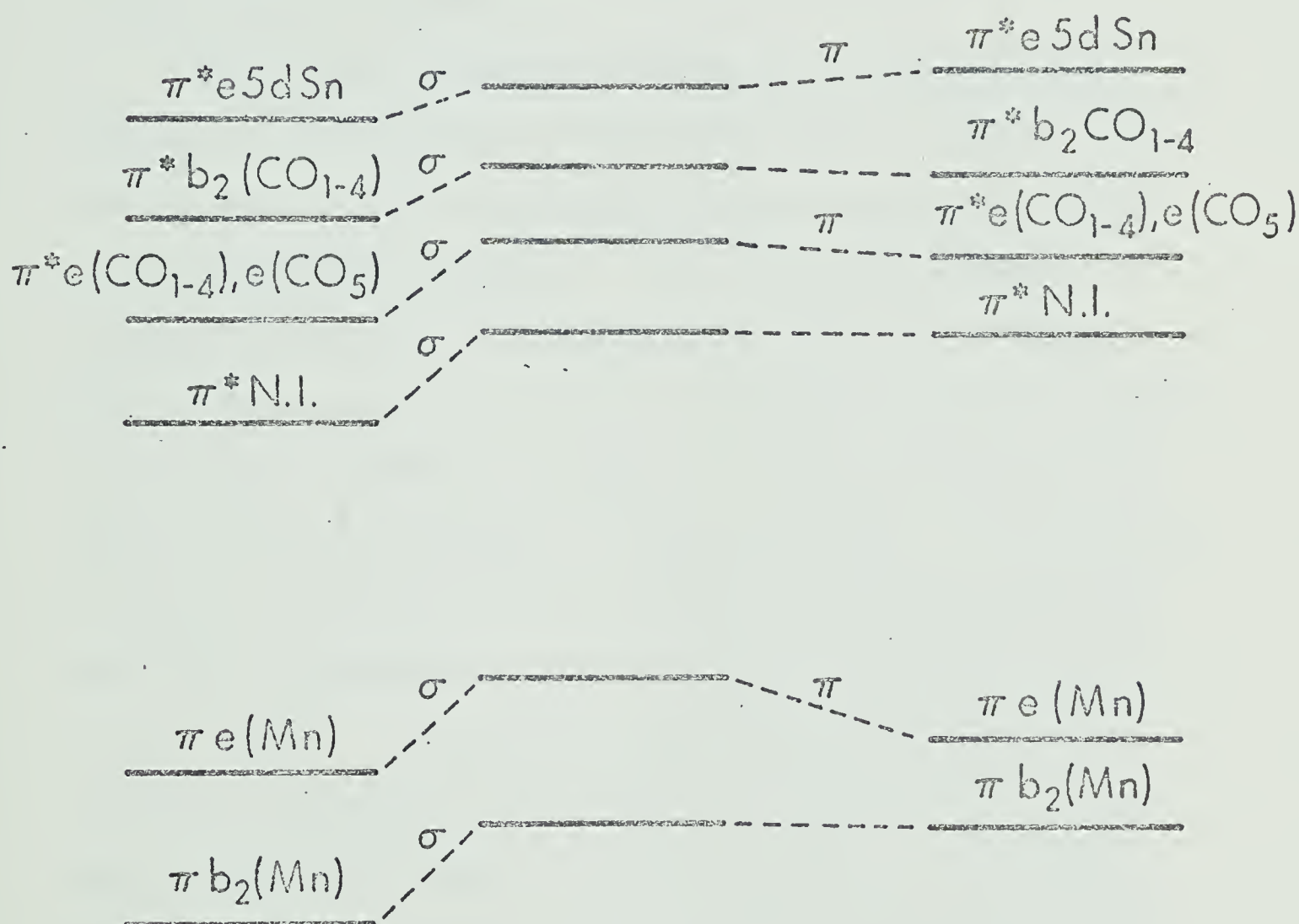


Figure 3.09 - Relative placement of $M(\pi)$ and $\pi^*(\text{CO})$ levels for



that the Mn-CO transitions are all blue shifted. In fact, the change of the 2655 Å band in $\text{Cl}_3\text{SnMn(CO)}_5$ to a shoulder at 2700 Å in $\text{Ph}_3\text{SnMn(CO)}_5$ indicates that the higher energy transitions in $\text{Ph}_3\text{SnMn(CO)}_5$ are red shifted more than the lower energy band.

3) $\text{Ph}_n(\text{Ph}_f)_{3-n}\text{SnMn(CO)}_5$

The electronic spectra for this series of compounds are outlined in Table 3-III with accompanying spectra in Figure 3.04. The absorptions in the phenyl compounds are expected to include a number of phenyl transitions. Since in photodecomposed compounds, phenyl types of absorption are observed as high as 2800 Å with an intensity less than ten percent of that of the original pentacarbonyl compound, the major part of the absorption in this region is assumed due to Mn- π^* (CO) transitions. The decrease in energy of the high λ band in proceeding from $(\text{Ph}_f)_3\text{SnMn(CO)}_5$ (2605 Å) to $\text{Ph}_3\text{SnMn(CO)}_5$ (2700 Å) can be accounted for by both σ and π effects. The greater σ withdrawal effect of Ph_f would result in a lower placement of the filled d orbitals on Mn and the higher energy of the Mn(d) - π^* (CO) transitions. Even though the high λ band red shifts from the Ph_f to the Ph compounds, the band changes from a well defined peak to a shoulder as higher energy transitions shift more markedly to the red. As Ph replaces Ph_f , Sn becomes a stronger σ donor and a slightly weaker π acceptor.¹⁵ Figure 3.10 depicts the corresponding changes in the energy level diagram.

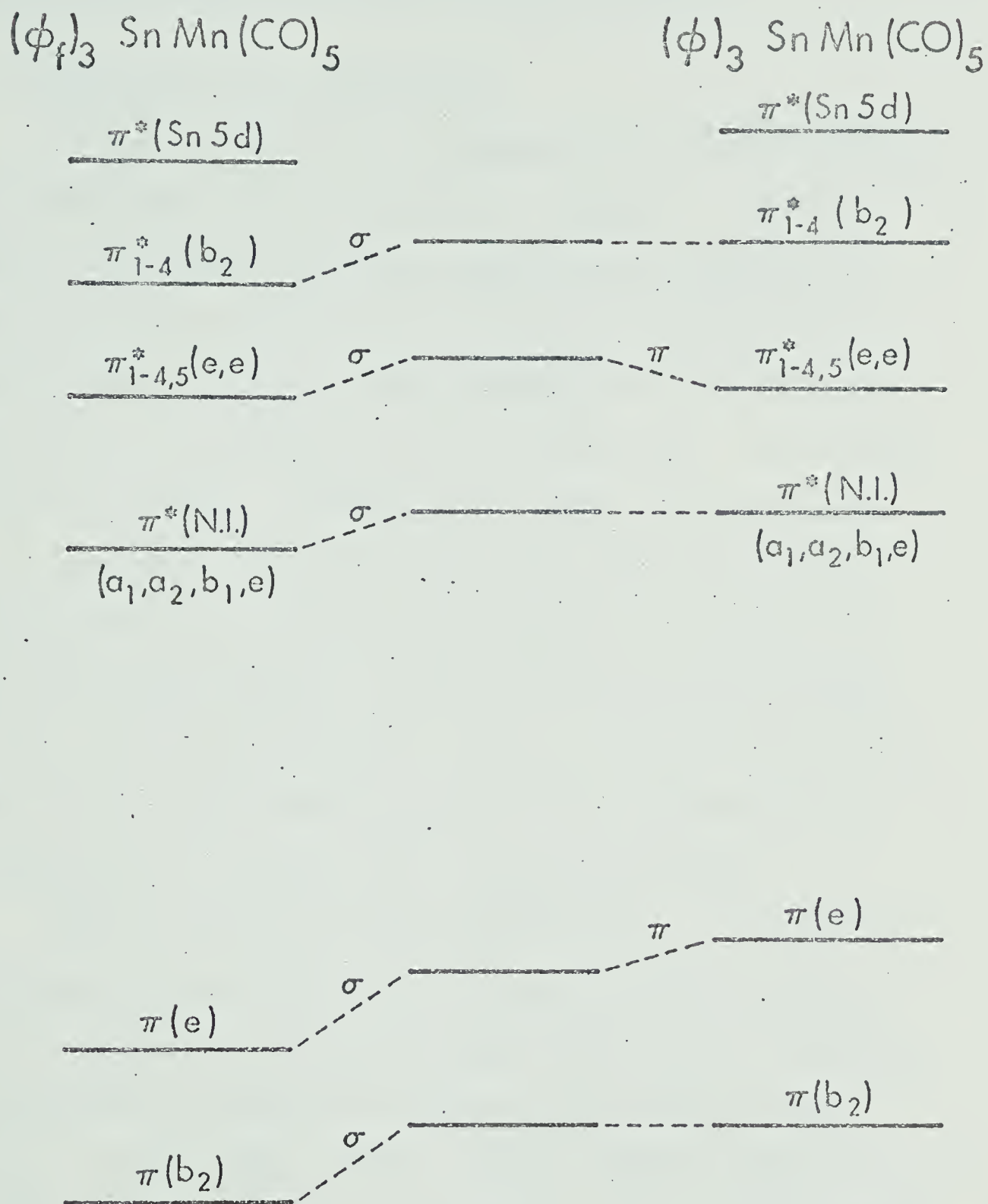


Figure 3.10 - Relative placement of $M(\pi)$ and $\pi^*(CO)$ levels for

$(\text{Ph}_f)_3 \text{SnMn(CO)}_5$ and $\text{Ph}_3 \text{SnMn(CO)}_5$.

Comparison of Mn and Re pentacarbonyl compounds

1) $\text{Cl}_3\text{SnMn}(\text{CO})_5$ and $\text{Cl}_3\text{SnRe}(\text{CO})_5$

The spectra of these two compounds are similar, that for the Re compound being somewhat more complex. Table 3-I shows λ maximum values and the appropriate assignments for these compounds and Figures 3.01 and 3.02 show the spectra. Because Re is slightly more electronegative than Mn both the e and b_2 levels are placed lower for Re than for Mn. This would result in less $M(d) - \pi^*(\text{CO})$ and $M - \text{Sn}(d - d)$ interaction for the Re compound. The blue shifts in the electronic spectra in going from Mn to Re are consistent with the placement of the levels and suggest that the σ effect is more important than the π effect in the placement of the e level. The asymmetry of the 2480 \AA band in $\text{Cl}_3\text{SnRe}(\text{CO})_5$ is ascribed to a splitting of the $\pi^*(\text{CO})$ levels, possibly due to f orbital interactions.

Although large blue solvent shifts for $M \rightarrow \pi^*(\text{CO})$ C.T. transitions are generally observed from non-polar to polar solvents (Figure 3.01), the low energy, high λ band at 3200 \AA in $\text{Cl}_3\text{SnRe}(\text{CO})_5$ is relatively indifferent to any solvent effects ($\text{C}_6\text{H}_{12} = 3200 \text{ \AA}$, $\text{CCl}_4 = 3200 \text{ \AA}$, $\text{CHCl}_3 = 3220 \text{ \AA}$, $\text{CH}_2\text{Cl}_2 = 3180 \text{ \AA}$, $\text{CH}_3\text{CN} \sim 3200 \text{ \AA}$). In addition, small ϵ values suggest assignment of this band to a $d - d$ type of transition. The band may be compared to a similar weak transition in this region in C_{4v} Mn pentacarbonyl compounds. The weaker shoulder at $\sim 3700 \text{ \AA}$ could conceivably be a $d - d$ type of transition, but weak

triplet components of the $e - \pi^*$ transitions are also a possibility for both of these bands.

Table 3-IV summarizes the observed spectra for other C_{4v} Re pentacarbonyl compounds shown in Figure 3.11. Spectra show additional splitting in the lowest energy band similar to that suggested by the $Cl_3SnRe(CO)_5$ spectrum. Ph, Cl substitution on the Sn has the same effect on the spectra of the Re pentacarbonyl compounds as that observed for the Mn ones.

2) $Ph_3M-Re(CO)_5$; $M = Si, Ge, Sn$ or Pb

Spectra for this group of compounds appear in Figure 3-12; band maxima and assignments are summarized in Table 3-IV. The $Ph_3MRe(CO)_5$ compounds all exhibit the splitting of the high λ band common to most C_{4v} Re and W pentacarbonyl compounds.⁴¹ The lowest energy transitions are undoubtedly still charge transfer in nature and comparable to the $Mn - \pi^*(CO)$ transitions observed in $L Mn(CO)_5$ compounds. The large red shift of the lowest energy band for the Pb compound as compared to the other Group IV atoms suggests that the σ property of the Ph_3M is the most important factor and that d orbital size may play a significant role in $M-M'$ π bonding. The large size of Pb d orbitals would then be expected to inhibit strong $M-M'$ overlap resulting in a higher placement of the Re (e) level and the large red shift of the lowest energy C. T. band.

TABLE 3-IV

Spectral Summary of Metal-Metal bonded Re Pentacarbonyl Compounds

Compound	λ max. (\AA)	$\bar{\nu}$ cm^{-1}	ϵ
Cl_3SnMe	1980	50,000	14,000
$\text{Me}_3\text{SnRe}(\text{CO})_5$	2580	38,750	7,000
	2480	40,300	6,000
$\text{Ph}_3\text{SnRe}(\text{CO})_5$	2780	36,000	13,000
	2670 (sh)	37,450	$\sim 3,000$
	2610 (sh)	38,300	$\sim 3,000$
$\text{Cl}_2\text{PhSnRe}(\text{CO})_5$	2520 (asymm)	39,700	$\sim 13,000$
$\text{Br}_3\text{SnRe}(\text{CO})_5$	2860	34,950	14,000
	2600 (sh)	38,500	$\sim 1,000$
	2400 (sh)	41,700	$\sim 2,000$
	2300 (sh)	43,500	$\sim 5,000$
	2100 (sh)	47,600	$\sim 25,000$
	1920	52,100	80,000
$\text{Ph}_3\text{GeRe}(\text{CO})_5$	2850	35,100	8,000
	2690 (sh)	37,200	$\sim 2,000$
	2620 (sh)	38,150	$\sim 2,000$
$\text{Ph}_3\text{SiRe}(\text{CO})_5$	2820	35,500	7,000
	2710 (sh)	36,900	$\sim 1,000$
	2640 (sh)	37,900	$\sim 1,000$
$\text{Ph}_3\text{PbRe}(\text{CO})_5$	3050	32,800	14,000
	2680 (sh)	37,300	$\sim 4,000$
	2560 (sh)	39,100	$\sim 4,000$

Figure 3.11 - Spectra of $X_3\text{SnRe}(\text{CO})_5$ compounds. Solvent - C_6H_{12} .

Path length - 1 mm vs 1 mm reference cell.

———— $\text{Cl}_3\text{SnRe}(\text{CO})_5$ - 4.5×10^{-4} M
----- $\text{Br}_3\text{SnRe}(\text{CO})_5$ - 3.2×10^{-4} M
— · — · — $\text{Ph}_3\text{SnRe}(\text{CO})_5$ - 11.8×10^{-4} M
- - - - - $\text{Me}_3\text{SnRe}(\text{CO})_5$ - 4.1×10^{-4} M
..... $\text{PhCl}_2\text{SnRe}(\text{CO})_5$ - 4.6×10^{-4} M

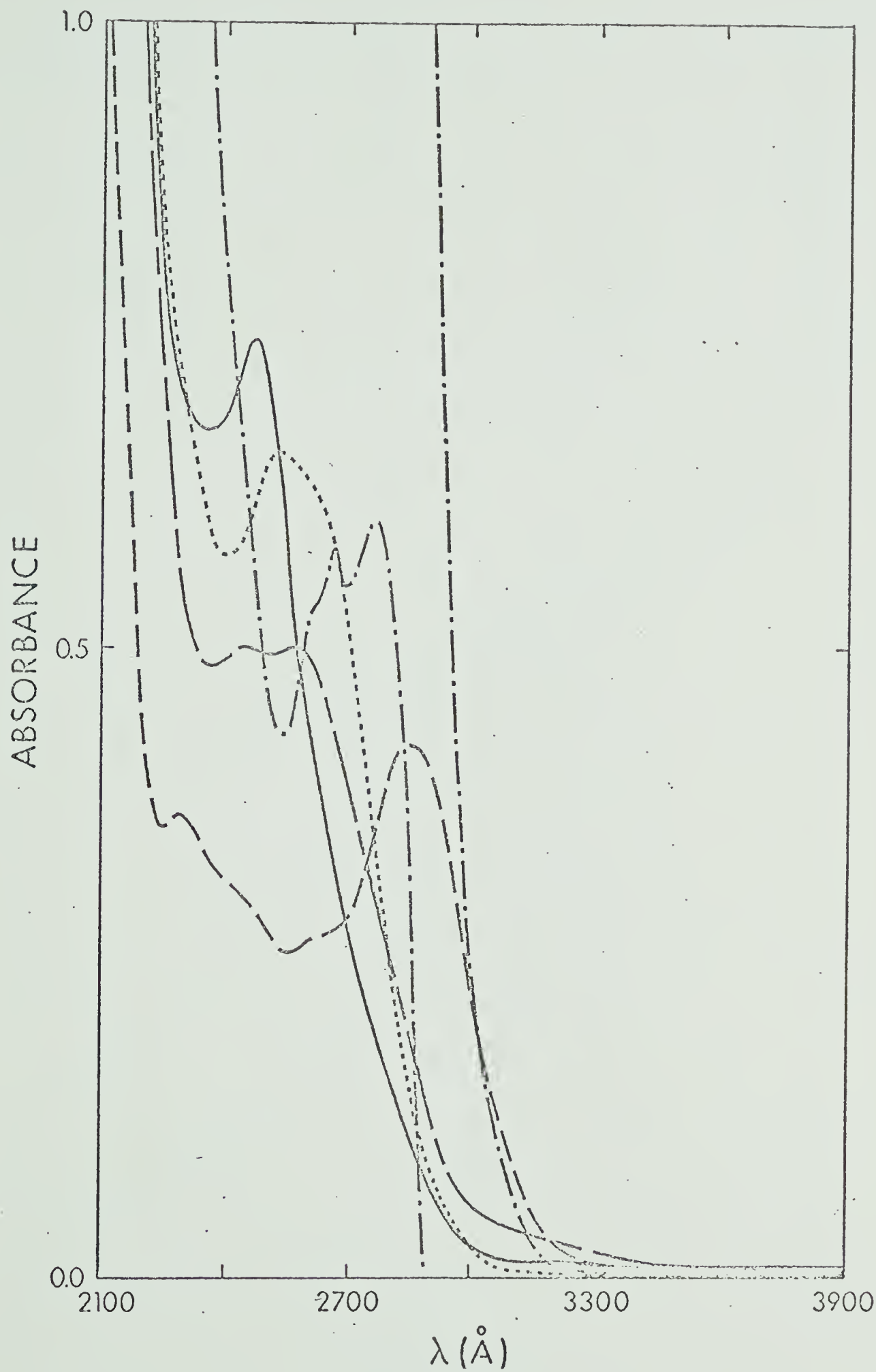
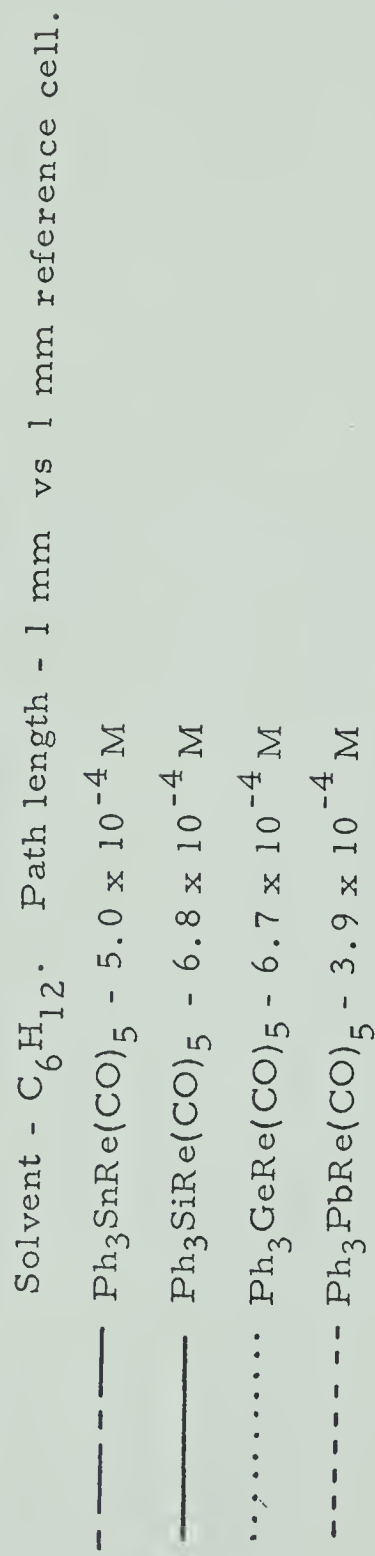
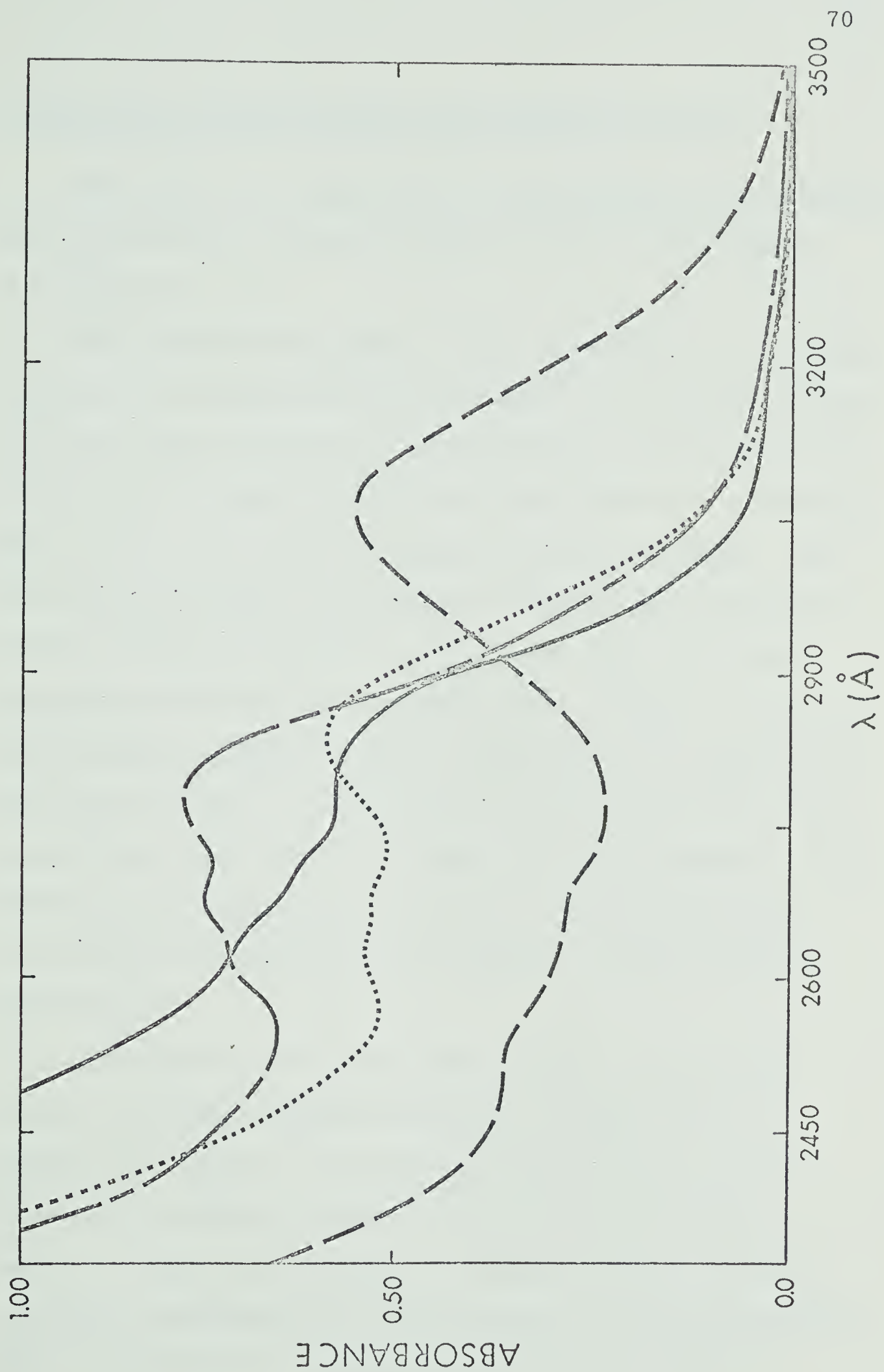


Figure 3.12 - Spectra of Group IVA triphenyl-Re pentacarbonyl compounds.





Comparison of $\text{Cl}_3\text{M}-\text{Mn}(\text{CO})_5$ compounds with varying M

The electronic spectral data for $\text{Cl}_3\text{SiMn}(\text{CO})_5$, $\text{Cl}_3\text{GeMn}(\text{CO})_5$ and $\text{Cl}_3\text{SnMn}(\text{CO})_5$ are given in Tables 3-I and 3-II and Figures 3.01 and 3.03.

Differences in the spectra of these compounds are necessarily dependent on the placement of the electronic levels in the molecules. This placement is expected to be related to the σ and π properties of the Group IV metal attached to Mn, which in turn are a function of size, shape and energy of the orbitals involved in bonding. The most striking change in the spectra is the blue shift of the 2655 \AA band in the Cl_3Sn compound to 2510 \AA in the Cl_3Ge one and the disappearance of this band in $\text{Cl}_3\text{SiMn}(\text{CO})_5$. Higher ϵ values for the transitions of higher energy in $\text{Cl}_3\text{SiMn}(\text{CO})_5$ also suggest that the lowest energy C.T. band has been blue shifted from the Cl_3Ge position and is now hidden by the higher energy absorptions. This shift indicates stabilization of the $\text{Mn}(\pi)$ level from Sn to Si which may be accounted for by increasing π acceptor properties from Sn to Si.

Although changes in the k values and the accompanying σ and π parameters suggest that Cl_3Si is a slightly better π acceptor than Cl_3Sn ,¹⁵ the changes in the electronic spectra are large and indicate significant differences in the bonding abilities of these three L groups. It is interesting to note that the phenyl substituted Si, Ge and Sn analogs show little significant difference in their U.V. spectra (Tables 3-II and 3-III) or in

bonding abilities calculated from I.R. studies.¹⁵

Comparison of $n - \sigma^*$ transitions in I_3Sn-Y compounds

Table 3-V gives the λ maximum and energy values for the two high λ bands which are present in I_3Sn-Y compounds. In the present case Y may be $Mn(CO)_5$, $Re(CO)_5$ or I. The C.T. transitions generally observed in compounds of this type are hidden or obscured by transitions arising from the I-Sn portion of the molecule. The compounds are examined however with respect to the effect that the Y substituent may have on the transitions arising from the I-Sn entities. Figure 3.13 shows the spectra.

There have been two approaches in the literature to the assignments of portions of halide spectra. Katzin⁴² has summarized initial work in this area by Franck and Scheibe⁴³ while Kimura and Nagakura⁴⁴ use a Mulliken approach to the assignment of the transitions in compounds of iodine and bromine.

Katzin's essentially atomic approach is based on the fact that the halogen atomic spectrum indicates two levels ($^2P_{3/2}$ and $^2P_{1/2}$) which show a spacing of approximately 7600 cm^{-1} for iodine compounds and smaller separations at higher energy for bromine and chlorine compounds. The absorption spectrum of the iodide ion shows two intense bands with this approximate spacing. The interpretation given is that an electron is removed from the ion leaving iodine in the ground ($^2P_{3/2}$) or excited ($^2P_{1/2}$) state. This approach assumes that transitions occurring in

TABLE 3-V

Summary of $\eta \longrightarrow \sigma^*$ Transitions in Iodo Tin Compounds

Compound	Band	$\lambda_{\text{max.}} (\text{\AA})$	$\bar{\nu} (\text{cm}^{-1})$	ϵ
$\text{I}_3\text{SnRe}(\text{CO})_5$	1	2785	35,900	5,900
	2	3560	28,100	11,700
	$\Delta 1-2$	-	7,800	-
I_4Sn	1	2875	34,780	2,200
	2	3650	27,400	9,000
	$\Delta 1-2$	-	7,400	-
$\text{I}_3\text{SnMn}(\text{CO})_5$	1	2955	33,840	6,400
	2	3705	27,000	12,800
	$\Delta 1-2$	-	6,800	-

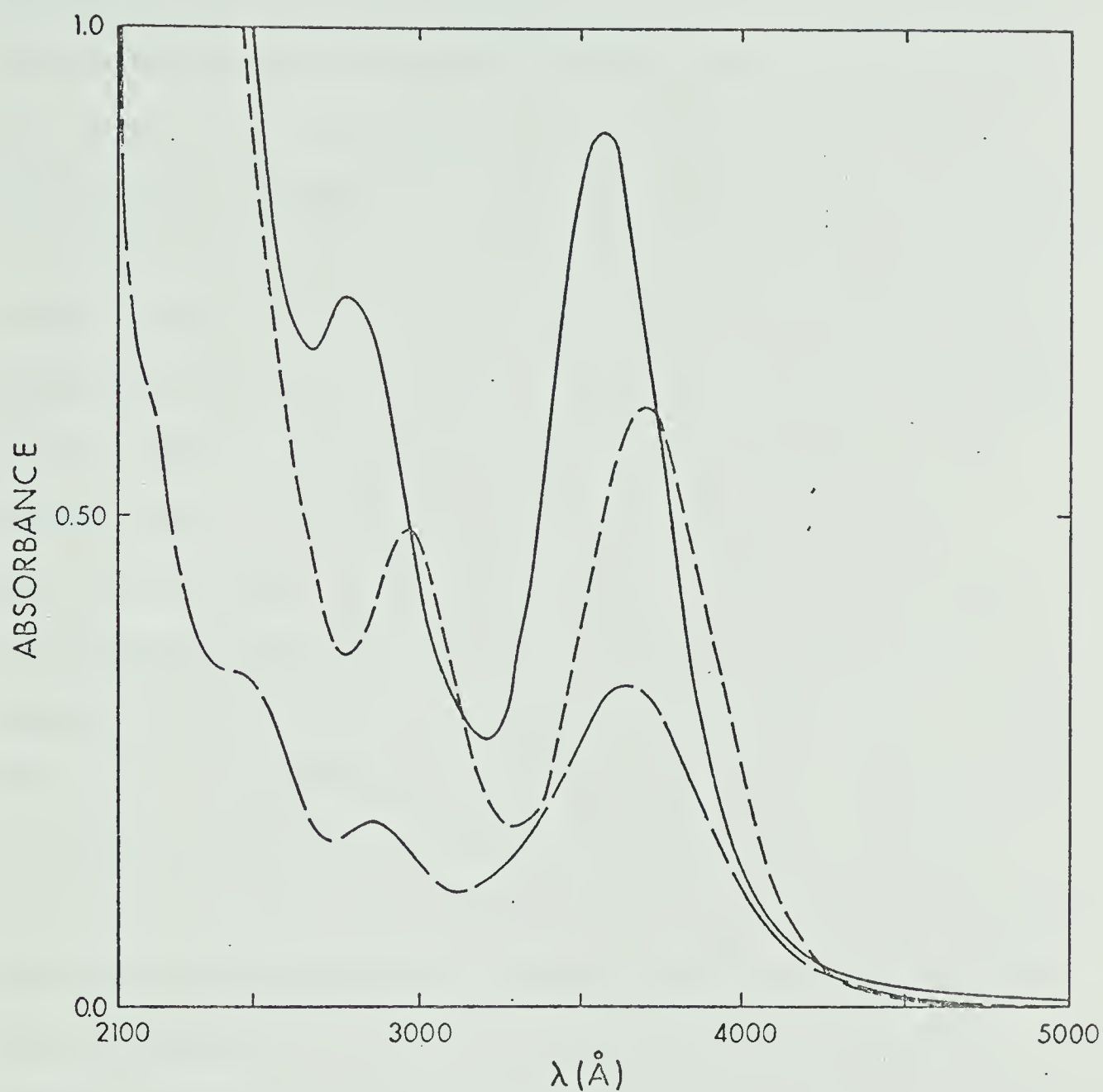


Figure 3.13 - Spectra of triiodo tin compounds. Solvent C_6H_{12} .

Path length - 1 mm vs 1 mm reference cell.

- $I_3SnRe(CO)_5$ - 7.3×10^{-4} M
- - - - I_3SnI - 3.7×10^{-4} M
- $I_3SnMn(CO)_5$ - 4.9×10^{-4} M

molecules containing halogen can be attributed to transitions of electrons localized on the halide portion of the molecule, such that removal to an excited state leaves an essentially neutral halogen atom as part of the excited state configuration. One of the shortcomings of this treatment however is the fact that only the two high wavelength bands were observed and higher energy transitions were not recorded. Kimura and Nagakura examined organic iodides and bromides for transitions in the U.V. and visible range. They indicate that for CHI_3 the four bands observed are $(\text{X})\text{n} - \pi^*(\text{C} - \text{X})$ transitions. They propose that the splittings in the spectrum are a result of I-I interactions of the nonbonding electrons. Although the splitting of approximately 7600 cm^{-1} as reported by Katzin⁴³ for the two low energy bands is present in the I_3SnY compounds examined here, a spectral form that is consistent with that reported for CHI_3 ⁴⁴ with changes only in the wavelength values is also observed. Assignment of the transitions as $\text{n} - \sigma^*$ is more appropriate since it gives a simpler and more complete interpretation of the observed spectra.

Both Katzin and Kimura observed red shifts in the bands as the C atom attached to I changes from primary to secondary to tertiary. In mixed alkyl iodides it is therefore assumed that the greater the withdrawing power of the Y substituent, the lower will be the placement of the nonbonding levels and the higher will be the energy of the $\text{n} - \sigma^*$ transitions. This same trend is apparent in the compounds examined here. The more electronegative

$\text{Re}(\text{CO})_5$ substituent accounts for the blue shifts in the bands in changing from the $\text{Mn}(\text{CO})_5$ and I to the $\text{Re}(\text{CO})_5$ compound. This places the σ withdrawing properties of I between that of the $\text{Re}(\text{CO})_5$ and $\text{Mn}(\text{CO})_5$ groups. This treatment is consistent with the approach taken in comparing the $\text{Cl}_3\text{SnMn}(\text{CO})_5$ and $\text{Cl}_3\text{SnRe}(\text{CO})_5$ compounds in which the greater inductive effect of the $\text{Re}(\text{CO})_5$ accounts in part for the observed blue shifts in going from Mn to Re.

Chapter 4 - Spectra and Reactivities of Bis and Tris Mn and Re Pentacarbonyl Compounds

BACKGROUND

In previous chapters the electronic spectra of C_{4v} pentacarbonyl compounds of Mn and Re were discussed and qualitative energy level diagrams were used to interpret the observed spectra. The present chapter involves a more general discussion of trends in various substituted tris and bis pentacarbonyl compounds.

Tris pentacarbonyl compounds have the general formula $X-M-(M'(CO)_5)_3$ and bis pentacarbonyls are $X_2-M-(M'(CO)_5)_2$ type compounds where X may be CH_3 , n-butyl (Bu), Cl, I, C_6H_5 or $CH_2=CH$; M is generally Sn and M' either Mn or Re. The bonding about M is essentially tetrahedral and each M' is octahedrally co-ordinated. The I.R. spectra of bis and tris pentacarbonyl compounds are complex and proposed interactions of the $M'(CO)_5$ groups within the compound are given to account for deviations from the number of expected bands based on a group theoretical approach²⁶.

The electronic spectra of these compounds may be examined in two ways:

- i) the effect of successive substitution of $M'(CO)_5$ groups for X beginning with the C_{4v} $X_3M-M'(CO)_5$ compounds.
- ii) the effect of changing the ligand X in the individual bis and tris compounds.

In addition, tris compounds undergo reactions in a variety of polar solvents. In MeOH solutions the tris compounds are converted to bis compounds with accompanying isobestic points. The products of some of these reactions in MeOH have been isolated and further examined spectroscopically.

EXPERIMENTAL PROCEDURE

The compounds examined here were obtained in generally pure form from W.A.G. Graham and J.J. Thompson. Purity and identity rechecks of the compounds were carried out using I.R. and mass spectrometry. Compounds were recrystallized, if necessary, from n-hexane. Visible and U.V. spectra were obtained using a Cary 14 spectrometer covering the range 5000-1900 Å. I.R. spectra were obtained using both the P.E. 421 and P.E. 337 with an external recorder and an expanded scale. Spectral grade solvents were used in all cases. Mass spectra were observed using an AEI MS 9 spectrometer, the sample being introduced by direct probe. NMR results were obtained from a Varian HA 100; the low solubilities in CCl_4 of the compounds examined made necessary the use of a CAT multiple scanner.

The compounds were prepared as outlined by Graham et al.²⁶ or by the references noted therein. Products obtained from the reaction of the tris Mn pentacarbonyl compounds in MeOH and MeOH-HCl solutions were isolated by low temperature vacuum distillation of solvent from the product mixture and subsequent dissolution in cyclohexane followed by another low temperature vacuum distillation. Cyclohexane generally dissolved only the desired pentacarbonyl compound product resulting in the elimination of side products of decomposition in the conversions of the tris compound to bis and mono products. $\text{MeCl}_2\text{SnMn}(\text{CO})_5$ and n-butyl- $\text{Cl}_2\text{SnMn}(\text{CO})_5$ were further purified by sublimation at room

temperature and 1 mm. pressure.

RESULTS

Tables 4-I, 4-II, 4-III summarize the U.V. results and Figures 4.01-4.04 show the spectra of the various bis and tris pentacarbonyl compounds.

TABLE 4-I

Summary of Electronic Spectra of Tris Mn Pentacarbonyl Compounds

Compound	C_6H_{12}		MeOH	
	$\lambda_{\text{max.}}$ (\AA)	$\bar{\nu}_{\text{max.}}$ cm^{-1}	ϵ	$\lambda_{\text{max.}}$ (\AA)
Cl-Sn(Mn(CO) ₅) ₃	3930	29,450	22,500	3890
	~3200 (sh.)	~31,250	~6,000	
	2055	48,660	159,000	
CH ₃ -Sn(Mn(CO) ₅) ₃	3775	26,490	22,700	3760
	~3000 (sh.)	~33,300	~13,000	
	~2700 (sh.)	~37,000	~12,000	
	2030	42,260	146,000	
I-Sn(Mn(CO) ₅) ₃	4165	24,020	16,000	3850
	~3500 (sh.)	~28,600	~5,500	
	~3000 (sh.)	~33,300	~9,000	
Bu-Sn(Mn(CO) ₅) ₃	3810	26,250	19,100	3780
	~3100 (sh.)	~32,250	~11,000	
	~2700 (sh.)	~37,000	~7,500	
CH ₂ =CH-Sn(Mn(CO) ₅) ₃	3805	26,280	17,900	3780
	~3000 (sh.)	~33,300	~8,500	
	~2700 (sh.)	~37,000	~8,500	
	2030	42,260	110,000	

TABLE 4-II

Summary of Electronic Spectra of Tris Re Pentacarbonyl Compounds

Compound	C_6H_{12}		MeOH	
	$\lambda_{\text{max.}}$ (Å)	$\bar{\nu}_{\text{max.}}$ cm^{-1}	ϵ	$\lambda_{\text{max.}}$ (Å)
Cl-Sn(Re(CO) ₅) ₃	4070	24,570	5,000	3600
	3635	27,510	19,500	
	~2700 (sh.)	~37,000	~5,000	
	~2400 (sh.)	~41,700	~13,000	
	1900	52,600	200,000	
CH ₂ =CH-Sn(Re(CO) ₅) ₃	4000 (sh.)	25,000	4,800	3600
	3625	27,590	20,100	
	~3100 (sh.)	~32,250	~2,500	
	~2700 (sh.)	~37,000	~6,000	
	~2100 (sh.)	~47,600	~25,000	
Bu-Sn(Re(CO) ₅) ₃	1900	52,600	204,000	3665
	~4050 (sh.)	~24,950	~6,500	
	3685	27,140	18,100	
	~3200 (sh.)	~31,250	~2,000	
	~2700 (sh.)	~37,000	~8,000	
C ₆ H ₅ -Sn(Re(CO) ₅) ₃	~2100 (sh.)	~47,600	~35,000	3650
	1900	52,600	198,000	
	4050 (sh.)	24,950	4,700	
	3680	27,170	16,800	
	~3100 (sh.)	~32,250	~1,500	
CH ₃ -Sn(Re(CO) ₅) ₃	~2700 (sh.)	~37,000	~9,000	3595
	~1900	~52,600	~200,000	
	4000 (sh.)	25,000	4,300	
	3625	27,590	19,300	
	~3100 (sh.)	~32,250	~1,000	
	~2650 (sh.)	~37,700	~5,000	
	~2150 (sh.)	~46,500	~32,000	
	1900	52,600	172,000	

TABLE 4-III

Summary of Electronic Spectra of Bis Mn and Re Pentacarbonyl

Compounds			
Compound ^a	$\lambda_{\text{max.}}$ (Å)	$\bar{\nu}_{\text{max.}}$ cm ⁻¹	ϵ
(C ₆ H ₅) ₂ -Pb(Mn(CO) ₅) ₂	3775	26,490	16,600
	~2650 (sh.)	~37,700	~12,000
	2005	49,875	107,000
Cl ₂ -Sn(Re(CO) ₅) ₂	3320	30,120	22,100
	~2550 (sh.)	~39,200	~4,500
	~2150 (sh.)	~46,500	~21,000
	1900	52,600	80,000
(CH ₃) ₂ -Sn(Re(CO) ₅) ₂	3300	30,300	18,900
	~2650 (sh.)	~37,700	~6,400
	~2100 (sh.)	~47,600	~18,000
	1900	52,600	110,000
Cl ₂ -Sn(Mn(CO) ₅) ₂	3400	29,410	23,500
	2150	46,500	18,000
	1960	51,020	65,000
(CH ₃) ₂ -Sn(Mn(CO) ₅) ₂	3140	31,850	22,500
	~2550 (sh.)	~39,200	~4,000
	1990	50,250	107,000

^a Cyclohexane was used as a solvent in all cases.

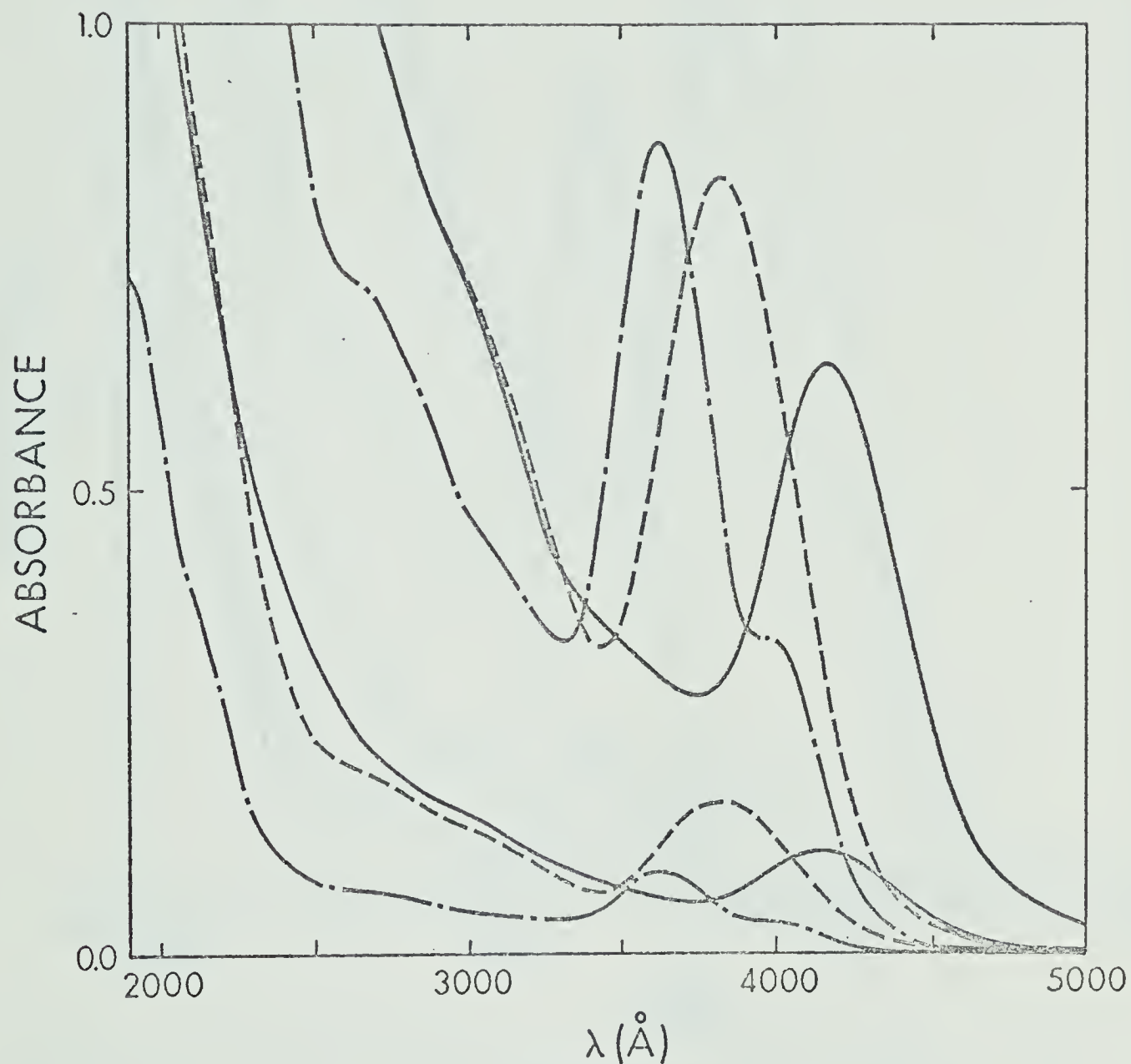


Figure 4.01 - Spectra of tris compounds in C_6H_{12}

- $ISn[Mn(CO)_5]_3$, $4.0 \times 10^{-5}M$, 1 cm and 2 mm path lengths
- $CH_2=CHSn[Mn(CO)_5]_3$, $4.7 \times 10^{-5}M$, 1 cm and 2 mm path lengths
- · - · - $CH_2=CHSn[Re(CO)_5]_3$, $3.7 \times 10^{-5}M$, 1 cm and 1 mm path lengths

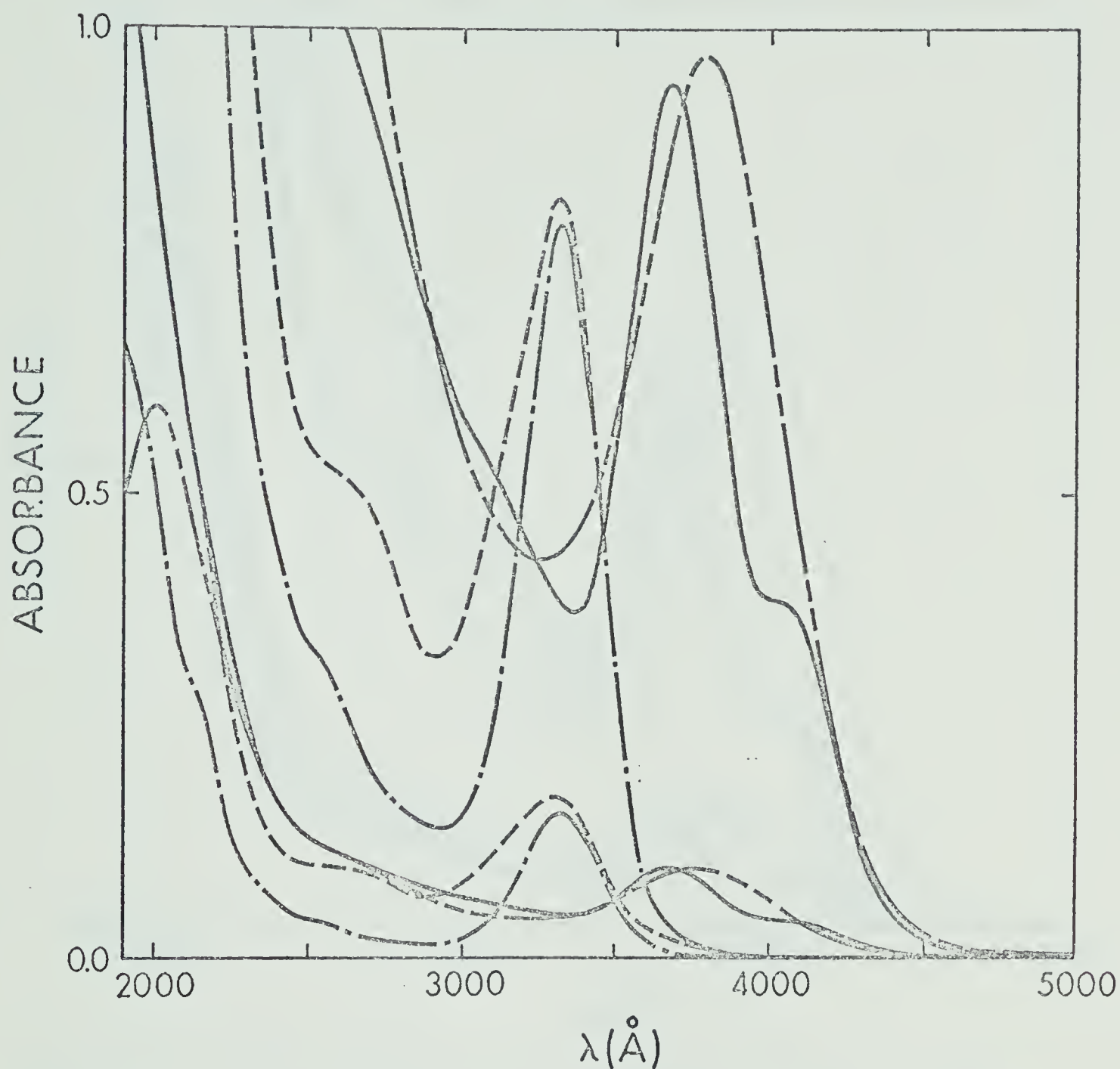


Figure 4.02 - Spectra of bis and tris compounds in C_6H_{12} .

- · — — — $Cl_2Sn[Re(CO)_5]_2$, 4.0×10^{-5} M., 1 cm and 2 mm path lengths
- - - - - $Me_2Sn[Re(CO)_5]_2$, 4.2×10^{-5} M., 1 cm and 2 mm path lengths
- · — — — $Ph_2Pb[Mn(CO)_5]_2$, 5.6×10^{-5} M., 1 cm and 1 mm path lengths
- $PhSn[Re(CO)_5]_3$, 4.9×10^{-5} M., 1 cm and 1 mm path lengths

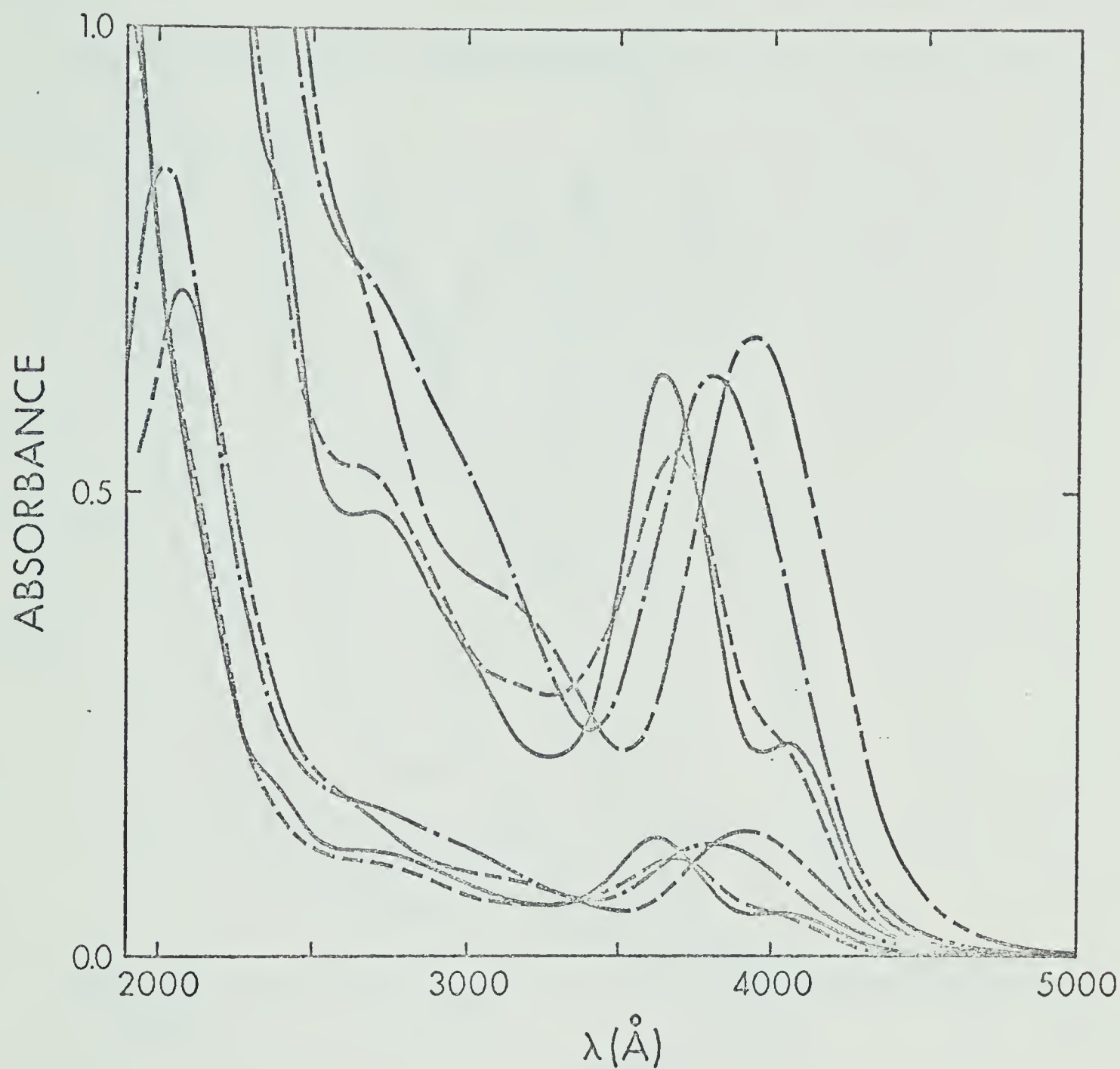


Figure 4.03 - Spectra of bis and tris compounds in C_6H_{12} ; each compound in both 5 mm and 1 mm path lengths.

- $BuSn[Re(CO)_5]_3$, 5.6×10^{-5} M.
- $ClSn[Re(CO)_5]_3$, 3.7×10^{-5} M.
- - - - - $ClSn[Mn(CO)_5]_3$, 5.7×10^{-5} M.
- · — · — $BuSn[Mn(CO)_5]_3$, 6.6×10^{-5} M.

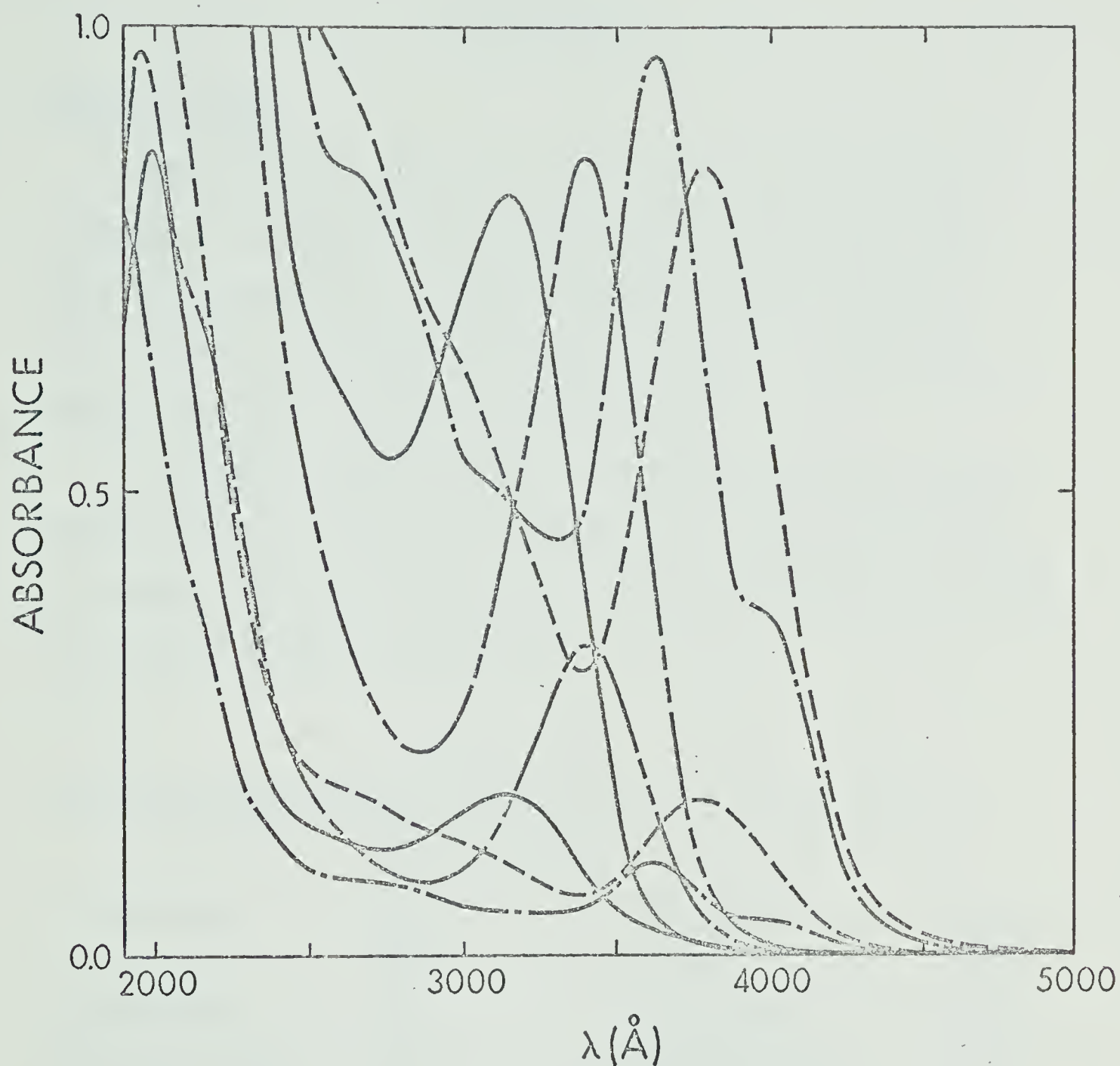


Figure 4.04 - Spectra of bis and tris compounds in C_6H_{12} .

- · — — — — — $MeSn[Re(CO)_5]_3$, 4.7×10^{-5} M., 1 cm and 1 mm path lengths
- - - - - $MeSn[Mn(CO)_5]_3$, 7.5×10^{-5} M., 5 mm and 1 mm path lengths
- - - - - $Cl_2Sn[Mn(CO)_5]_2$, 7.2×10^{-5} M., 5 mm and 2 mm path lengths
- $Me_2Sn[Mn(CO)_5]_2$, 3.7×10^{-5} M., 1 cm and 2 mm path lengths

DISCUSSION

Spectral Trends

The transitions observed in the tris and bis pentacarbonyl compounds are expected to be charge transfer transitions from filled $M' d_{\pi}$ orbitals to π^* (CO) antibonding orbitals similar to those in the C_{4v} compounds previously examined. Some of the observed spectral trends are examined below.

As $M'(CO)_5$ groups are successively added to the Sn atom in the progression from the mono to the bis and tris pentacarbonyl compounds, the lowest energy charge transfer band shifts markedly to the red as shown in Table 4-IV.

TABLE 4-IV

Low Energy Band Maxima Comparison for Mono, Bis and Tris

Pentacarbonyls			
Compound	$\lambda_{\text{max.}}$ (Å)	Compound	$\lambda_{\text{max.}}$ (Å)
$\text{Cl}_3\text{SnMn}(\text{CO})_5$	2655	$\text{Cl}_3\text{SnRe}(\text{CO})_5$	2480
$\text{Cl}_2\text{Sn}(\text{Mn}(\text{CO})_5)_2$	3385	$\text{Cl}_2\text{Sn}(\text{Re}(\text{CO})_5)_2$	3320
$\text{ClSn}(\text{Mn}(\text{CO})_5)_3$	3930	$\text{ClSn}(\text{Re}(\text{CO})_5)_3$	3630
$\text{Me}_3\text{SnMn}(\text{CO})_5$	$\sim 2500^a$	$\text{Me}_3\text{SnRe}(\text{CO})_5$	$\left. \begin{array}{l} 2480 \\ 2580 \end{array} \right\}$
$\text{Me}_2\text{Sn}(\text{Mn}(\text{CO})_5)_2$	3130	$\text{Me}_2\text{Sn}(\text{Re}(\text{CO})_5)_2$	3300
$\text{MeSn}(\text{Mn}(\text{CO})_5)_3$	3780	$\text{MeSn}(\text{Re}(\text{CO})_5)_3$	3620

^a estimated value

These large red shifts may be accounted for by the σ and π effects of X and $M'(CO)_5$ and by the intramolecular $M'(CO)_5$ group interactions. In both the series of compounds $Cl_{4-n}Sn(Mn(CO)_5)_n$ and $Me_{4-n}Sn(Mn(CO)_5)_n$ these red shifts appear with increasing n despite the variations in σ and π abilities of the X ligands. For this reason it is suggested that the shifts are a result of intramolecular $M'(CO)_5$ group interactions, i.e. interactions of filled d orbitals of similar symmetry on each of the Mn atoms. This should result in an elevation of the highest occupied orbitals and a lowering of the remaining filled orbitals on the metal. An approach of this type is analagous to a case where L-L repulsions become important in a molecule of T_d symmetry such as SnI_4 . $M'(CO)_5$ group interactions have also been used to explain the observed I.R. spectra of the bis and tris pentacarbonyl compounds.²⁶

The changes which occur in the λ_{max} . values as Mn is replaced by Re in the bis and tris compounds are shown in Tables 4-I, 4-II and 4-III. The blue shifts in the high intensity, lowest energy C.T. band in going from Mn to Re may be a general reflection of the σ properties of Re as illustrated in most Class 1 and Class 2 compounds. The exceptions to this trend appear in the mono and bis methyl rhenium pentacarbonyl compounds.

The ligands attached to Sn appear to have little effect on the position of the C.T. bands in the bis and tris series of Re pentacarbonyl compounds. In the analagous Mn compounds however some general trends are observed for the ligands attached to the Sn.

Table 4-I shows that the λ max. values for the low energy band in tris and bis carbonyl compounds of Mn follow a trend that was also evident for Class 3 compounds. Halide ligands such as Cl and I red shift the band from that of the strong σ donors such as Me and n-butyl. It appears that the filled p orbitals on the halides are responsible for the changes in the spectra by inducing a charge on Sn thereby reducing the ability of Sn to accept charge from the $M'(CO)_5$ groups. These filled halide p orbitals could also have $p_{\pi} - d_{\pi}$ interactions with the filled d orbitals on the Mn atom which should also result in a higher placement of the Mn d levels.

Reactivity of Tris Pentacarbonyl Compounds

It has been observed that a variety of polar solvents decompose or react with the tris compounds examined here. Of the compounds belonging to the mono, bis and tris groups, the tris compounds are generally the least stable in solution. The behaviour of these compounds was examined in a number of solvents to determine the effect of solvents on the low energy band and to check for possible reactions. A number of fleeting isobestic points and conversion of the high λ band to a lower λ are suggested but it appears that decomposition of the product compound is rapid enough to prevent the observation of an isobestic point for more than a period of 30 minutes. Appendix I summarizes the reactivities of a number of pentacarbonyl compounds in a variety of solvents.

n-Bu-Sn($Mn(CO)_5$)₃ serves as a sample compound for discussion of behaviour in a number of solvents and solvent mixtures. In

C_6H_{12} the compound proved extremely susceptible to photo-decomposition but was stable in the dark. Dimethyl formamide decomposed the compound rapidly while in pyridine the high λ band slowly shifted to the blue with accompanying decomposition. CH_3CN and 95% EtOH converted the high λ band to lower λ shoulders with simultaneous decomposition; in tetrahydrofuran and dioxane the compound appeared to decompose slowly. Reactions of the tris compounds in MeOH and MeOH-conc. HCl however offer the most interesting and fruitful approach to the examination of the reactivities of these compounds. All tris compounds examined here reacted when dissolved in MeOH with the conversion of the λ band to a lower λ one. The presence of isobestic points in each case indicated that a chemical equilibrium existed between the tris compound and its product and that the product compound was stable for at least the period of spectroscopic examination. For some compounds the complete conversion takes place in 30 mins. $ISn(Mn(CO)_5)_3$ whereas others such as $CH_2=CHSn(Mn(CO)_5)_3$ and $ClSn(Mn(CO)_5)_3$ may take a few hours. Over a longer period of time (2 days) both bands disappear completely as the conversion product decomposes. Tris compounds show the same sensitivity to photolytic decomposition in polar solvents that were shown in C_6H_{12} and care must therefore be taken to prevent undue exposure to light if isobestic points are to be observed. The relative stability of the products formed from the reactions in MeOH allows isolation and spectroscopic examination of many of these products. It was not possible

to identify positively all the products but the spectroscopic results outlined in the next section indicate the nature of these products.

The spectroscopic behaviour of tris Mn pentacarbonyl compounds in MeOH and MeOH-HCl is dependent on the nature of X in $\text{XSn}(\text{Mn}(\text{CO})_5)_3$. The discussion of this behaviour is divided into two categories: one in which L is an alkyl group (Me, Bu, $\text{CH}_2=\text{CH}$) and one in which X is a halogen atom (Cl, I).

1) X is an alkyl group

The positions of the λ max. for the methanol reaction products for all the compounds examined are in the region of the spectrum corresponding to the bis compounds which have already been examined ($\text{Me}_2\text{Sn}(\text{Mn}(\text{CO})_5)_2$, $\text{Cl}_2\text{Sn}(\text{Mn}(\text{CO})_5)_2$). The band position for mono, bis and tris Sn-Mn pentacarbonyl compounds is so specific for each that it may be used as a means of judging the type of MeOH conversion product. The position of these bands for the reaction products in MeOH of the alkyl tris Mn compounds varies from 3230 \AA to 3290 \AA and indicates that the product is a bis compound. Other spectroscopic evidence to be presented in the following section clearly shows that bis compounds are products of tris compound reactions in MeOH-HCl. Figures 4.05 and 4.06 show the U.V. study of the tris to bis conversion with the accompanying isobestic points for two representative compounds, $\text{MeSn}(\text{Mn}(\text{CO})_5)_3$ and $\text{BuSn}(\text{Mn}(\text{CO})_5)_3$. Table 4-V gives the λ max. values for the low energy parent and conversion product bands and the isobestic points for the available tris Mn pentacarbonyl compounds.

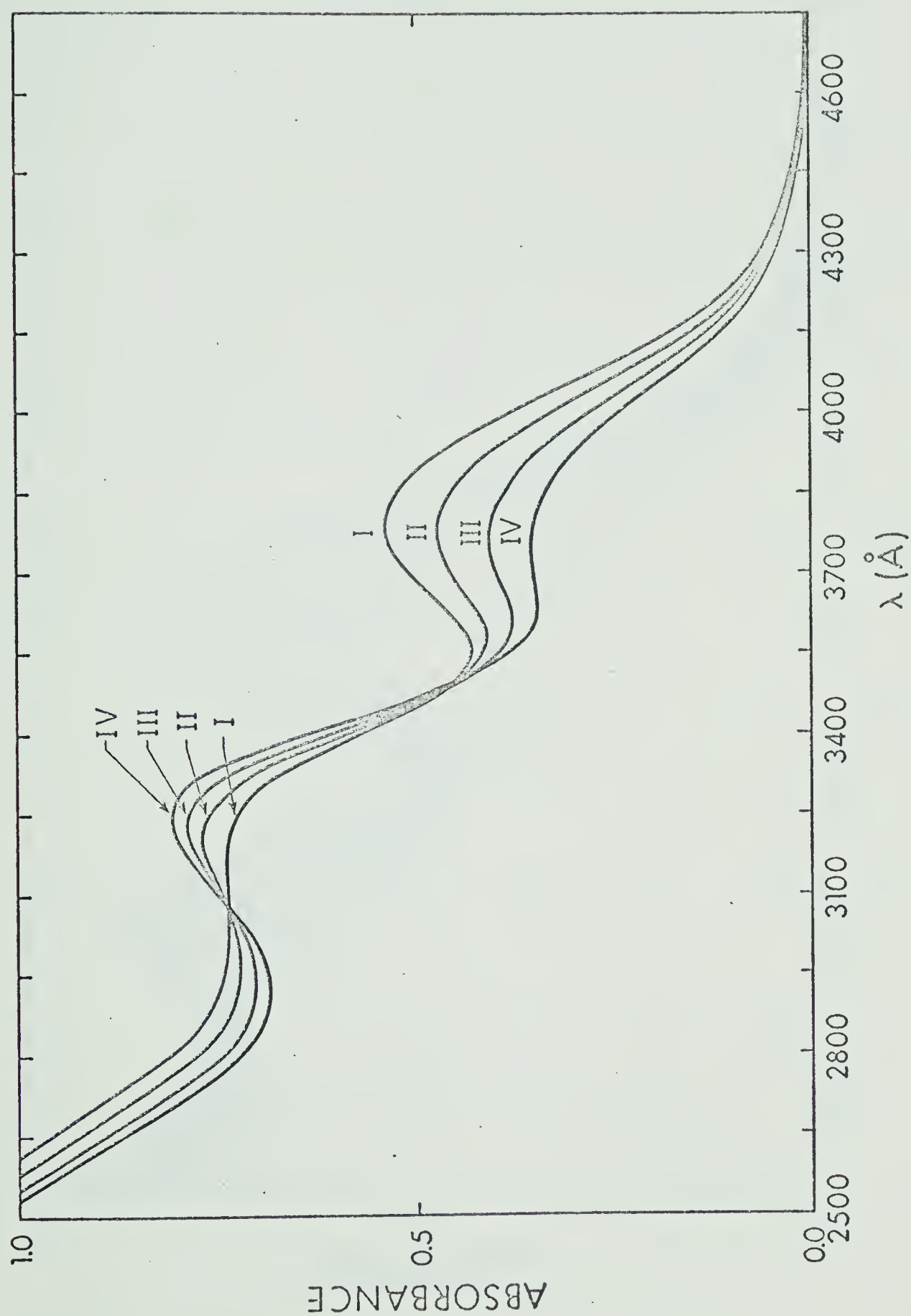


Figure 4.05 - Isobestic point data for $\text{CH}_2=\text{CHSn}[\text{Mn}(\text{CO})_5]_3$ in MeOH. Spectral Curves

I, II, III and IV are taken at 15 minute intervals.

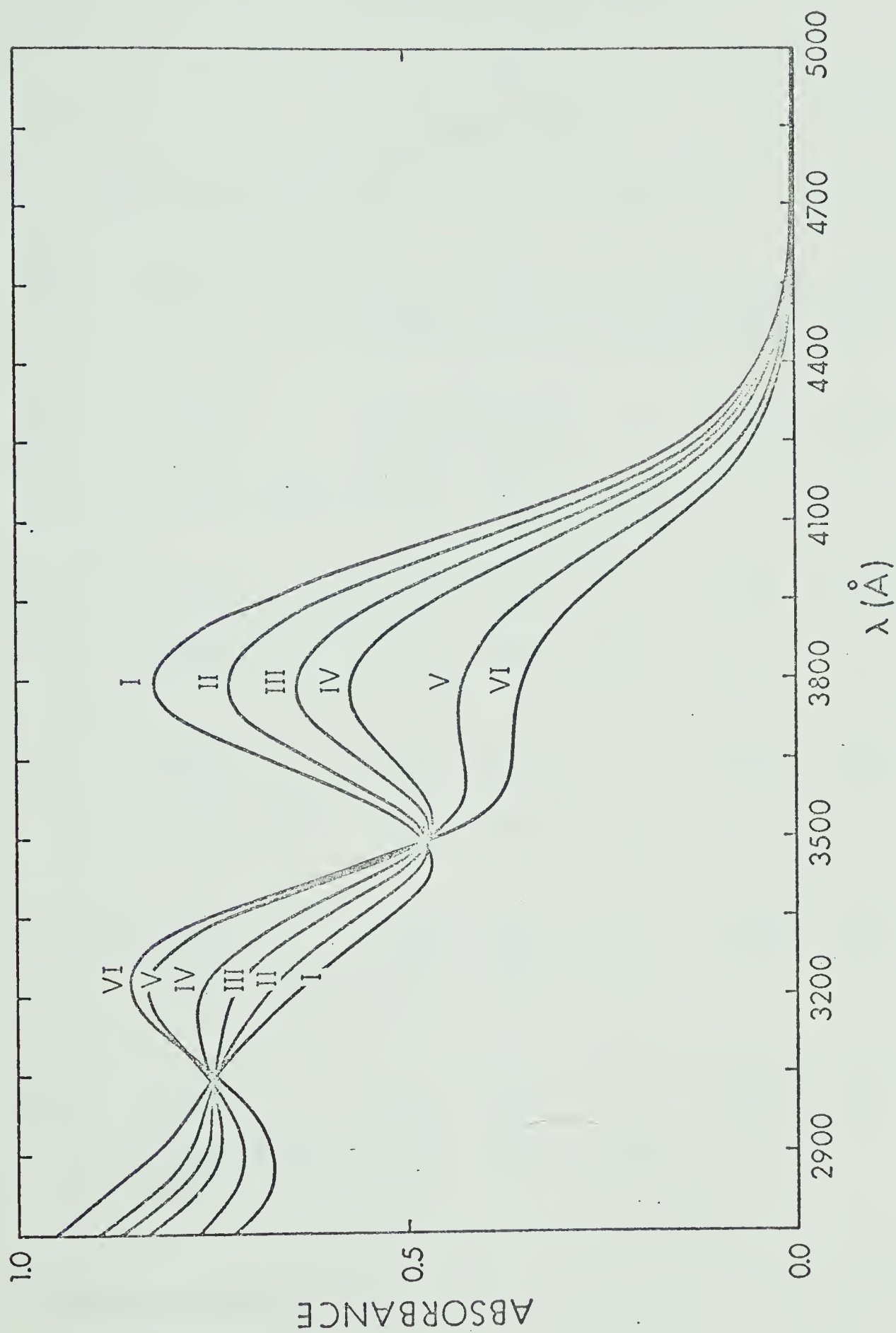


Figure 4.06 - Isobestic point data for $\text{BuSn}[\text{Mn}(\text{CO})_5]_3$ in MeOH. Curves I through VI represent spectra taken successively at 15 minute intervals.

TABLE 4-V

Isobestic Point Data for Tris Mn Pentacarbonyl Compounds

X^a	Solvent	Parent $\lambda_{\max.}$	Product $\lambda_{\max.1}$	Product $\lambda_{\max.2}$	Isobest. Point 1	Isobest. Point 2	Isobest. Point 3
Bu	MeOH	3780 Å	3250 Å	-	3500 Å	3050 Å	-
	MeOH-1% HCl	3780	3280	2645 Å	-	-	2803 Å
Cl	MeOH	3875	3290	-	3560	3060	-
	MeOH-1% HCl	3875	3375	-	-	-	-
I	MeOH	3880	3285	-	3560	3050	-
	MeOH-1% HCl	3880	3350	-	-	-	-
$\text{CH}_2=\text{CH}$	MeOH	3780	3245	-	3075	3075	-
	MeOH-1% HCl	3780	3275	-	-	-	-
Me	MeOH	3760	3230	-	3510	3015	-
	MeOH-1% HCl	3760	3260	2625	-	-	2740

^a in $\text{XSn}(\text{Mn}(\text{CO})_5)_3$

If a small amount of HCl (1%) is added to a tris Mn pentacarbonyl in MeOH solution there is a rapid conversion of the high λ band to the lower λ band. Figures 4.07 and 4.08 show the U.V. spectral results for these compounds. For the tris methyl and butyl compounds this conversion is rapid and leaves no trace of the parent tris compound spectrally upon the addition of the HCl. An isobestic point can be observed however in the further conversion of the bis compound to the final mono pentacarbonyl product. The final products of the reactions of the butyl and methyl tris tin Mn pentacarbonyl compounds in MeOH-HCl were isolated and further examined spectroscopically. Table 4-VI summarizes the I.R. results for these products. Spectra observed for these compounds prepared in this manner compare with those reported previously and synthesized in the standard way.⁴⁵ The I.R. spectra indicate that the final products of the above reactions are the mono pentacarbonyl compounds $n\text{-BuCl}_2\text{SnMn(CO)}_5$ and $\text{MeCl}_2\text{SnMn(CO)}_5$. Figure 4.09 shows the I.R. spectra for the separated product of the tris vinyl Sn-Mn pentacarbonyl reaction in pure MeOH.

The chloro substituted products that were examined above in the I.R. were also investigated mass spectrally. These results are summarized in Table 4-VII. The peaks observed for these compounds can be attributed to the parent pentacarbonyl product compound and the possible fragmentation products. Two weak peaks (possible impurity) appear at mass numbers 429 and $429 + 57$ (Bu) for $n\text{-BuCl}_2\text{SnMn(CO)}_5$ and cannot be assigned. The apparent impurity

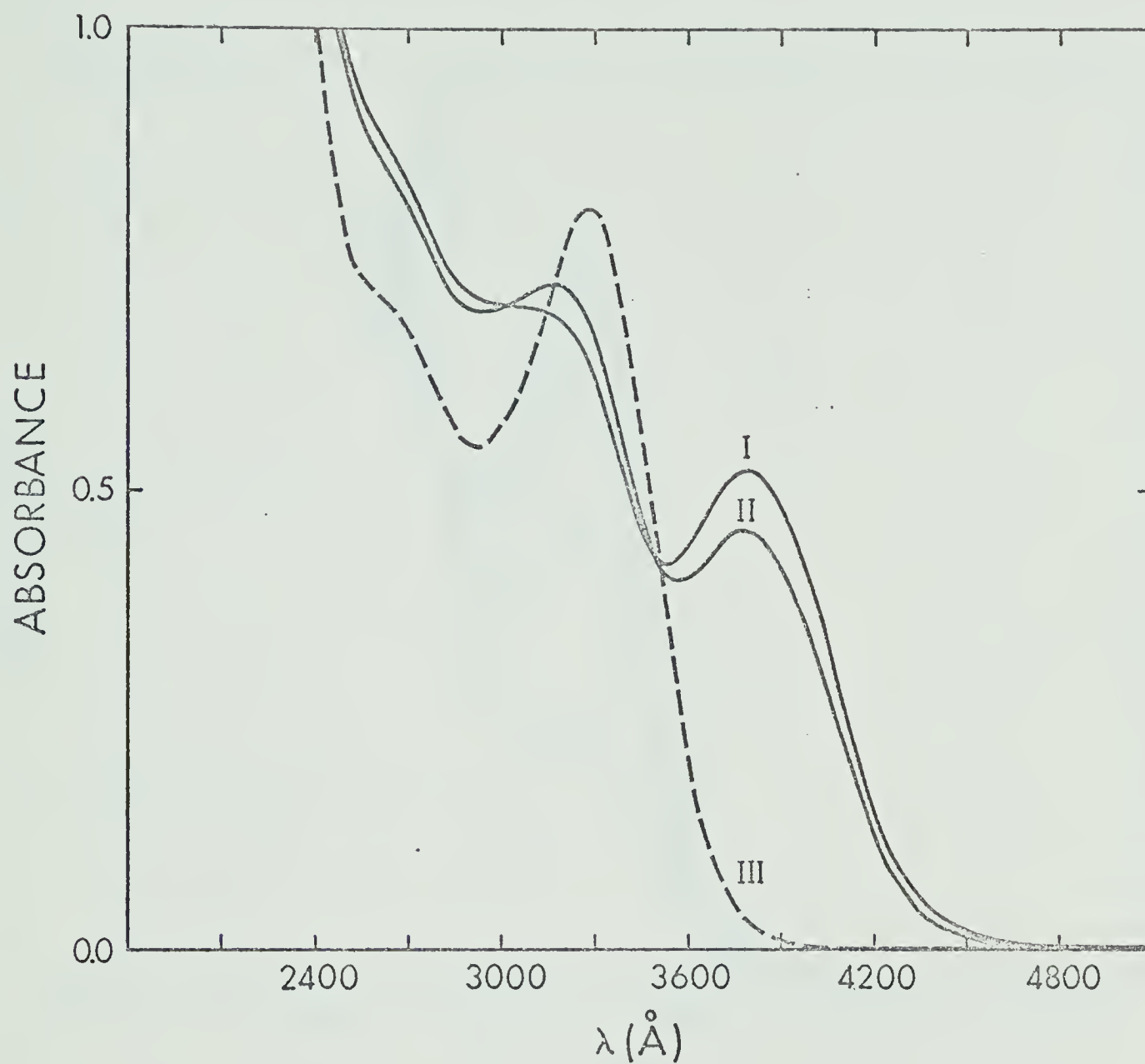


Figure 4.07 - Spectra of $\text{BuSn}[\text{Mn}(\text{CO})_5]_3$ in MeOH and in MeOH-1% HCl

Curve I - MeOH solution spectra

Curve II - MeOH solution spectra taken 10 minutes after
Curve I.

Curve III - MeOH-1% HCl spectra taken 5 minutes after
Curve II.

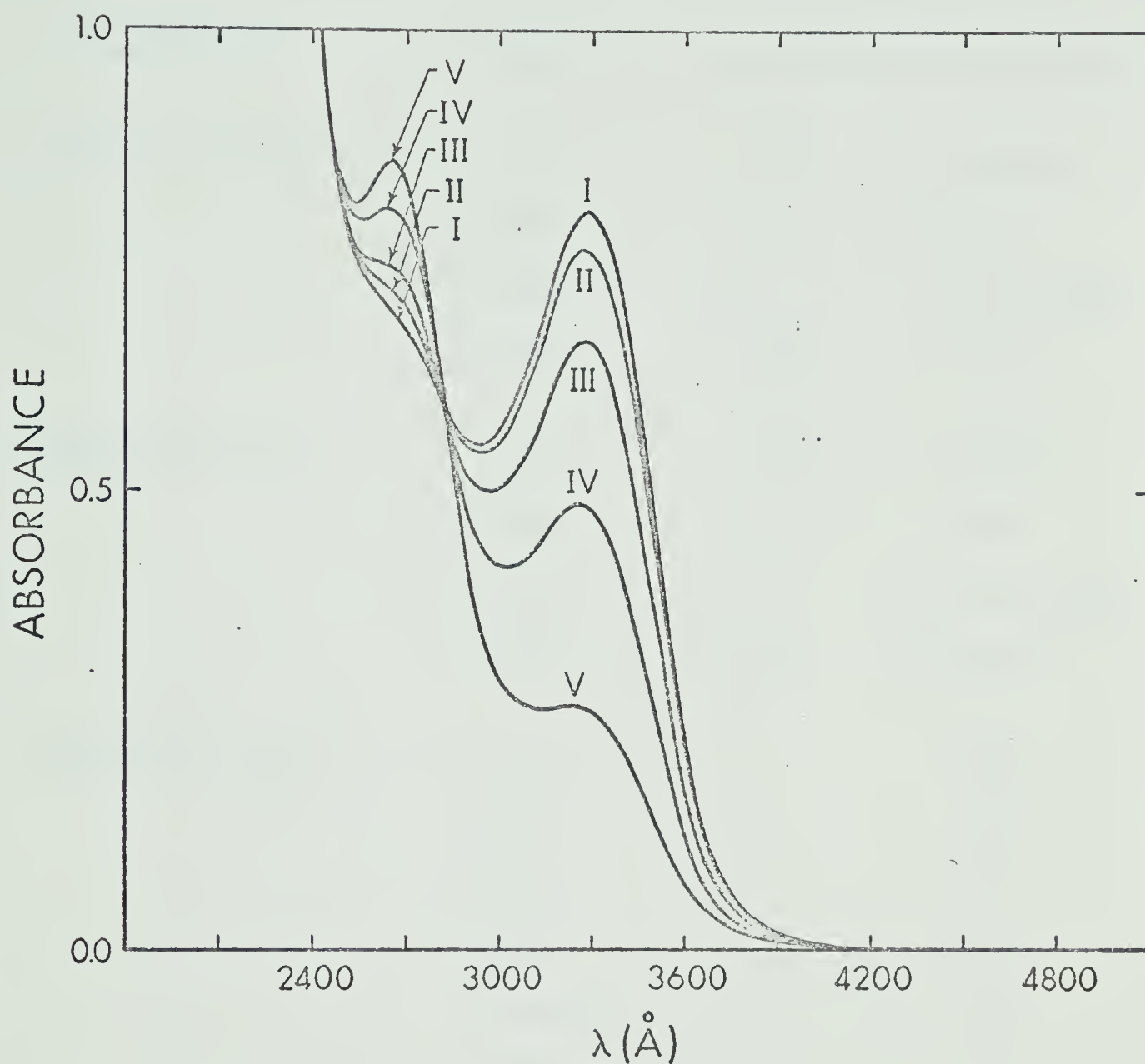


Figure 4.08 - Isobestic point data for $\text{BuSn}[\text{Mn}(\text{CO})_5]_3$ in MeOH - 1% HCl.

Curve I represents a spectrum taken 5 minutes after 1% HCl added to the MeOH solution.

Curve II, III, IV and V represent spectra taken at 10, 25, 50 and 90 minutes after Curve I.

TABLE 4-VI

Summary of I.R. Spectra of Reaction Products in MeOH-HCl

Compound ^a	$\bar{\nu}$ (cm ⁻¹)	Assignment	Relative Int.
BuCl ₂ SnMn(CO) ₅ ^b	2113	A ₁ ⁽²⁾	medium
	2057	B ₁	weak
	2030	E	very strong
	2017	A ₁ ⁽¹⁾	strong
MeCl ₂ SnMn(CO) ₅ ^c	2115	A ₁ ⁽²⁾	medium
	2058	B ₁	weak
	2031	E	very strong
	2019	A ₁ ⁽¹⁾	strong
Cl ₂ Sn(Mn(CO) ₅) ₂ ^d	2119		0.4
	2095		5.9
	2055		2.0
	2030		10.0
	2024 (sh)		4.0
	2000		3.9
	2011		1.9

^a All spectra taken in cyclohexane solution, 0.5 mm cells and concentration 1 mg/ml.

^b Assignments are consistent with those put forward for C_{4v} penta-carbonyls as proposed by Cotton and Kraihanzel and adopted by Graham et al.

^c Spectra compares with that reported in Reference 45.

^d Spectrum compares with that reported by Graham and Thompson in Reference 26.

Figure 4.09 - Spectra of the product from the reaction of



- | | |
|-----------|---|
| — | Curve I - CCl_4 spectra of fresh solution |
| - - - - - | Curve II - CCl_4 spectra of solution left 4 hrs. in dark |
| — - - — - | Curve III - CCl_4 spectra of solution left 8 hrs. in dark |
| - - — - - | Curve IV - C_6H_{12} spectra which shows no change after 8 hrs. |

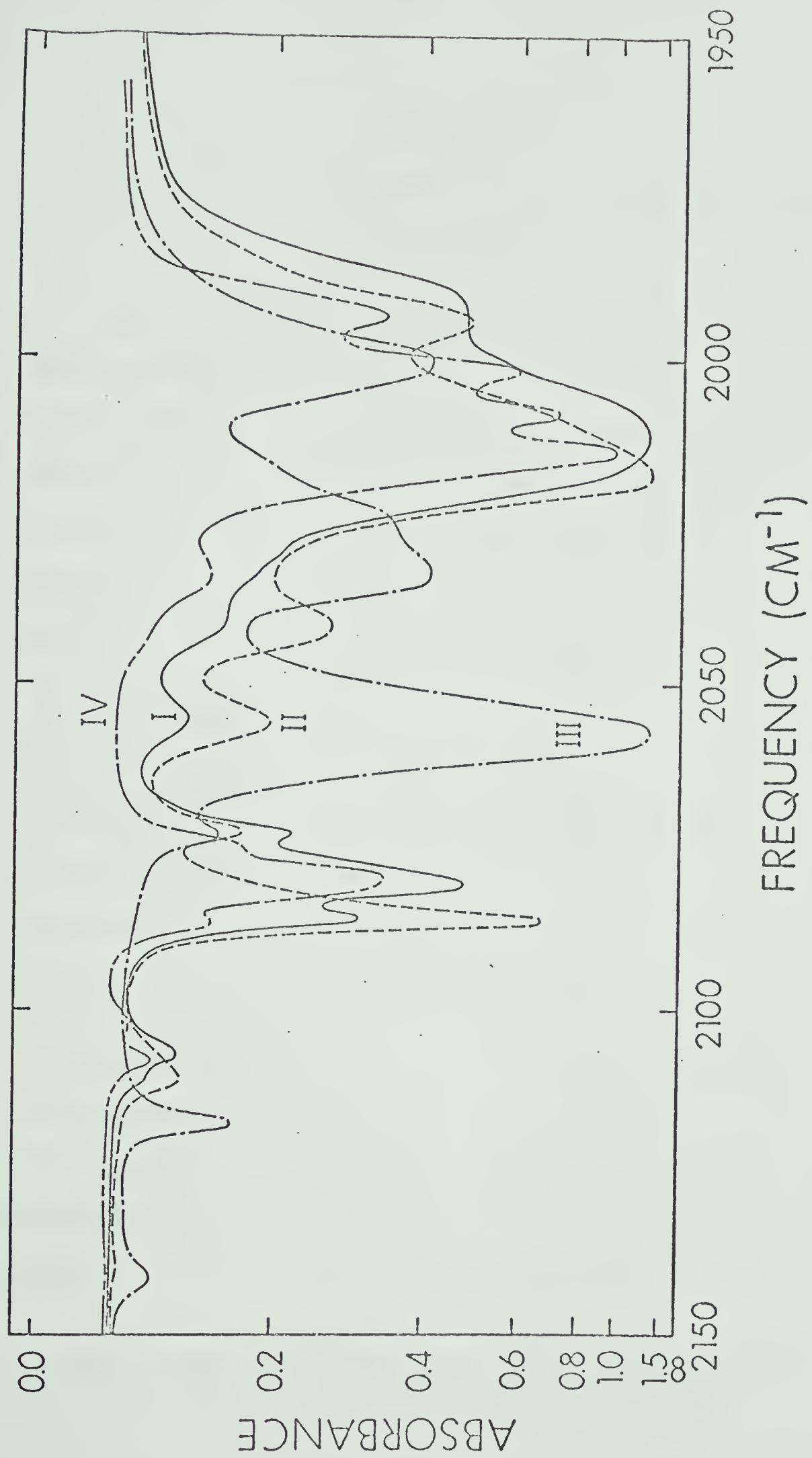


TABLE 4-VII

Mass Spectral Data for $\text{Cl}_2\text{Sn}(\text{Mn}(\text{CO})_5)_2$, $\text{BuCl}_2\text{SnMn}(\text{CO})_5$ and
 $\text{MeCl}_2\text{SnMn}(\text{CO})_5$

	x^a										
	0	1	2	3	4	5	6	7	8	9	10
$\text{Cl}_2\text{Sn}(\text{Mn}(\text{CO})_5)_2^b$											
$\text{Cl}_2\text{SnMn}_2(\text{CO})_x^+$	vs	w ^c	w	-	-	m	vw	-	-	-	s
$\text{ClSnMn}_2(\text{CO})_x^+$	m	-	-	vw	w	w	vw	vw	-	-	m
$\text{Cl}_2\text{SnMn}(\text{CO})_x^+$	w	w	w ^c	w ^c	m	vs					
$\text{SnMn}(\text{CO})_x^+$	vs	w	m	vs	vs	vs					
$\text{Mn}(\text{CO})_x^+$	vs	-	m	w	w	m					
$\text{BuCl}_2\text{SnMn}(\text{CO})_5^d$											
$\text{BuCl}_2\text{SnMn}(\text{CO})_x^+$	-	vw ^c	-	-	-	s					
$\text{Cl}_2\text{SnMn}(\text{CO})_x^+$	s	m	m ^c	s	vs	vs					
$\text{BuClSnMn}(\text{CO})_x^+$	w	-	-	-	w	m					
$\text{ClSnMn}(\text{CO})_x^+$	s	vw	-	-	vw	w					
$\text{Mn}(\text{CO})_x^+$	vs	vs	m	m	m	s					
$\text{MeCl}_2\text{SnMn}(\text{CO})_5^e$											
$\text{MeCl}_2\text{SnMn}(\text{CO})_x^+$	m	w	-	-	-	w					
$\text{Cl}_2\text{SnMn}(\text{CO})_x^+$	m	w	w	m	m	s					
$\text{MeClSnMn}(\text{CO})_x^+$	w	vw	vw	-	-	w					
$\text{Mn}(\text{CO})_x^+$	vs	s	m	m	w	m					

^a Entries in table are approximate relative peak intensities:
vw = very weak, w = weak, m = medium, s = strong,
vs = very strong and dash indicates absence of peak.

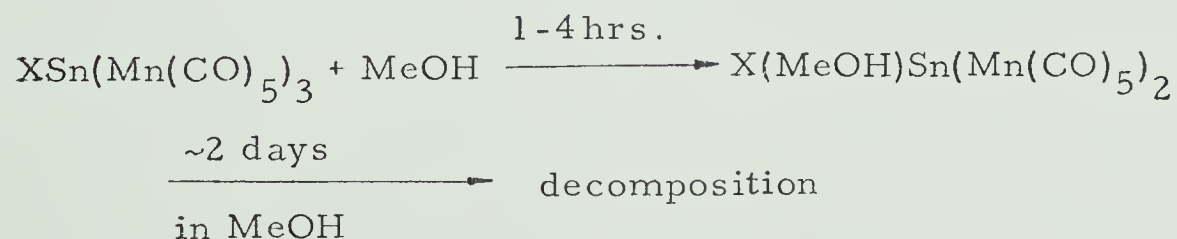
- b Other fragments observed are ClSnMn^+ , Mn_2^+ , ClSn^+ , Mn^+ , Sn^+ , ClMn^+ , CO^+ , H_2O^+ , mass #149(?).
- c Assignments are not certain due to overlap with fragments of other series.
- d Other fragments observed are BuClSn^+ , BuClSn^+ , ClSnHMn^+ , BuSn^+ , ClSn^+ , HSn^+ , ClSn^+ , SnMn^+ , mass #'s 429 and $429 + 57(\text{Bu})$ are weak unassigned peaks. Bu fragments are present also.
- e Other fragments observed are SnMn^+ , ClSnMn^+ , MeSn^+ , ClSn^+ , Sn^+ , ClMn^+ , HMnCO^+ , MeMn^+ , HMn^+ , CO^+ , H_2O^+ .

does not appear in the I.R. even at increased concentrations and for this reason it is assumed that it is not a carbonyl compound.

The NMR spectra of the parent tris $\text{BuSnMn}_3(\text{CO})_{15}$ shows the familiar CH_3 triplet at 9.1τ and the CH_2 triplet at 8.1τ with a low intensity multiplet between. The product of the MeOH-HCl reaction with this tris compound gives an NMR spectrum that shows the two triplets of the butyl substituent at the same τ values indicating that the butyl ligand remains as part of the reaction product.

NMR spectra were also taken in CCl_4 solution for the tris vinyl Sn Mn pentacarbonyl compound and its suspected bis reaction product obtained in MeOH . Table 4-VIII gives the τ values for the protons in these two compounds. The two peaks which appear at 6.20 and 7.05τ for the product compound in an intensity ratio of 1:3 suggest that MeOH is involved as a ligand in the product compound. The vinyl proton pattern also indicates that $\text{CH}_2=\text{CH}$ remains as a ligand in the product compound.

The reactions of tris Sn Mn pentacarbonyl compounds in MeOH and MeOH-HCl suggested by the spectroscopic evidence presented above are as follows:

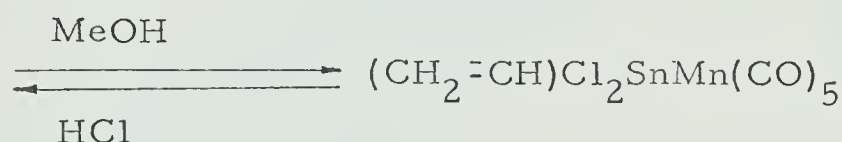
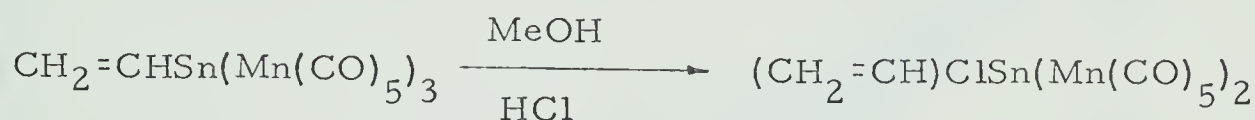
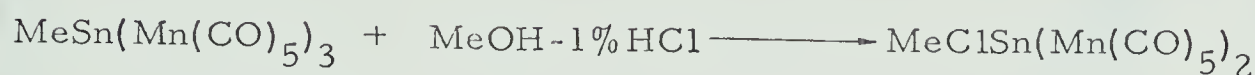
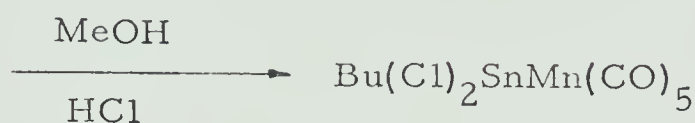
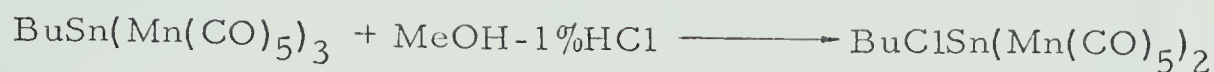


where X = methyl, butyl, vinyl

TABLE 4-VIII

Summary of NMR spectra of Tris Vinyl Compound and the Reaction
Product in MeOH

Compound	=C-H quadruplet τ Values	CH ₂ cis Proton τ Values	CH ₂ trans Proton τ Values	Other τ Values
CH ₂ =CHSn(Mn(CO) ₅) ₃	2.47	3.60	4.04	
	2.60	3.73	4.23	
	2.67			
	2.80			
Reaction product in MeOH	2.47	3.67	4.10	6.20
	2.61	3.80	4.30	7.05
	2.82			
	2.98			



2) X is a halogen atom

Table 4-V outlines the λ max. values and isobestic points for the products of the MeOH and MeOH-HCl reactions. Figures 4.10 and 4.11 show the MeOH isobestic points of the tris compounds of Cl and I. The positions of the bands in the U.V. again suggest that the products are bis pentacarbonyl compounds. The compound $\text{Cl}_2\text{Sn}(\text{Mn}(\text{CO})_5)_2$ was available in pure form prepared in a standard manner and the λ max. values for this compound were identical to those λ max. values for the product of the $\text{ClSn}(\text{Mn}(\text{CO})_5)_3$ reaction in MeOH-HCl. The product of the reaction of the tris Cl compound in pure MeOH shows a different low energy λ max. (3295 \AA) but one that is closely related to the value of the bis Cl-Sn-Mn pentacarbonyl compound. A quantity of the tris Cl compound was dissolved in MeOH and allowed to stand until the band at 3295 \AA

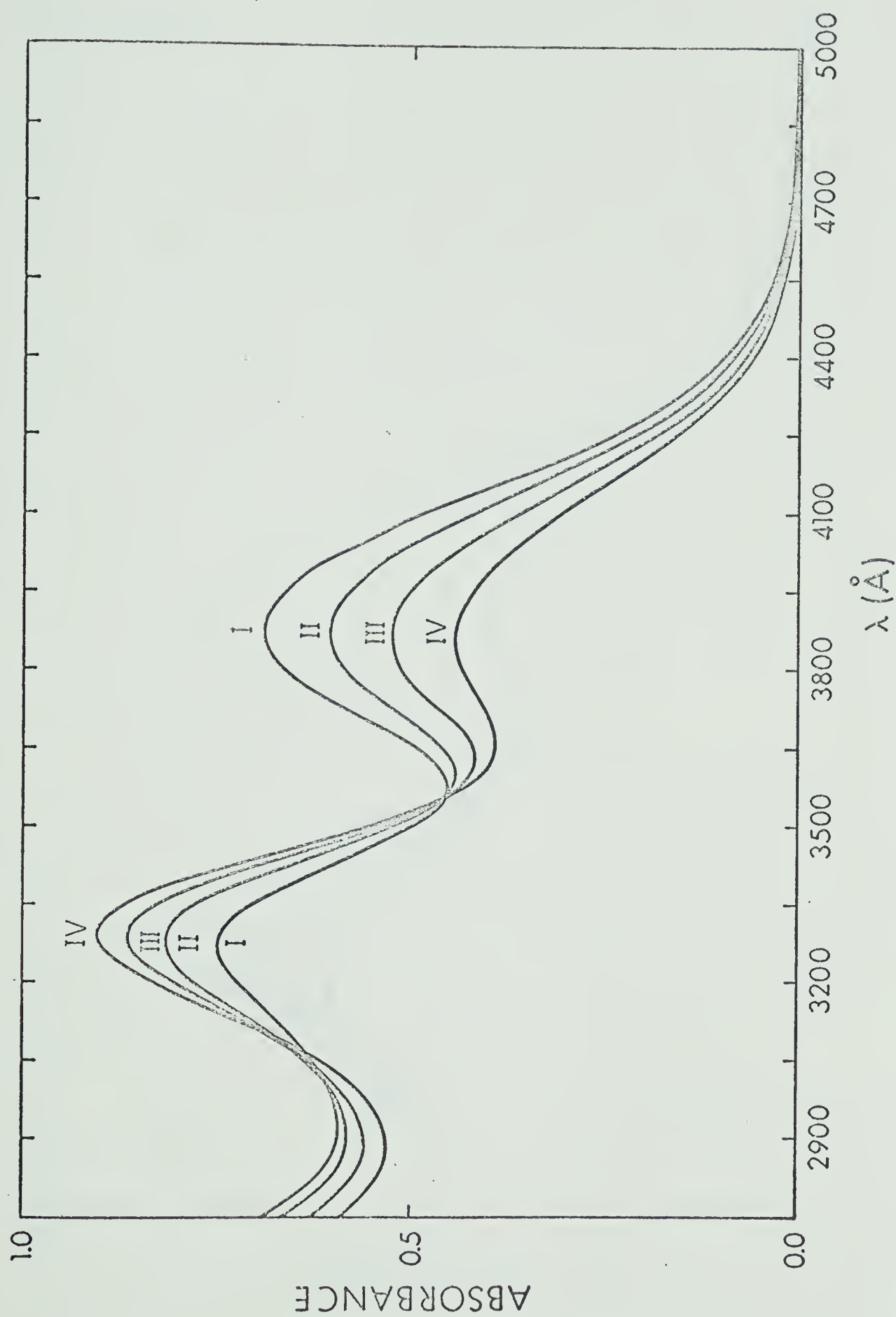


Figure 4.10 - Isobestic point data for $\text{ClSn}[\text{Mn}(\text{CO})_5]_3$ in MeOH. Curves I through IV represent spectra taken successively at 15 minute intervals.

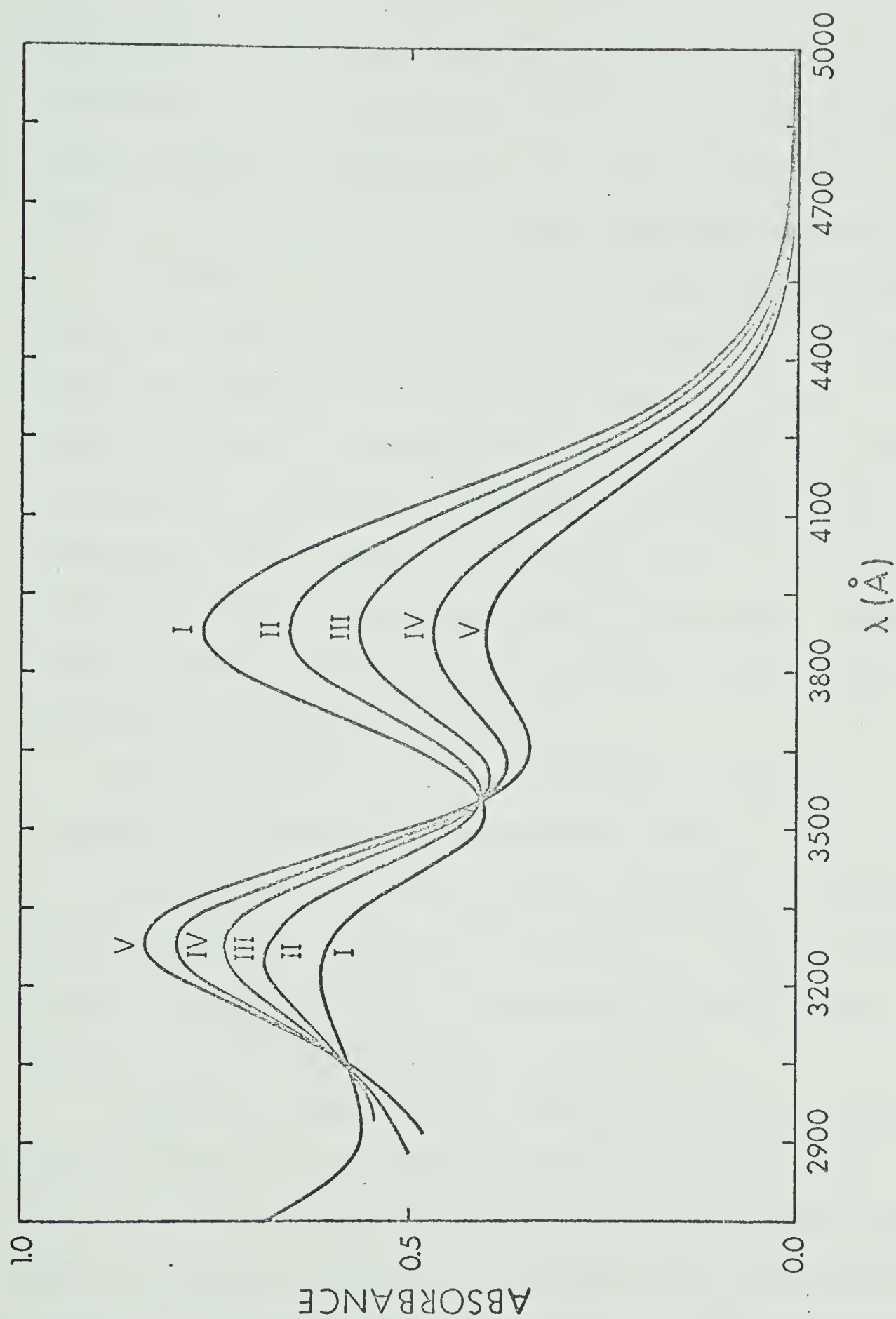


Figure 4.11 - Isobestic point data for $\text{ISn}[\text{Mn}(\text{CO})_5]_3$ in MeOH. Curves I through V represent spectra taken successively at 10 minute intervals.

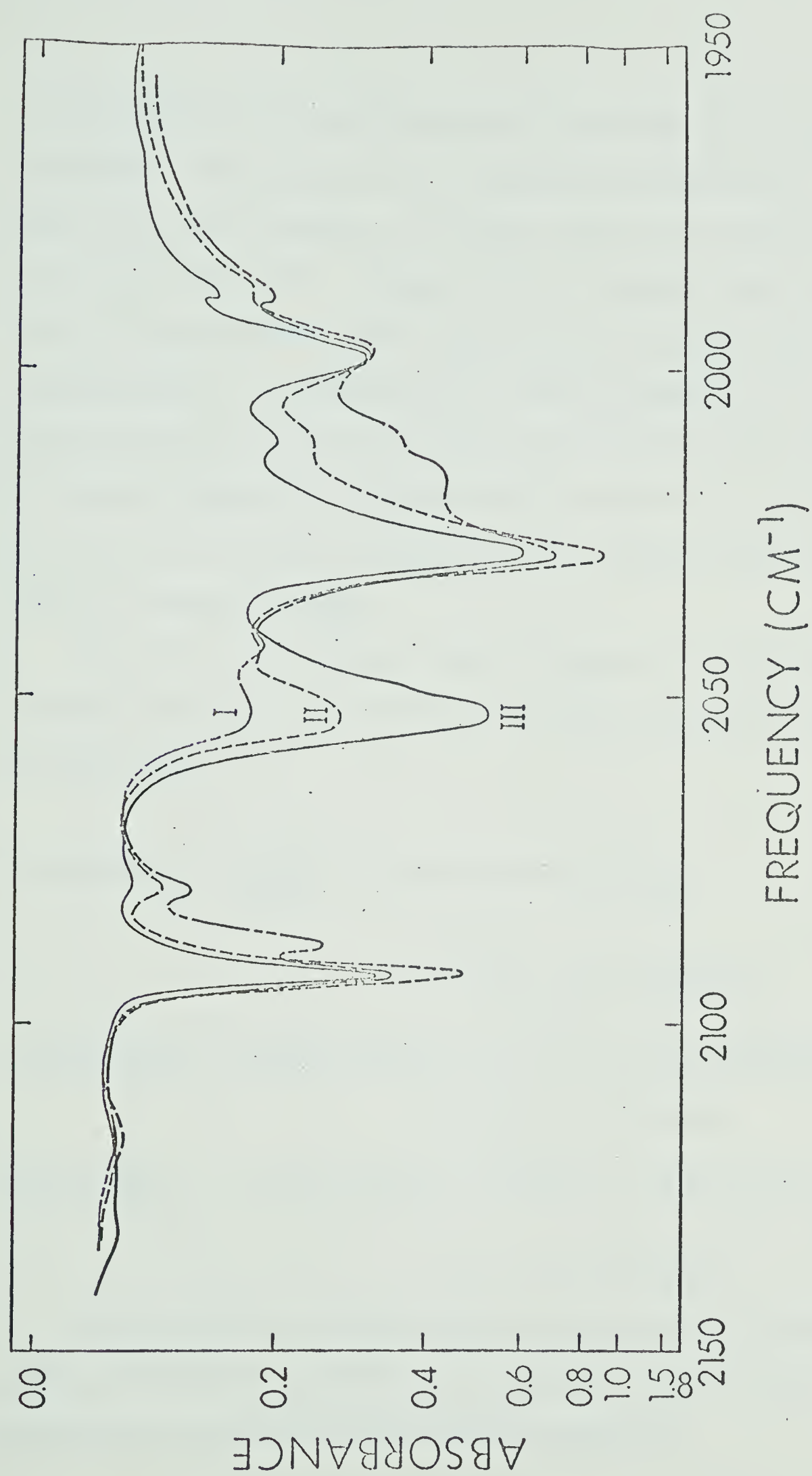
developed. At this point 1% HCl was added to the solution causing an immediate shift of this band to $3375 \text{ }^{\circ}\text{A}$. This is the $\lambda \text{ max}$. for the authentic $\text{Cl}_2\text{Sn}(\text{Mn}(\text{CO})_5)_2$ compound in MeOH. The position does not change when 1% HCl is added to the MeOH solution.

Ligands such as Cl, I, σ withdrawing ligands, attached to the Sn in the tris compounds, prevent the formation of the mono product and stop the reaction at the bis stage. The rate of change of the tris to the bis compound in the HCl spiked solutions differs markedly for the Me and Bu compounds as compared to the Cl and I compounds. This may be related to the σ and π properties of L and the type of charge that L may induce at the Sn site. Changes which are observed above occur also in isopropanol and 1% HCl solution and lead to identical products.

The I.R. spectrum of the product of the reaction of $\text{ClSn}(\text{Mn}(\text{CO})_5)_3$ in MeOH-HCl is reported in Table 4-VI and has a 1:1 correspondence with the spectrum reported for the authentic $\text{Cl}_2\text{Sn}(\text{Mn}(\text{CO})_5)_2$ by Graham and Thompson.²⁶ Mass spectral results as shown in Table 4-VII add further evidence that the product of this reaction is $\text{Cl}_2\text{Sn}(\text{Mn}(\text{CO})_5)_2$.

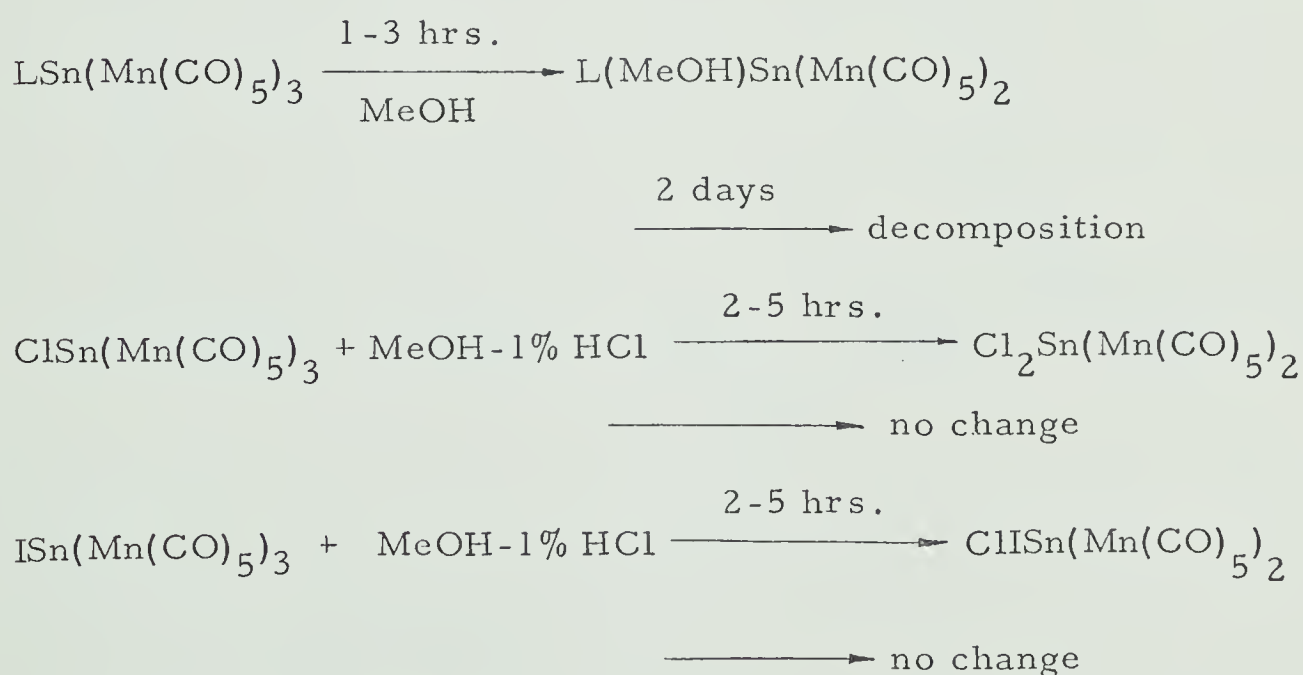
Figure 4.12 shows the I.R. spectra for the product of the reaction of the tris Cl compound in MeOH only. The mass spectrum of the suspected bis compound formed from the reaction of tris Cl Mn pentacarbonyl compound yields little information since the compound is involatile and decomposes on heating to 80°C . The spectrum does show however very large intensity peaks at

Figure 4.12 - Spectra in CCl_4 of the product from the reaction of $\text{ClSn} [\text{Mn}(\text{CO})_5]_3$ and MeOH . Spectra II and III indicate changes which take place after solution remains in dark for 4 and 8 hrs. respectively.



mass numbers 32, 31 and 18 which are characteristic methanol fragments. The products of tris compound reactions with MeOH + HCl were prepared in the same manner and showed only a very weak water peak. Despite the low volatility of the compound, very weak fragmentation peaks appear at mass numbers 405 ($\text{ClSnMn}_2(\text{CO})_5^+$), 315 ($\text{SnMn}(\text{CO})_5^+$) and 287 ($\text{SnMn}(\text{CO})_4^+$). For these reasons it is suspected that the bis compound product from the reaction of the tris compound in pure methanol is a methanolated one, possibly $\text{Cl}(\text{MeOH})\text{Sn}(\text{Mn}(\text{CO})_5)_2$ or a compound held together weakly by methanol bridges.

The above spectroscopic evidence suggests that the following reactions take place for the tris Cl and iodine compounds in MeOH and MeOH-HCl:



With the addition of HCl to the tris compounds the product yields are essentially quantitative and provide a means for the preparation of mixed bis pentacarbonyl compounds.

Usually tris Re compounds require a large amount of time (~ 3 weeks) to undergo a noticeable conversion to a bis type of product in a MeOH solution. With the addition of a few %HCl to the methanol solution it is possible to observe a partial conversion of the lower energy tris band to a band which is probably attributable to a bis product observed in analagous Mn compounds. Figures 4.13 and 4.14 show spectra of MeOH solutions of tris compounds of Re and MeOH solutions with HCl added.

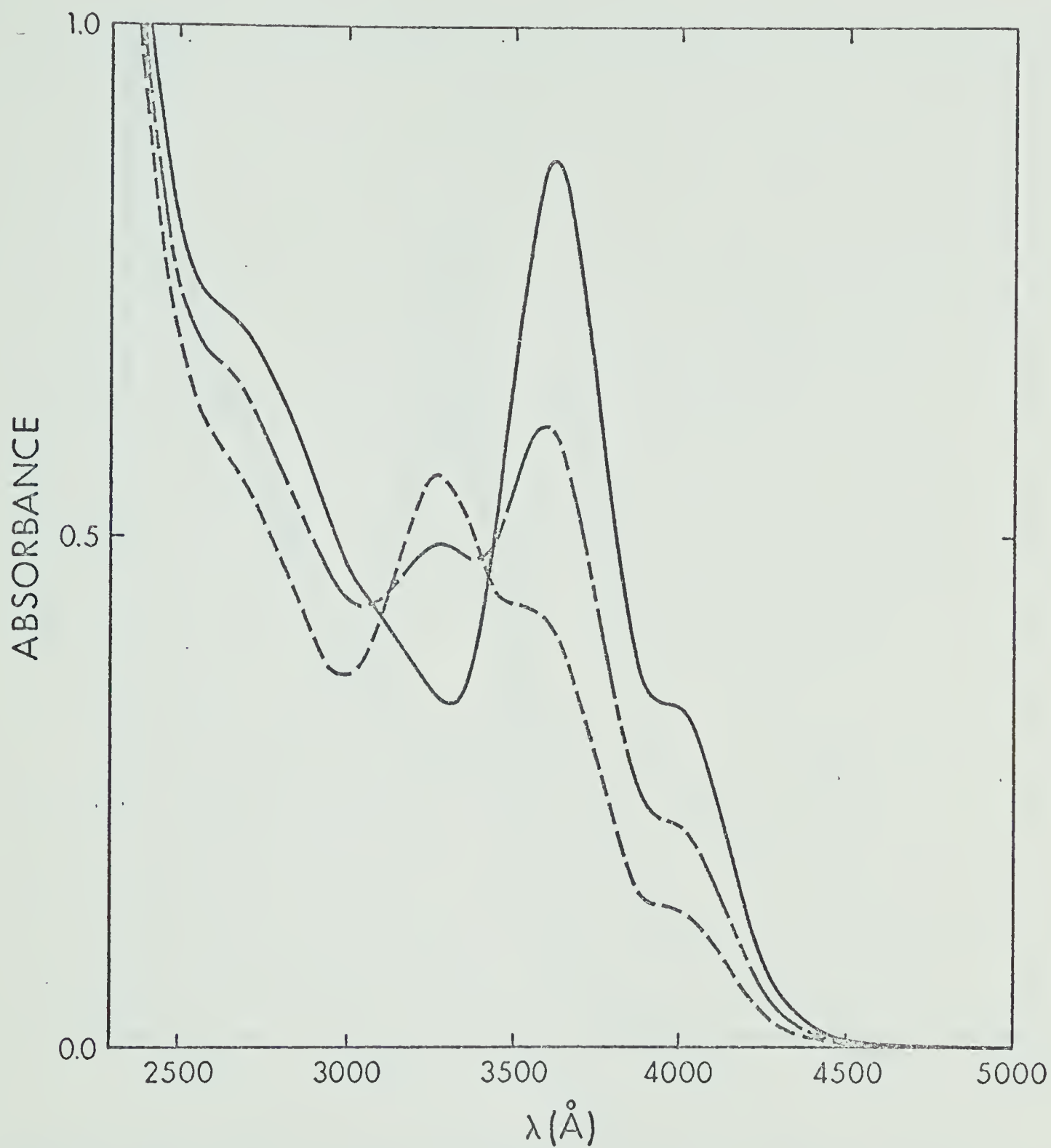


Figure 4.13 - Spectra of $\text{CH}_2=\text{CHSn}[\text{Re}(\text{CO})_5]_3$ in MeOH.

- fresh solution
-- solution 2 weeks in dark
- - - solution 4 weeks in dark

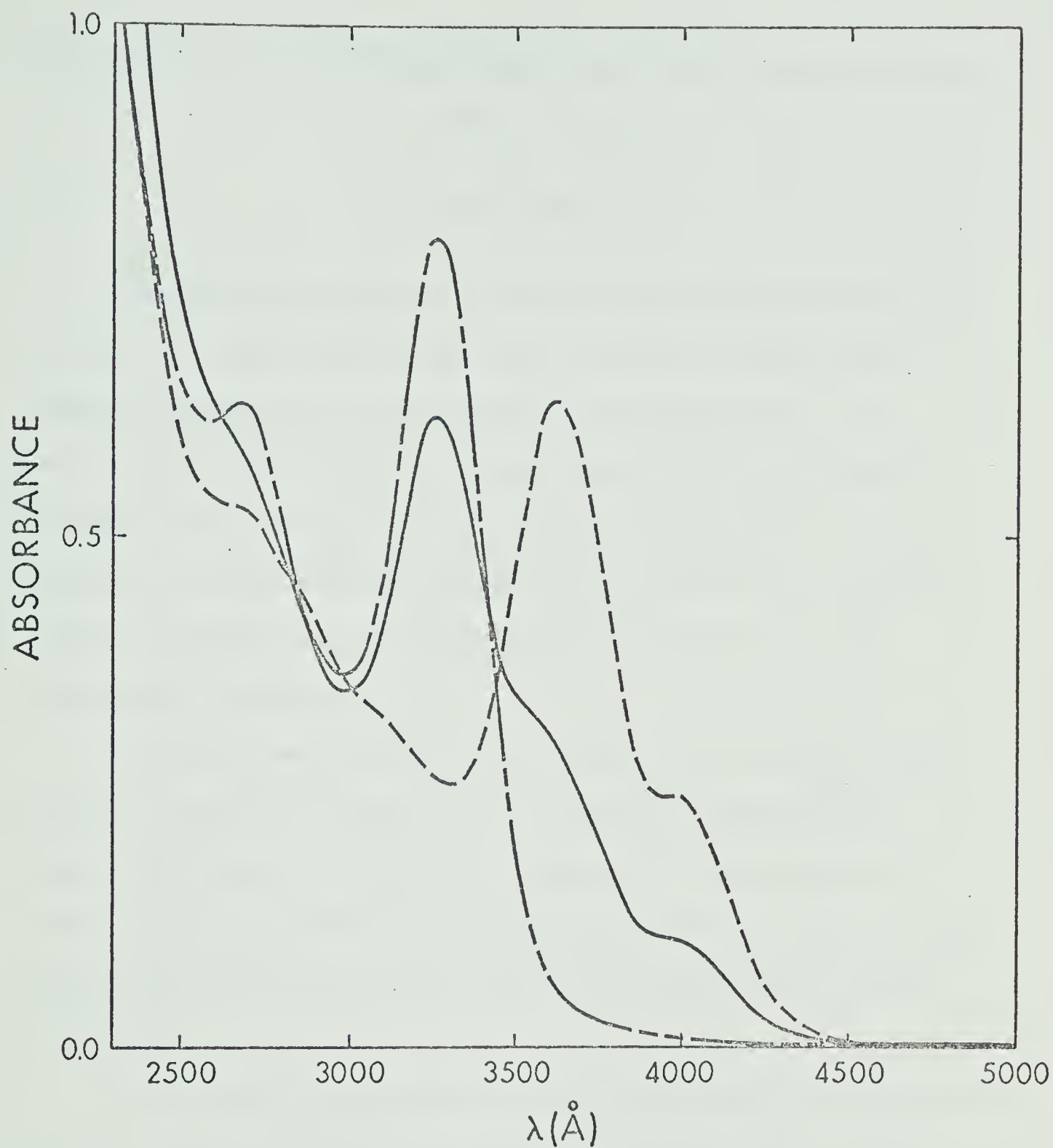


Figure 4.14 - Spectra of $\text{CH}_2=\text{CHSn}[\text{Re}(\text{CO})_5]_3$ in $\text{MeOH} - 1\% \text{HCl}$.

- - - - - fresh solution
- solution 1 week in dark
- · - · - solution 2 weeks in dark

Chapter 5 - Spectra and Reactivities of the Tetracarbonyl Dimers of Cl, Br and I.

BACKGROUND

During the investigation of the Mn pentacarbonyl halides of Cl and Br, it was observed that these compounds underwent spectral changes over a period of time in cyclohexane. In non-polar solvents the tetracarbonyl dimers of Mn are formed from the corresponding Br and Cl pentacarbonyl halides. Small quantities of these reaction products were isolated and examined spectroscopically, spectra were compared with those of the pentacarbonyl halides.

The structure of the tetracarbonyl dimers has been shown from I.R. data and analysis to be D_{2h} but the molecules bear close resemblance to $L_2M(CO)_4$ compounds as investigated by Cotton and Kraihanzel¹² and for simplicity may be treated as C_{2v} compounds to facilitate comparisons with related pentacarbonyl compounds.

In this chapter a qualitative energy level diagram is proposed and the electronic bands are assigned. The p_π levels of the halide are placed below those of the filled d_π levels of Mn. This placement takes into account photoelectron spectral data²⁰, calculated energy levels for the pentacarbonyl halides²¹ and the changes in bonding expected to take place in changing from the monomer to the dimer.

The I.R. and U.V. spectra of the tetracarbonyl dimers were examined in C_6H_{12} , in CCl_4 and in CCl_4 with small quantities of MeOH added. The changes in the I.R. spectra suggest the formation of methanolated $X-Mn(CO)_4$ compounds. The U.V. comparisons with the pentacarbonyl halides in MeOH suggest that the same product is formed whether the pentacarbonyl halides or the tetracarbonyl dimers of Mn are dissolved in MeOH.

EXPERIMENTAL PROCEDURE

The Mn tetracarbonyl dimers of Br and Cl examined here were obtained from the conversion of their respective pentacarbonyl halide in C_6H_{12} . When a saturated solution of the pentacarbonyl halide was allowed to stand in the dark for a period of two weeks red needle like crystals were formed from the pentacarbonyl bromide and orange crystals from the chloride. Small quantities of these were recovered. Although the amount of compound isolated was insufficient for chemical analysis, the I.R. spectra of C_6H_{12} solutions of the products agreed closely (Table 5-II) with those reported by Kaesz for the tetracarbonyl dimers.²⁹ No extraneous CO bands corresponding to carbonyl impurities were observed. A small quantity of the iodine tetracarbonyl dimer was isolated during the preparation of $IMn(CO)_5$ by reaction of $NaMn(CO)_5$ and I_2 in THF solution.

Visible and U.V. spectra were obtained using a Cary 14 spectrometer covering the range 5500-1900 $\overset{\circ}{A}$. I.R. spectra were obtained using the Perkin-Elmer 337 spectrometer with an external recorder and an expanded scale. Spectral grade solvents were used in all cases.

RESULTS

Figure 5.01 gives the electronic spectra for $\text{Cl}_2\text{Mn}_2(\text{CO})_8$, $\text{Br}_2\text{Mn}_2(\text{CO})_8$ and $\text{I}_2\text{Mn}_2(\text{CO})_8$. Table 5-I summarizes the λ max. values in the U.V. and visible regions for the tetracarbonyl dimers in C_6H_{12} and MeOH and includes the λ max. values for the Br pentacarbonyl halide in MeOH after a period of 12 hours. Table 5-II compares the I.R. spectra of the tetracarbonyl dimers isolated here with those reported in the literature.²⁹

Figure 5.01 - Spectra of the tetracarbonyl dimers of Cl, Br and I in C_6H_{12}

—————	$Cl_2Mn_2(CO)_8$, 1×10^{-4} M, 3 cm and 2 mm path lengths
- - - - -	$Br_2Mn_2(CO)_8$, 2×10^{-4} M, 2 cm and 1 mm path lengths
-----	$I_2Mn_2(CO)_8$, 3×10^{-4} M, 1 cm, 5 mm and 1 mm path lengths

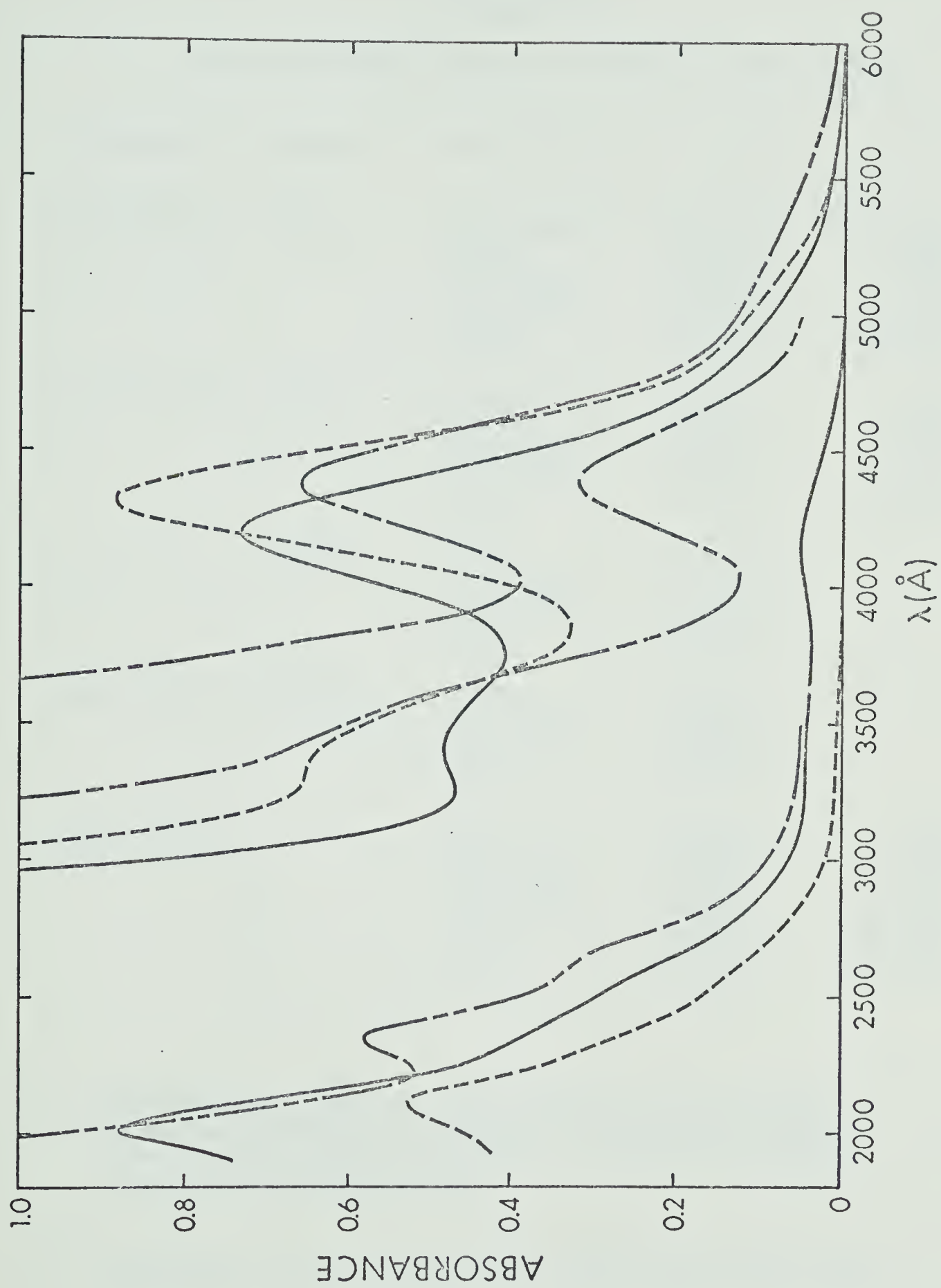


TABLE 5-I

Summary of U.V. Spectra of Tetracarbonyl Dimers

Compound	Solvent	$\lambda_{\text{max.}} (\text{\AA})$	$\nu_{\text{cm}^{-1}}$	ϵ^a
$\text{Cl}_2\text{Mn}_2(\text{CO})_8$	C_6H_{12}	~5000 (sh)	20,000	100
		4200	23,800	2,000
		3450 (sh)	29,000	500
		~2500 (sh)	40,000	5,000
		2000	50,000	40,000
$\text{Br}_2\text{Mn}_2(\text{CO})_8$	C_6H_{12}	~5100 (sh)	19,600	200
		4330	23,100	2,000
		~3400 (sh)	29,400	600
		~2600 (sh)	38,500	3,000
		2120	47,200	25,000
	MeOH	3880	25,800	b
		~2700 (sh)	37,000	
		~2150 (sh)	46,500	
		<2000	>50,000	
$\text{BrMn}(\text{CO})_5$	MeOH 12 hrs.	3880	25,800	b
		~2700 (sh)	37,000	
		~2150 (sh)	46,500	
		<2000	>50,000	
$\text{I}_2\text{Mn}_2(\text{CO})_8$		~5200 (sh)	19,200	200
		4400	22,700	2,000
		~3500 (sh)	28,600	1,000
		~2700 (sh)	37,000	5,000
		2350	42,550	20,000
		<2000	>50,000	30,000

^a The absolute values of ϵ have large uncertainties due to the uncertainty in weighing the very small sample of pure material that was available. The relative values are quite accurate however.

^b See Figure 5.08 for spectra and relative intensity values.

TABLE 5-II

Summary of I.R. Data for Tetracarbonyl Dimers

Compound ^a	$\lambda_{\text{max.}}$	Assignment	Relative Intensity	Literature Values ¹³	Relative Intensity
$\text{Cl}_2\text{Mn}_2(\text{CO})_8$	2105	B_{3u}	w	2104	w
	2046	B_{1u}	s	2045	s
	2015	B_{3u}	m	2012	m
	1979	B_{2u}	m	1977	m
$\text{Br}_2\text{Mn}_2(\text{CO})_8$	2099	B_{3u}	w	2099	w
	2043	B_{1u}	s	2042	s
	2013	B_{3u}	m	2011	m
	1978	B_{2u}	m	1975	m
$\text{I}_2\text{Mn}_2(\text{CO})_8$	2088	B_{3u}	w	2087	w
	2034	B_{1u}	s	2033	s
	2009	B_{3u}	m	2009	m
	1976	B_{2u}	m	1976	m

^a Spectra recorded in CCl_4

DISCUSSION

The structure of the tetracarbonyl dimers as determined by I.R. analysis²⁹ and crystallographic studies³⁰ is shown in Figure 5.02. The number of observed bands in the I.R. coincides with the number expected for a molecule of D_{2h} symmetry. In the I.R. analysis it is assumed that there is no interaction across the bridging halides. It is therefore possible to treat the tetracarbonyl bands as analogous to $ML_2(CO)_4$ molecules of C_{2v} symmetry. Figure 5.03 shows Orgel's diagrams¹³ for the vibrations which apply to cis $ML_2(CO)_4$ compounds. These are accompanied by their appropriate C_{2v} symmetry labels with the corresponding D_{2h} symmetry labels in brackets. The bonding in the tetracarbonyl dimer (TCD) molecules may be treated in a variety of ways. For direct comparison with $LMn(CO)_5$ molecules the changes in bonding can be qualitatively described by treating the $X_2Mn(CO)_4$ portion of the molecule within the same reference axis frame as the C_{4v} compounds. For completeness the bonding can also be treated using the actual D_{2h} symmetry of $Mn_2X_2(CO)_8$. The final bonding pictures for each treatment are comparable.

Treating the $M(CO)_4X_2$ portion of the molecule as a molecule with C_{2v} symmetry and the axis presentation given in Figure 5.04 indicates that one of the equatorial CO's in $XMn(CO)_5$ has been replaced by a halide. The same Mn d orbitals (d_{xz} , d_{yz} , d_{xy}) are involved in π bonding in each case. On the basis of decreased total π interaction, as discussed in Chapter 2, the d_{xz} , d_{yz} (e) orbitals in

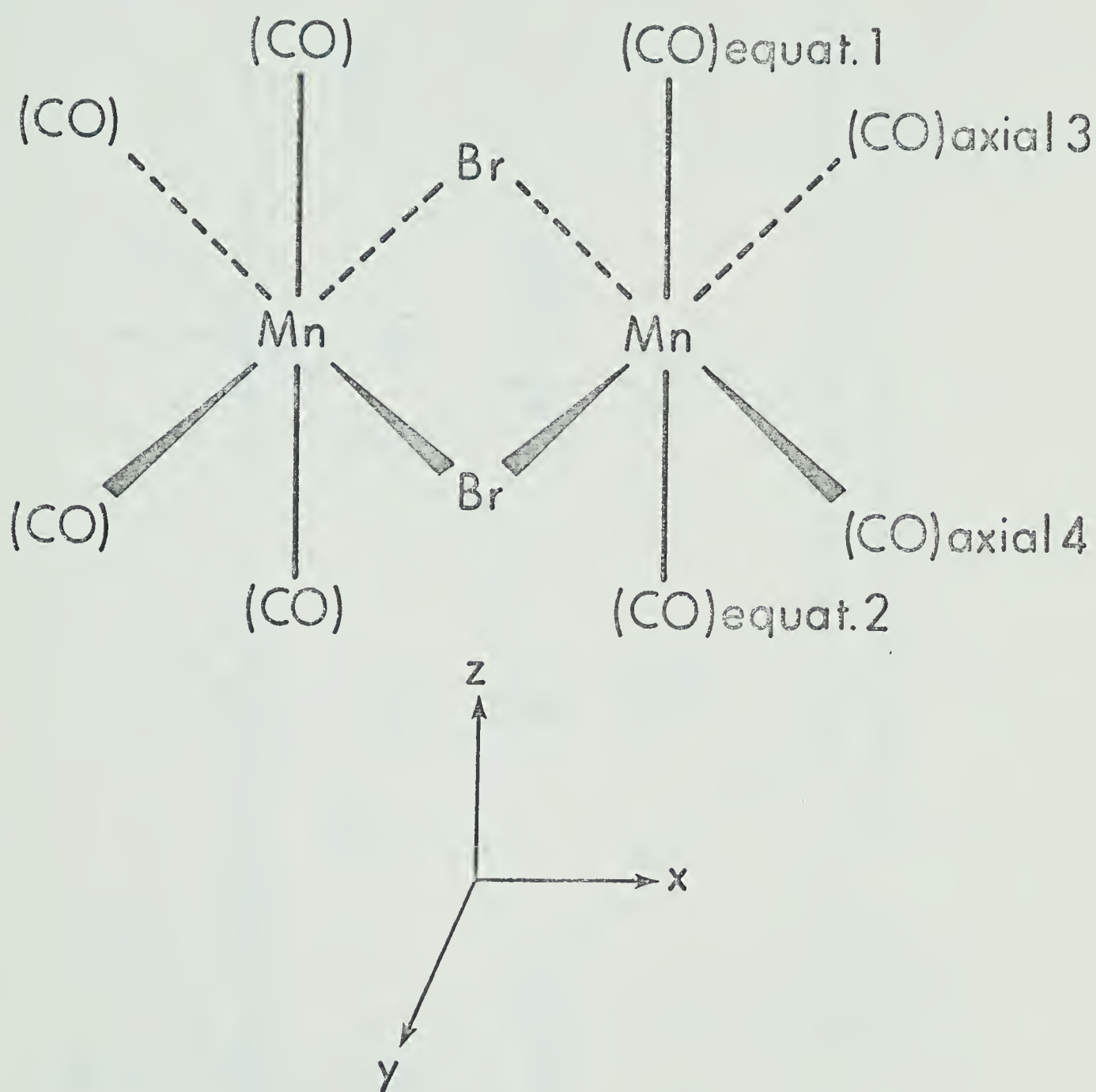


Figure 5.02 - Structure and axes representation for $\text{Br}_2\text{Mn}_2(\text{CO})_8$

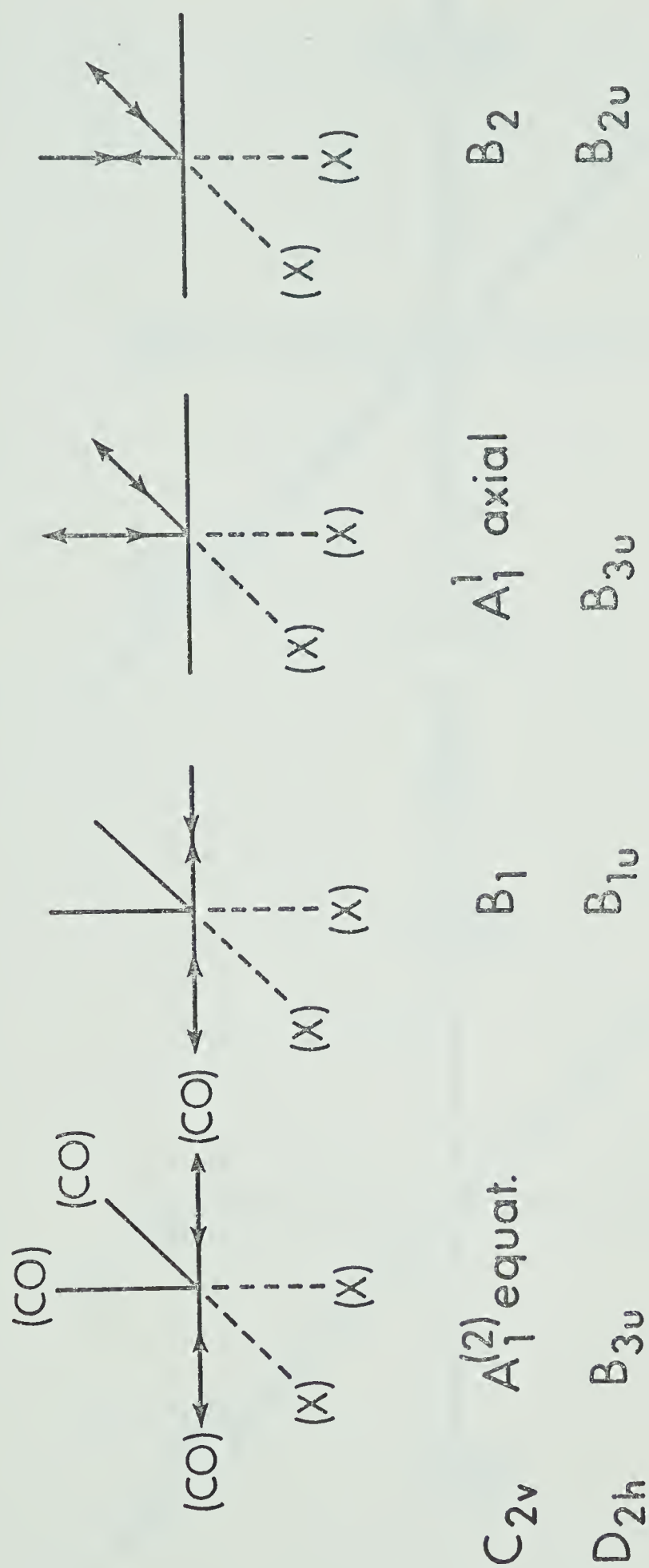


Figure 5.03 - Representations of carbonyl vibrations which apply to C_{2v} cis $ML_2(CO)_4$ compounds. Comparative D_{2h} representations are given below the C_{2v} ones.

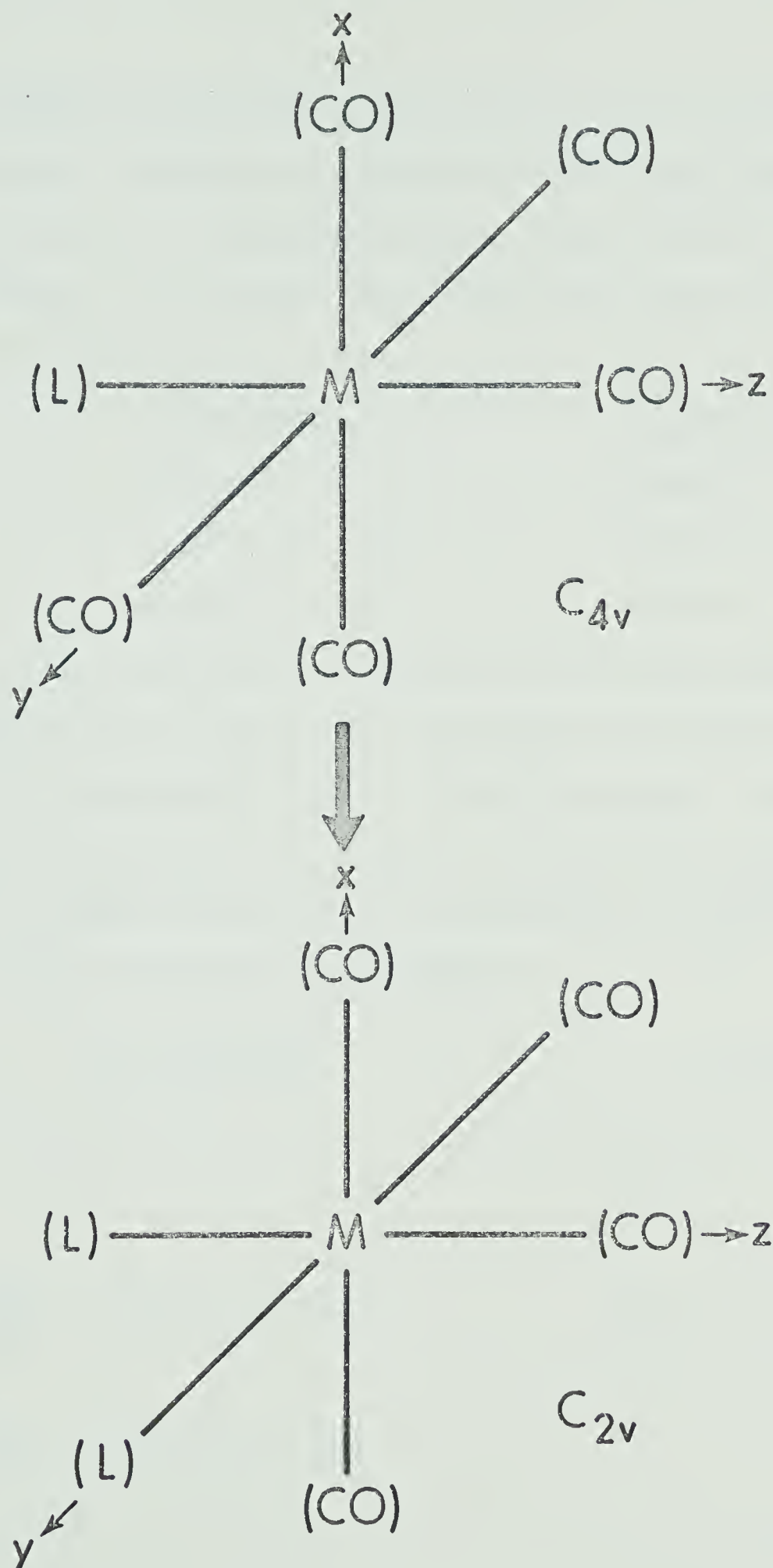


Figure 5.04 - Axes representations used in bonding comparisons of LMn(CO)_5 compounds and the $\text{L}_2\text{Mn(CO)}_4$ portion of tetracarbonyl dimer molecules.

C_{4v} symmetry are placed above that of the d_{xy} (b_2) in an energy level diagram. Replacing an equatorial CO by a halide influences the amount of total π interaction with the various CO's for each metal d orbital. The number of CO's interacting with each d orbital is outlined below:

	$C_{4v}(XMn(CO)_5)$	$C_{2v}(X_2Mn(CO)_4)$
d_{xy}	4 CO's	3 CO's + 1 X
d_{xz}	3 CO's + 1 X	3 CO's + 1 X
d_{yz}	3 CO's + 1 X	2 CO's + 2 X

Since the halides have no capacity for π acceptance and varying abilities as π donors, the stabilization of the filled d orbitals is accomplished by $M(d) - \pi^*(CO)$ interaction. Ignoring σ effects for the present, the changes in the placement of the filled Mn d orbitals based on total π interaction are depicted in Figure 5.05 for $XMn(CO)_5$ and $X_2Mn(CO)_4$.

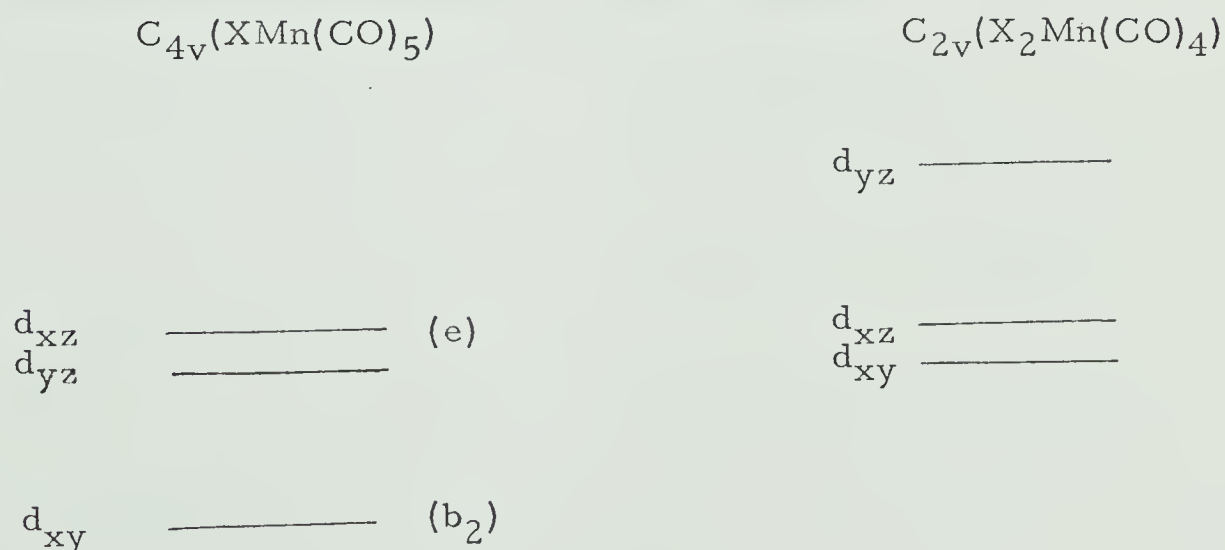


Figure 5.05

In addition to the π effects just described, the halide ligands also influence the relative placement of the d levels in accordance with their abilities to pull charge from the Mn through the X-Mn σ bond and to interact with the filled Mn(d_{π}) levels through their filled X(p_{π}) orbitals. It has been previously shown that in $\text{XMn}(\text{CO})_5$ the halide exerts a σ effect that lowers both the e and b_2 levels of Mn and a π effect that raises the Mn (e) level through interaction with the halogen p_{π} (e) level. The nature of the σ bonding of the bridging halides in the TCD's suggests that the σ withdrawing efficiency of the halides is likely to be decreased from that in the $\text{XMn}(\text{CO})_5$ compounds. In addition the number of the filled p_{π} levels available for interaction with each Mn is decreased in the TCD from that of the pentacarbonyl compound. This π interaction now takes place between the lower filled M(π) orbitals (d_{xz} , d_{xy}) and the (X) p_{π} levels. Figure 5.06 shows a qualitative placement of these filled levels considering these additional σ and π effects.

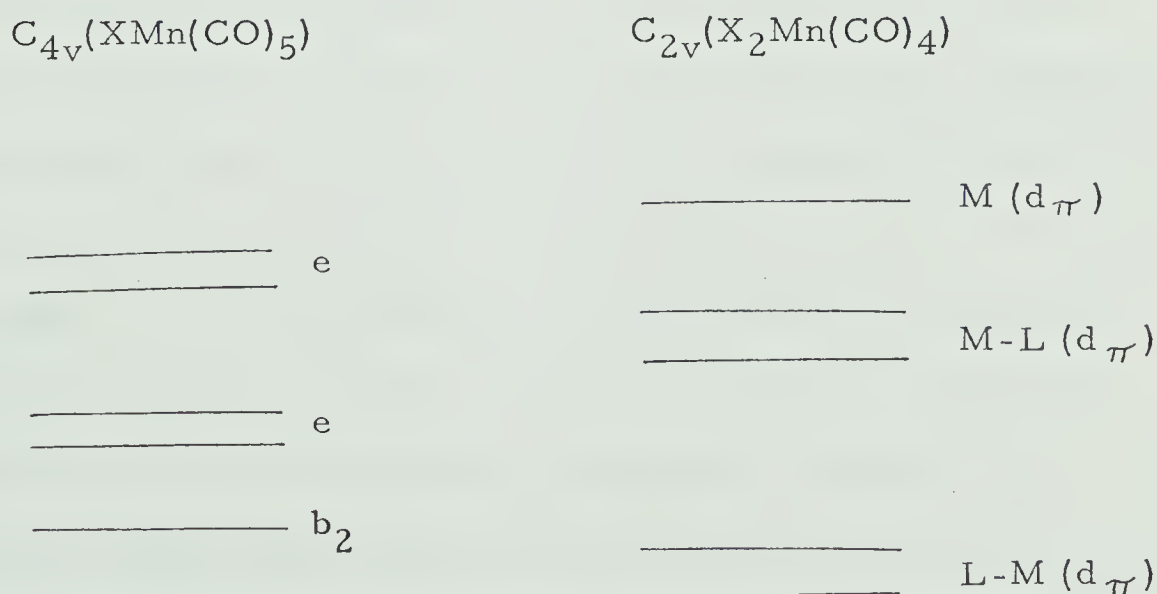


Figure 5.06

It is useful at this point to examine the observed changes in the CO stretching force constants for ClMn(CO)_5 ($k_{\text{ax.}} = 16.22$, $k_{\text{eq.}} = 17.50$ m. dynes/A) and for $\text{Cl}_2\text{Mn}_2(\text{CO})_8$ ($k_{\text{ax.}} = 16.07$, $k_{\text{eq.}} = 17.23$). In each case the axial force constants are weaker than the equatorial ones since there is greater interaction per CO for the trans CO's with the $\text{M}(\pi)$ d orbitals. In addition the force constants for the TCD are weaker than for the corresponding pentacarbonyl compound. This indicates that there is greater d - π^* interaction for each CO as a result of the $\text{Mn}(\text{d}_{\pi})$ orbitals backbonding with only 4 CO's compared to 5 in the pentacarbonyl compound. The total π backbonding however is still less in the TCD than it is in the corresponding pentacarbonyl halide. This results in a higher placement of the Mn d orbitals as shown in Figure 5.06 and accounts for the red shifts in many of the observed electronic transitions in going from XMn(CO)_5 to the TCD.

Figure 5.07 shows a more complete energy level diagram for the tetracarbonyl dimer compounds using the group theoretical approach presented in Appendix II for molecules of D_{2h} symmetry. The placement of the filled $\text{M}(\pi)$ and $\text{X}(\text{p}_{\pi})$ orbitals is equivalent to the descriptive presentation but the symmetry labels do not of course bear a 1:1 correspondence to the d orbitals in the more qualitative treatment since the reference axes in the qualitative treatment vary from those for D_{2h} symmetry. Table 5-III summarizes the assignments proposed for the electronic bands in $\text{Br}_2\text{Mn}_2(\text{CO})_8$, $\text{Cl}_2\text{Mn}_2(\text{CO})_8$ and $\text{I}_2\text{Mn}_2(\text{CO})_8$ using the labels for

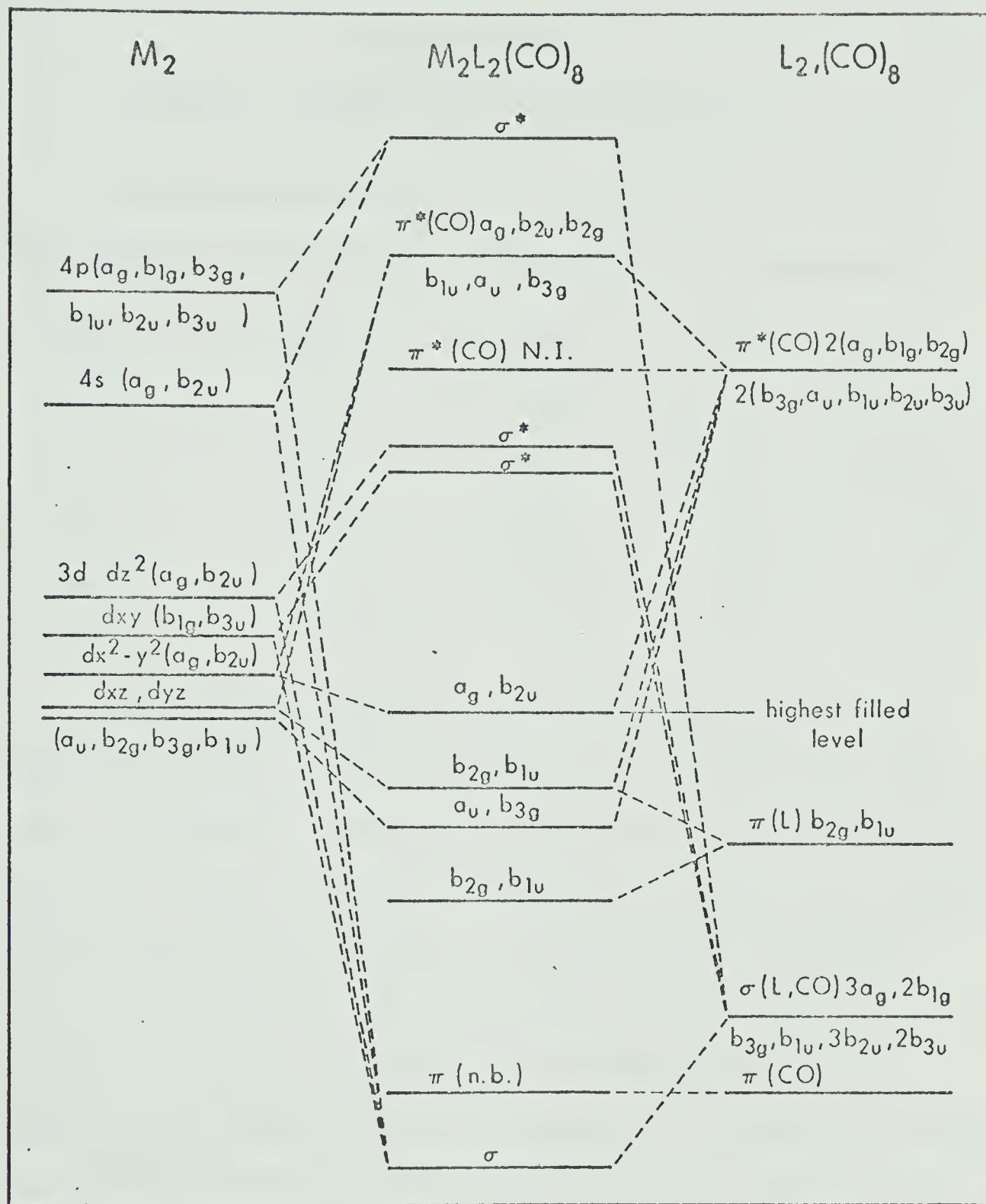


Figure 5.07 - Qualitative energy level diagrams for the Cl, Br, and I tetracarbonyl dimers based on D_{2h} symmetry.

the energy levels given in Figure 5.07.

TABLE 5-III

Proposed Assignments for TCD Compounds

Band Maxima (\AA)			
$\text{Cl}_2\text{Mn}_2(\text{CO})_8$	$\text{Br}_2\text{Mn}_2(\text{CO})_8$	$\text{I}_2\text{Mn}_2(\text{CO})_8$	Assignment
~5000	~5100	~5200	$\text{M}(\pi) \rightarrow \text{M}(\sigma^*)$
4200	4330	4400	$a_g, b_{2u} \rightarrow \pi^*(\text{CO}) \text{ N.I.}$
3450	~3400	~3500	$b_{2g}, b_{1u} \rightarrow \pi^*(\text{CO}) \text{ N.I.}$
~2500	~2600	~2700	$\text{M}(\pi) \rightarrow \pi^*(\text{CO})$
2000	2120	2350	$\text{M}(\pi) \rightarrow \pi^*(\text{CO})$

Figure 2.01 in Chapter 2 shows the ready conversion of $\text{ClMn}(\text{CO})_5$ to the Cl TCD in cyclohexane. The intensity of the lower energy band is obviously greater for the dimer than for the monomer. This transition is assigned as coming from a level in the TCD that is not involved in π interaction with the halides. Decreasing halide character in the highest filled e level in the monomer compounds appeared to increase the intensity of a similar type of band as shown in Chapter 2. The amount of halide character in the levels for the TCD's would also seem to affect the intensity of the band arising from these levels. The assignments as proposed in Table 5-III indicate a splitting of approximately 6000 cm^{-1} in the two uppermost filled π levels.

As Figure 5.07 shows, no attempt has been made to order the antibonding CO levels which interact with the $M(\pi)$ levels. The two general $\pi^*(CO)$ levels shown are $\pi^*(N.I.)$ and $\pi^*(CO)$. For this reason higher energy bands in the TCD's are assigned only as $M(\pi) - \pi^*(CO)$ transitions. The red shifts which occur in the observed bands as X is changed from Cl to Br to I (Table 5-III) reflect the changing σ property of X.

Table 5-I outlines the comparison of the $Br_2Mn_2(CO)_8$ spectra in C_6H_{12} and MeOH that is shown in Figure 5.08. The large differences in the band positions indicate more than just a solvent shift. The MeOH spectrum of the TCD bears a marked resemblance to the spectrum of $BrMn(CO)_5$ after this compound has remained in MeOH for a period of 12 hours. Figure 5.08 includes the spectrum of a freshly prepared MeOH solution of $BrMn(CO)_5$ and the spectrum of the same solution after 12 hours in the dark. It is possible that the dimer may be slowly formed in MeOH from the pentacarbonyl bromide and then rapidly reacts with MeOH to give the product that is observed immediately when the bromine tetracarbonyl dimer is dissolved in MeOH. A similar behaviour is apparent for the $Cl_2Mn_2(CO)_8$ in methanol solution.

A reaction takes place when $Br_2Mn_2(CO)_8$ is dissolved in CCl_4 solution with 2% MeOH added. Table 5-IV shows the λ max. values in the I.R. for the dimer in CCl_4 and after the MeOH has been added. This new formed compound is stable in solution for a short time (a few hours) and the observed I.R. bands resemble in position and

Figure 5.08 - Spectra of products formed from the reaction of BrMn(CO)_5 and

$\text{Br}_2\text{Mn}_2(\text{CO})_8$ with MeOH. Reactant spectra are included for

comparison. Cell path lengths of 2 cm and 1 mm are used in

each case.

----- $\text{Br}_2\text{Mn}_2(\text{CO})_8$, 1×10^{-4} M in C_6H_{12}

----- $\text{Br}_2\text{Mn}_2(\text{CO})_8$, 1.5×10^{-4} M in MeOH

----- BrMn(CO)_5 , 5.0×10^{-4} M in MeOH

----- BrMn(CO)_5 , above solution of 5.0×10^{-4} M after 12 hrs in dark

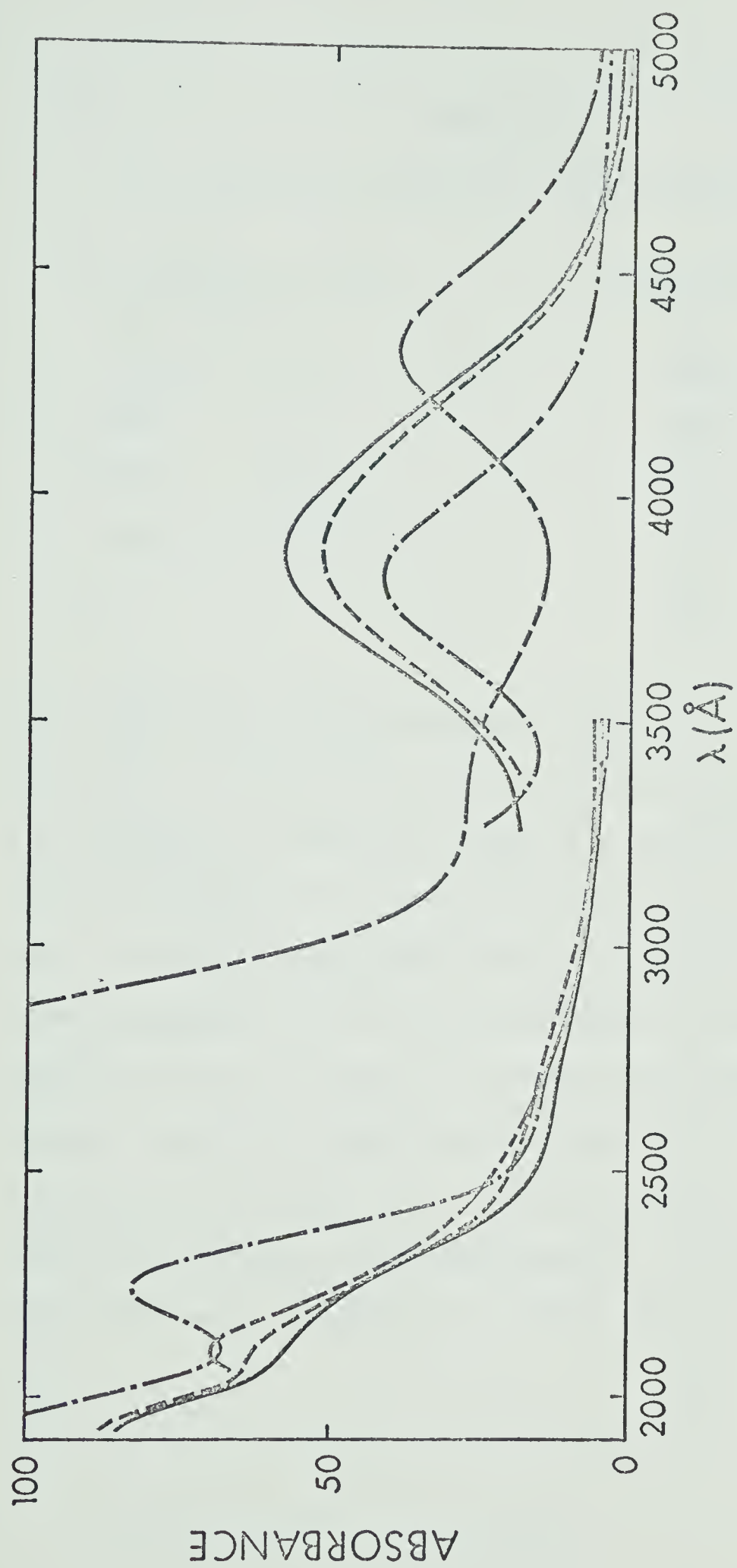


TABLE 5-IV

I.R. Comparison of BrTCD in CCl_4 and CCl_4 -2% MeOH

$\text{Br}_2\text{Mn}_2(\text{CO})_8$ (CCl_4)	$\text{Br}_2\text{Mn}_2(\text{CO})_8$ (CCl_4 -2% MeOH)
2099 cm^{-1} (w)	2053 cm^{-1} (vs)
2043 (s)	2030 (w)
2013 (m)	2002 (m)
1979 (m)	1942 (m)
	1927 (m)

form those of $\text{ML}_2(\text{CO})_4$ compounds reported by Cotton⁴⁶ and by Sheline⁴⁷. In this latter case it was shown by Sheline that CH_3CN can substitute as a ligand in solution for $\text{Mo}(\text{CO})_n\text{CH}_3\text{CN}_{6-n}$ compounds where $n = 3, 4, 5$ and that alcohols can act as ligands for $n = 5$ in these compounds leaving a molecule of C_{4v} symmetry. These compounds were not isolated either by Sheline or in this work. The spectroscopic evidence presented above and the results of Sheline suggest that MeOH has the ability to act as a ligand in substituted metal carbonyls. A possible product for the reaction of the TCD in MeOH is $\text{Br}(\text{MeOH})\text{Mn}(\text{CO})_4$. The I.R. spectra for the BrTCD and its methanolysis product are shown in Figure 5.09.

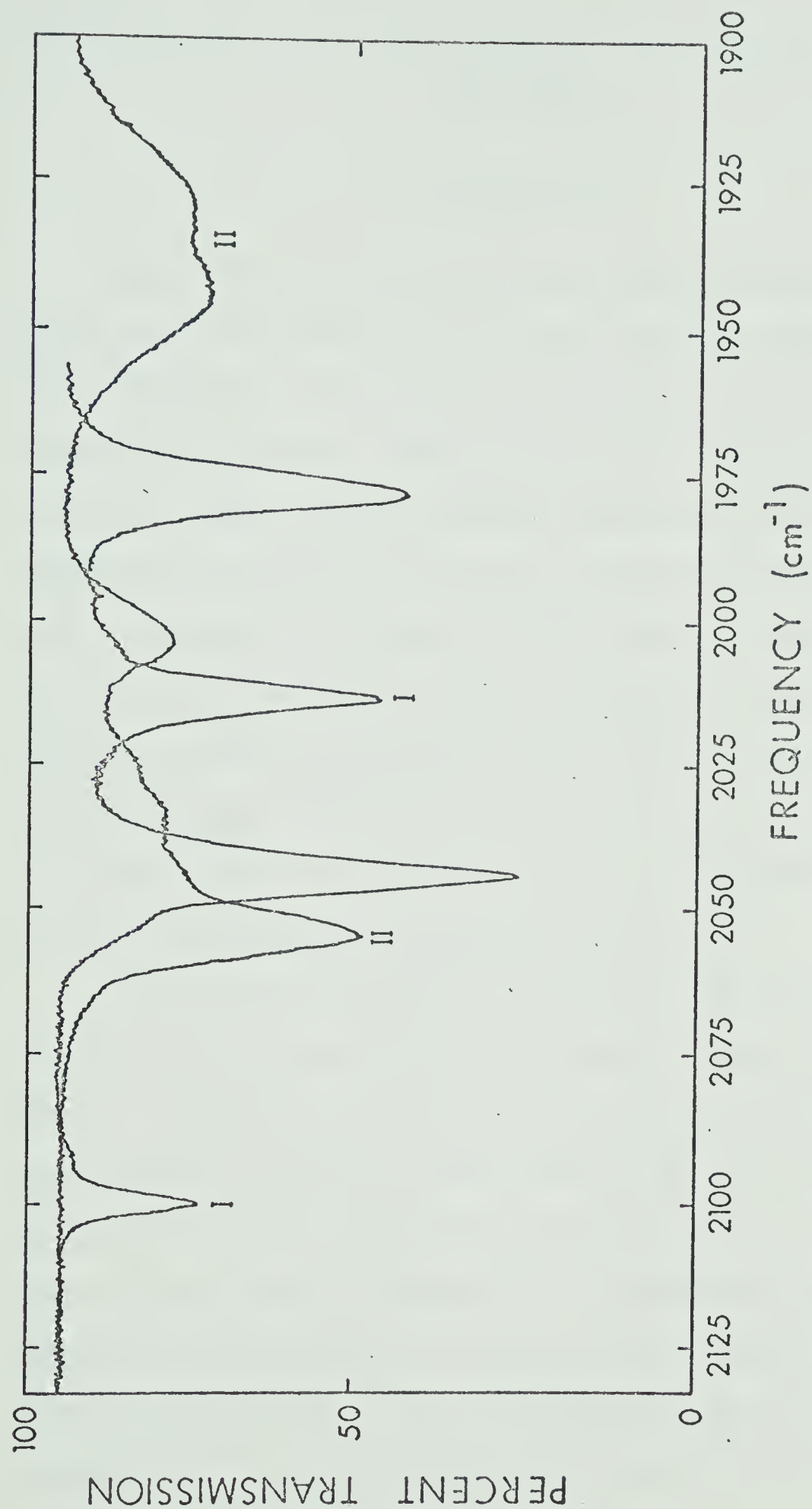


Figure 5.09 - Spectra of $\text{Br}_2\text{Mn}_2(\text{CO})_8$ in CCl_4 and CCl_4 -2% MeOH.

Curve I $\text{Br}_2\text{Mn}_2(\text{CO})_8$ in CCl_4

Curve II $\text{Br}_2\text{Mn}_2(\text{CO})_8$ in CCl_4 -2% MeOH. Spectra taken 10 minutes after MeOH added.

Chapter 6 - Electronic Spectra of the Pentacarbonyl Dimers of Mn and Re

BACKGROUND

The ready availability of the pentacarbonyl dimers of Mn and Re for use in the synthesis of a variety of metal carbonyls³⁵ has also facilitated various structural and spectroscopic investigations of the dimers and their related substituted compounds.^{31, 48, 49} X-ray diffraction results on the Mn pentacarbonyl dimer (Mn PCD) suggested the structure to be of D_{4d} symmetry with a direct M-M bond, staggered CO groupings for the individual $Mn(CO)_5$ moieties with respect to each other and no bridging CO groups.³³ I.R. spectral results and assignments were consistent with a molecular symmetry of D_{4d} indicating the same symmetry for solution as for the crystal phase. Recent I.R. polarization studies³² verify the earlier interpretation of the $M_2(CO)_{10}$ spectra.⁵⁰

Little information appears however for the electronic structure of the dimers despite the activity in other spectroscopic areas. Polarization spectra of the low energy band in Mn PCD has appeared with a proposed abbreviated energy level diagram.³² The electronic structure suggested here however is not consistent with that proposed from PES studies.²⁰ A qualitative energy level diagram is presented here to account for the complete electronic spectra of the dimers. It is consistent with other experimental results.^{20, 51} The low temperature spectra of the dimers are

also examined in solution; the presence or absence of wavelength shifts serves as an aid in making the proposed assignments.

EXPERIMENTAL

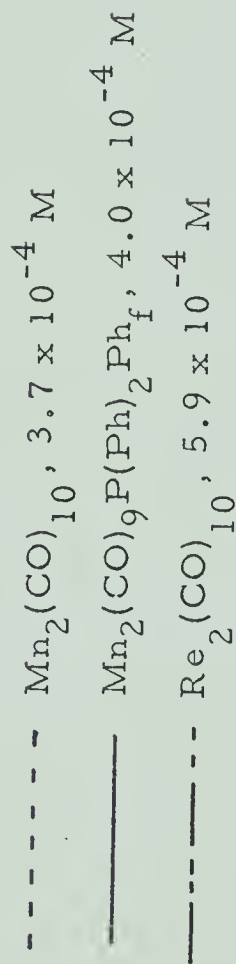
The compounds $\text{Mn}_2(\text{CO})_{10}$, $\text{Re}_2(\text{CO})_{10}$ and $\text{Mn}_2(\text{CO})_9$ trans $\text{P}(\text{Ph})_2\text{Ph}_f$ were obtained from W.A.G. Graham and coworkers. These compounds were purified by recrystallization from n-hexane and their I.R. spectra were checked on a PE 337 spectrometer using an external recorder and an expanded scale.

Visible and U.V. spectra were obtained on either a Cary 14 spectrometer or a Jasco UV-5 spectrometer. The Cary 14 was adapted to handle a modified version of a recommended solution low temperature cell.⁵¹ A low temperature cell of this type allows examination in a variety of solvents but suffers from poor temperature control and inexact temperature measurement. The lowest temperature obtainable with a cell of this type is estimated to be -100°C . For the low temperature spectra of the dimers, MeOH was used as a solvent and the temperature was estimated to be -70°C .

RESULTS

Figure 6.01 shows the U.V. spectra of $\text{Mn}_2(\text{CO})_{10}$, $\text{Re}_2(\text{CO})_{10}$ and $\text{Mn}_2(\text{CO})_9\text{P}(\text{Ph})_2\text{Ph}_f$. Table 6-I summarizes the λ max. values for these compounds and includes the proposed assignments. Low temperature results are reported in the discussion section.

Figure 6.01 - Spectra of carbonyl dimers in C_6H_{12} with 1 mm path lengths.



Concentrations given apply to higher wavelength region of the spectrum, solutions have been diluted to show lower wavelength region.

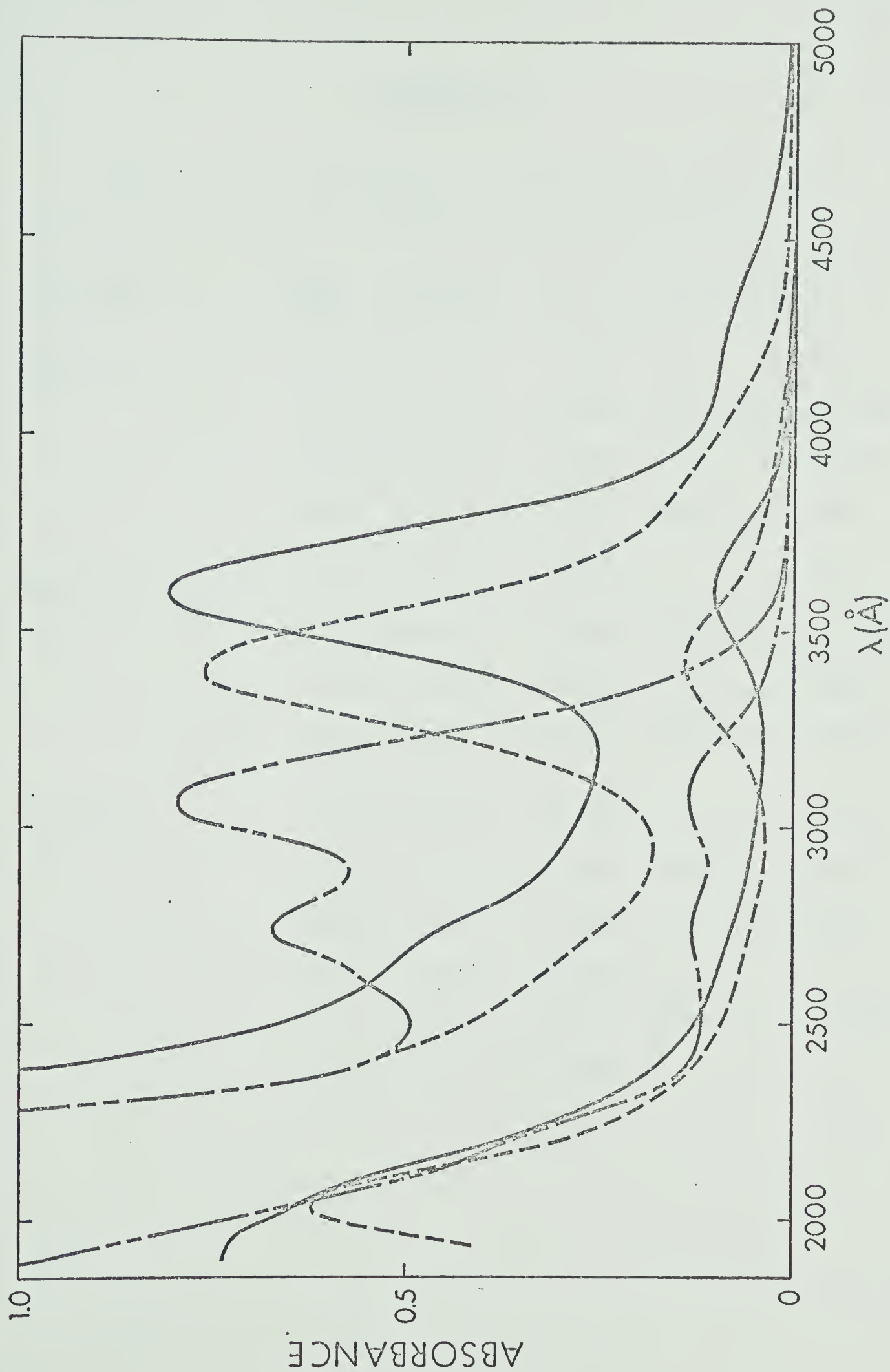


TABLE 6-I

Summary of Electronic Spectra for PCD Compounds

Compound	$\lambda_{\max.}$ (Å)	$\bar{\nu}_{\max}$ (cm ⁻¹)	ϵ	Assignment
$\text{Mn}_2(\text{CO})_{10}$	~4000	25,000	~1,200	$a_1 \longrightarrow \pi^*\text{N.I.}$
	3432	29,140	20,500	$a_1 \longrightarrow \sigma^*(b_2), e_3 \longrightarrow \pi^*\text{N.I.}$
	~2700	37,000	~4,000	$e_1, e_2 \longrightarrow \pi^*\text{N.I.}$
	2042	48,970	90,000	$M(\pi) \longrightarrow \pi^*\text{CO}$
$\text{Mn}_2(\text{CO})_9\text{P}(\text{Ph})_2\text{Ph}_f$	~4300	23,250	~2,000	$a_1 \longrightarrow \pi^*\text{N.I.}$
	3610	27,700	20,000	$a_1 \longrightarrow \sigma^*, e_3 \longrightarrow \pi^*\text{N.I.}$
	2750	36,360	~5,000	$e_1, e_2 \longrightarrow \pi^*\text{N.I.}$
	~2000	50,000	120,000	$M(\pi) \longrightarrow \pi^*(\text{CO})$
$\text{Re}_2(\text{CO})_{10}$	3105	32,210	13,500	$a_1 \longrightarrow \sigma^*(b_2)$
	2765	36,170	9,000	$M(\pi)e_3 \longrightarrow \pi^*\text{N.I.}$
	~2620	38,170	~1,000	$a_1 \longrightarrow \pi^*\text{N.I.}$
	~2230	44,840	~20,000	} $M(\pi) \longrightarrow \pi^*(\text{CO})$
	~2050	48,780	~40,000	
	< 1900	52,630	>100,000	

DISCUSSION

Despite the expected similarity in bonding, the electronic spectra of the dimers vary significantly from those of the hexacarbonyls. Introduction of a metal-metal bond and the possibility of $d_{\pi} - d_{\pi}$ interaction of the $M(CO)_5$ entities would seem to be responsible for these changes.

The observed similarities in the electronic spectra of $Cr(CO)_6$ ²⁴ and $Mn_2(CO)_{10}$ are listed below:

- i) both compounds show two well defined U.V. bands in addition to a number of weaker shoulders.
- ii) the higher energy band is much more intense in both cases.
- iii) the higher energy band shows a strong red shift from vapor to solution phase while the lower energy band shows only small shifts (Table 6-II).

The lowest energy C.T. band ($M_{\pi} - (CO)\pi^*$) in $Cr(CO)_6$ occurs at $35,800\text{ cm}^{-1}$.²⁴ Splittings in the t_{2g} level of the hexacarbonyls brought about by the introduction of L in C_{4v} $LMn(CO)_5$ compounds have been shown by PES²⁰ and U.V. spectra (Chapters 2-3) to vary from $6,000 - 13,000\text{ cm}^{-1}$. In $LMn(CO)_5$ compounds in which L may have π interaction with the metal d orbitals U.V. bands are observed at energies as low as $25,000\text{ cm}^{-1}$ (Chapter 2). In an I.R. analysis of the PCD's, Cotton suggests a similar π repulsion interaction between the filled d orbitals of the individual $M(CO)_5$ groups.³¹ C.T. transitions are also observed as low as $26,000\text{ cm}^{-1}$ in $LCr(CO)_5$ compounds⁴¹ and in $LMo(CO)_5$ compounds in which L has no π

TABLE 6-II

Solvent Effects on U.V. Bands of $\text{Mn}_2(\text{CO})_{10}$ and $\text{Re}_2(\text{CO})_{10}$

Solvent	$\text{Mn}_2(\text{CO})_{10}$		$\text{Re}_2(\text{CO})_{10}$	
C_6H_{12}	3432 Å (29,140 cm^{-1})	2042 Å (48,970 cm^{-1})	3105 Å (32,210 cm^{-1})	2765 Å (36,170 cm^{-1})
MeOH	3422 Å (29,220 cm^{-1})	2058 Å (48,500 cm^{-1})	3095 Å (32,310 cm^{-1})	2770 Å (36,100 cm^{-1})
CH_3CN	3422 Å (29,220 cm^{-1})	2043 Å (48,950 cm^{-1})	3100 Å (32,260 cm^{-1})	2775 Å (36,040 cm^{-1})
Vapor	3395 Å (29,460 cm^{-1})	1982 Å (50,460 cm^{-1})	-	-

accepting properties.²² In addition the average I.P. for the highest occupied levels in $\text{Mn}_2(\text{CO})_{10}$ are lower than for corresponding $\text{LMn}(\text{CO})_5$ compounds.²⁰ For these reasons, a strong possibility exists for a $\text{M}(\pi) - \pi^*(\text{CO})$ transition at a wavelength above 3000 \AA ($33,000 \text{ cm}^{-1}$). The observation of this transition may be complicated however by the formation of the Mn-Mn σ bond resulting in a high lying $\sigma(a_1)$ level. Transitions from this level may obscure or combine with transitions from the metal π levels.

Recent assignments for the low energy portion of the electronic spectrum of $\text{Mn}_2(\text{CO})_{10}$, which are based partially on polarization data, indicate that the highest filled orbitals are $\text{Mn}(d_\pi)$ and that the Mn-Mn $a_1(\sigma)$ level is placed slightly below these in energy.³² The band at $29,200 \text{ cm}^{-1}$ is then assigned as a $\text{Mn}(\sigma) - \text{Mn}(\sigma^*)$ transition based on the z polarization of this band and the shoulder at $26,000 \text{ cm}^{-1}$ is assigned as a $\text{Mn}(d_\pi) - \text{Mn}(d_{\sigma^*})$ transition. The placement of the highest filled levels and the assignments proposed on the basis of these polarization spectra are not however consistent with the electronic structure that is indicated by recent photoelectron studies.²⁰ These studies suggest that the highest lying level is an (a_1) level which is 3000 cm^{-1} above the first $\text{Mn}(d_\pi)$ level. A splitting of $5,000 \text{ cm}^{-1}$ in the metal d_π levels is indicated.

Figure 6.02 shows a qualitative energy level diagram using the PES placement of the ground state levels and symmetry labels corresponding to the D_{4d} symmetry of the molecule. The transformation properties of the metal and ligand orbitals under this D_{4d}

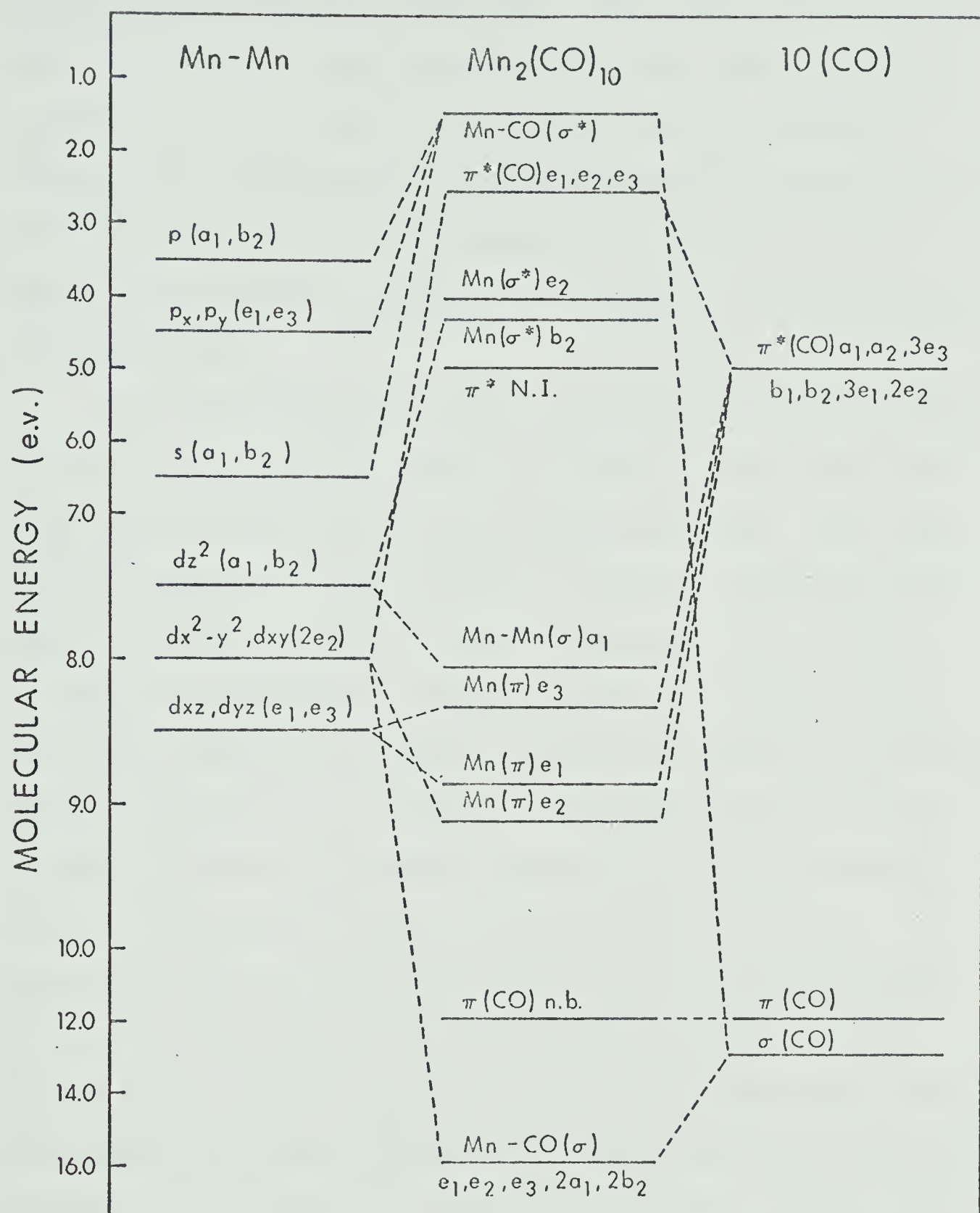


Figure 6.02 - Qualitative energy level diagram for the pentacarbonyl dimer of Mn.

symmetry are outlined in Table 6-III. The antibonding levels are placed in accordance with the observed spectra and the expected positioning of these levels from previous studies of $\text{LMn}(\text{CO})_5$ compounds. The placement of the $d(\sigma^*)$ levels is difficult to predict in the absence of d-d transitions but these levels are expected to lie close in energy to the $\pi^*(\text{CO})$ N.I. levels depicted in Figure 6.02.²⁴

The assignments of the bands for the PCD compounds outlined in Table 6-I are proposed partly on the basis of their consistency with both the results of PES and polarization studies. The simultaneous assignment of the $29,000 \text{ cm}^{-1}$ band to a combination of a $M(\pi) - \pi^*(\text{CO})$ and a $M(\sigma) - M(\sigma^*)$ transition is based on the following considerations. A number of $M(\pi) - \pi^*(\text{CO})$ bands in $\text{LMn}(\text{CO})_5$ compounds are shown to be relatively weak and could be hidden by more intense transitions. In addition, the increased number of bands for the RePCD compound in this region and the solvent and temperature effects on these bands serve as an indication that coincidence absorption may occur in the Mn PCD. Low temperature data in MeOH for the PCD's indicate that the lowest energy band in $\text{Re}_2(\text{CO})_{10}$ ($32,200 \text{ cm}^{-1}$) is the $M(\sigma) - M(\sigma^*)$ transition as previously suggested.³² This band shows a blue shift of 300 cm^{-1} in MeOH at low temperatures (approx. -70°C) similar to the $29,000 \text{ cm}^{-1}$ of the Mn PCD whereas the band at $36,050$ shows little change with temperature. The observation that the total intensity of the three bands for Re PCD is equivalent to the total intensity for the two bands of Mn PCD in the lower energy region

TABLE 6-III

Transformation Properties of Metal and Ligand Bonding Orbitals in
 $M_2(CO)_{10}$ Molecules

Metal Orbitals	Transformation	Ligand π^*CO Orbitals	Transformation
p_z	$a_1 + a_2$	π^*CO axial	$e_1 + e_3$
p_x, p_y	$e_1 + e_3$	π^*CO equatorial	$2a_1 + 2b_2$ $+2e_1 + 2e_2 + 2e_3$
s	$a_1 + b_2$		
d_{z^2}	$a_1 + b_2$		
$d_{x^2-y^2}, d_{xy}$	$2e_2$		
d_{xy}, d_{yz}	$e_1 + e_3$		

may serve as further indication that two bands are coincident in Mn PCD at $29,000\text{ cm}^{-1}$.

The spectra of the substituted Mn PCD compound shows red shifts of both the band and shoulder that are observed in the lower energy region for the Mn PCD compound. The shifts are expected to be a result of decreased total π bonding due to the introduction of the phosphine group and an accompanying elevation in the uppermost π level and a general raising of all levels due to the slightly increased σ donor property of the phosphine group compared to a CO. The spectra of this compound also indicates a shoulder at 2700 Å which is more definite than the shoulder which appears in the Mn PCD compound.

SUMMARY

Although there has been a great deal of activity in the metal carbonyl field in X-ray diffraction and I.R. determinations of structure, only scattered and incomplete electronic spectral data are available. This study has provided reliable U.V. and visible spectral data over the entire U.V. and visible range for some seventy carbonyl compounds of Mn and Re. For most of these compounds, one-electron energy level diagrams have been constructed using the available structural information with group theoretical and symmetry approaches. The various concepts of bonding that have been popular in descriptions of bonding for substituted metal carbonyl compounds have been incorporated into the electronic structural pictures presented. These concepts include π -back-bonding, π -repulsion, dative σ bonding and separated σ and π effects which are used in the correlation of I.R. data and interpretations with the information and models derived from the U.V. and visible spectral results.

A number of compounds have been examined in a variety of solvents and the influence of solvent and of phase have been discussed with reference to their effect on observed wavelength positions. Data has also been provided on the solvent reactions of some of these carbonyl compounds. Specific indications are reported suggesting that the MeOH molecule may serve as an co-ordinating ligand in a number of the carbonyl compounds examined.

BIBLIOGRAPHY

1. L. Mond, C. Langer and F. Quincke, *J. Chem. Soc.*, 749 (1890).
2. T. J. Kealy and P. L. Pauson, *Nature*, 168, 1039 (1951).
3. S. A. Miller, J. A. Tebboth and J. F. Tremaine, *J. Chem. Soc.*, 632 (1952).
4. E. O. Fischer and W. Hafner, *Z. Naturforsch.*, 106, 665 (1955).
5. E. W. Abel and F. G. A. Stone, *Quart. Res.*, 325 (1969).
6. J. Ladell, B. Post, and I. Fankuchen, *Acta Cryst.*, 5, 795 (1952).
7. J. Donahue and A. Caron, *Acta Cryst.*, 17, 663 (1964).
8. W. Rudorff and U. Hoffmann, *Z. Phys. Chem. (B)* 28, 351 (1935).
9. G. Natta et al., *Atti. Accad. Naz. Lincei, Rend. Classe Sci. fis. mat. nat. (8)*, 27, 107 (1959).
10. H. P. Weber and R. F. Bryan, *Chem. Comm.*, 443 (1966).
11. R. F. Bryan, *J. Chem. Soc.*, (A) 696 (1968).
12. F. A. Cotton and C. S. Kraihanzel, *ibid.*, 84, 4432 (1962).
13. L. E. Orgel, *Inorg. Chem.*, 1, 726 (1962).
14. W. Jetz, P. B. Simons, J. A. J. Thompson and W. A. G. Graham, *ibid*, 5, 2217 (1966).
15. W. A. G. Graham, *ibid*, 7, 315 (1968).
16. F. A. Cotton, *ibid*, 3, 707 (1964).

17. F. A. Cotton, A. Musco and G. Yagupsky, *ibid*, 6, 1357 (1967).
18. H. B. Gray, E. Billig, A. Wojcicki and M. Farona, *Can. J. Chem.*, 41, 1281 (1963).
19. R. T. Lundquist and M. Cais, *J. Org. Chem.*, 27, 1167 (1962).
20. S. Evans, J. C. Green, M. L. H. Green, A. F. Orchard and D. W. Turner, *Discussions Faraday Soc.*, 47, 112 (1969).
21. R. F. Fenske and R. L. DeKock, *Inorg. Chem.*, 9, 1053 (1970).
22. D. J. Darensbourg and T. L. Brown, *ibid*, 7, 959 (1968).
23. K. Caulton and R. F. Fenske, *ibid*, 7, 1273 (1968).
24. N. A. Beach and H. B. Gray, *J. Am. Chem. Soc.*, 90, 5713 (1968).
25. E. W. Abel, R. A. N. McLean, S. D. Tyfield, P. S. Braterman, A. P. Walker and P. J. Hendra, *J. Molec. Spec.*, 30, 29 (1969).
26. J. A. J. Thompson and W. A. G. Graham, *Inorg. Chem.*, 9, 1053 (1970).
27. B. T. Kilbourne and H. M. Powell, *Chem. Ind.*, 1578 (1964).
28. J. H. Tsai, J. T. Flynn and F. P. Baer, *Chem. Comm.*, 702 (1967).
29. M. A. El-Sayed and H. D. Kaesz, *Inorg. Chem.*, 2, 158 (1963).
30. L. F. Dahl and C. H. Wei, *Acta Cryst.*, 16, 611 (1963).
31. F. A. Cotton and R. M. Wing, *Inorg. Chem.*, 4, 1328 (1965).
32. R. A. Levenson, H. B. Gray and G. P. Ceasar, *J. Am. Chem. Soc.*, 92, 3653 (1970).

33. L. F. Dahl and R. E. Rundle, *Acta Cryst.*, 16, 419 (1963).
34. L. F. Dahl, E. Ishishi and R. E. Rundle, *J. Chem. Phys.*, 26, 1750 (1957).
35. R. B. King, *Organometallic Synthesis*, Vol. 1, Academic Press, New York and London (1965).
36. H. B. Gray and N. A. Beach, *J. Am. Chem. Soc.*, 85, 2922 (1963).
37. A. F. Schreiner and T. L. Brown, *ibid*, 90, 3366 (1968).
38. D. S. Carroll and S. P. McGlynn, *Inorg. Chem.*, 7, 1285 (1968).
39. F. A. Cotton and J. A. McCleverty, *J. Organometal. Chem.*, 4, 490 (1965).
40. P. S. Braterman, R. W. Harrill and H. D. Kaesz, *J. Am. Chem. Soc.*, 89, 2851 (1967).
41. M. Y. Darensbourg and D. J. Darensbourg, *Inorg. Chem.*, 9, 32 (1970).
42. J. Franck and G. Scheibe, *Z. Physik. Chem.*, A1 39, 22 (1928).
43. L. I. Katzin, *J. Chem. Phys.*, 23, 2055 (1955).
44. K. Kimura and S. Nagakura, *Spectrochim. Acta*, 17, 166 (1961).
45. N. A. D. Carey and H. C. Clark, *Inorg. Chem.*, 7, 95 (1968).
46. F. A. Cotton, *ibid.*, 5, 702 (1964).
47. G. R. Dobson, M. F. A. El-Sayed, I. W. Stolz and R. K. Sheline, *ibid*, 1, 526 (1962).
48. D. J. Parker and M. H. B. Stiddard, *J. Chem. Soc.*, (A) 695 (1966).

49. R. M. Wing and D. C. Crocker, *Inorg. Chem.*, 6, 289 (1967).
50. N. Flitcroft, D. K. Huggins and H. D. Kaesz, *ibid*, 3, 1123 (1964).
51. W. B. Rose, J. W. Nebgen, and F. Metz, *Rev. Sci. Instr.*, 36(9), 1319 (1965).

APPENDIX I

Summary of Reactivities of Pentacarbonyls in Various Solvents

Compound	Solvent	Remarks on Behavior
$\text{Me}_3\text{SnMn}(\text{CO})_5$	MeOH	decomposes immediately, band at 3770 Å, $\epsilon \sim 1000$.
$\text{Cl}_3\text{SnMn}(\text{CO})_5$	MeOH - 1% HCl	stable in methanol and acidified methanol if kept in the dark.
$\text{Me}_2\text{SnMn}_2(\text{CO})_{10}$	MeOH - 1% HCl	decomposes (1 hr) in MeOH and the 3300 Å band disappears, no isobestic point. In HCl acidified MeOH 3300 Å band disappears immediately and a shoulder appears at 2200 Å.
$\text{Cl}_2\text{SnMn}_2(\text{CO})_{10}$	MeOH - 1% HCl	resistant to any change in MeOH and HCl acidified MeOH when kept in the dark.
$\text{MeSnMn}_3(\text{CO})_{15}$	MeOH - 1% HCl	In pure MeOH 3760 Å band shifts to 3230 Å in 2 hrs. and with the addition of HCl a band which may be attributed to $\text{MeCl}_2\text{SnMn}(\text{CO})_5$ appears at 2625 Å.
$\text{CH}_2=\text{CHSnMn}_3(\text{CO})_{15}$	MeOH - 1% HCl	In pure MeOH band at 3780 Å shifts to 3245 Å. With addition of HCl there is a fast conversion to the bis compound and an equilibrium set up between the bis and mono compound.
$\text{BuSnMn}_3(\text{CO})_{15}$	C_6H_{12} MeOH	- limited solubility, stable in dark, photodecomposes. - conversion of low energy band to a higher energy band as a result of a bis compound formation.

Compound	Solvent	Remarks on Behavior
$\text{BuSnMn}_3(\text{CO})_{15}$	MeOH - 1% HCl	- change of bis band ($\text{BuClSnMn}_2(\text{CO})_{10}$) to the mono compound ($\text{BuCl}_2\text{SnMn}(\text{CO})_5$) at 2645 Å. Product stable in the dark and may be isolated.
	dimethyl-formamide	- decomposes rapidly after the appearance of tris compound low energy band at 3750 Å.
	i-PrOH	- main band at 3750 Å. Conversion of this band takes place more slowly than in MeOH and results in a lower λ shoulder at 3200 Å. This conversion is accompanied for a short time by an isobestic point but conversion product decomposes and the isobestic point disappears after 1 hr.
	CH_3CN	- the 3790 Å tris band disappears and a 3200 Å shoulder appears. Both decrease in intensity with time. Total time ~3 hrs. for 3790 Å band to disappear.
	EtOH 95%	- Two shoulders appear in the 3200 and 3800 Å area but the λ max's cannot be determined exactly. The solubility is very low and the stability of the intermediate is less than the solubility of the tris compound.
	Pyridine	- The band at 3800 Å slowly shifts to the blue with a decrease in absorbance value. The absorbance at 3540 Å is constant for 1 hr. The pyridine cut off at 3050 Å inhibits observation of any lower λ shoulders.
$\text{BuSnMn}_3(\text{CO})_{15}$	Dioxane	- Stable in dioxane for 8 hrs. in the dark with a 5% decrease in the 3800 Å absorbance value. There is a hint of a shoulder at ~3100 Å.
	T.H.F.	- Compound very soluble. Decrease in the absorbance value over a 5 hr period in the dark from 0.63-0.29. At $\lambda = 3410$ Å for (continued)

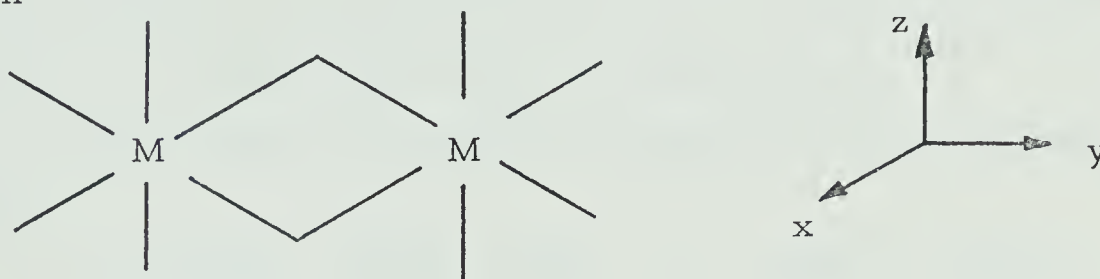
Compound	Solvent	Remarks on Behavior
$\text{BuSnMn}_3(\text{CO})_{15}$	T.H.F. (Cont'd)	3 hrs have a constant Absorbance value.
	MeOH-NH ₄ OH	- 3780 Å band disappears and is replaced by a band at 3500 Å of unknown origin.
$\text{ISnMn}_3(\text{CO})_{15}$	MeOH - 1% HCl	- In pure MeOH conversion of 3880 Å band to the 3285 Å band with an isobestic point. In HCl acidified MeOH a product, possibly $(\text{ISnMn}_2(\text{CO})_{10})$, stable for a week in the dark is formed. Product in pure MeOH slowly decomposes within one day.
	C ₆ H ₁₂	- Stable in the dark but photo-decomposes rapidly.
	CH ₃ CN	- Compound appears stable indefinitely in the dark.
	i-PrOH	- 3840 Å band shifts to 3365 Å. Compound has limited solubility in this solvent but after 10 hrs. both bands are present and the intermediate appears to be fairly stable.
	EtOH 95%	- A stable intermediate band comparable to the 3285 Å band in MeOH is suggested but insolubility of the compound makes the observation of low energy bands difficult. Both bands disappear 8 hrs after makeup in the dark.
	Pyridine	- Over a 90 min period the λ max shifts 100 Å from 3840 → 3740 Å. There is a constant absorbance value for the first 20 min at ~3600 Å. The absorbance value of the main band decreases from 0.58-0.28 in the 90 mins.
	Dioxane	- 4125 Å main band decreases in absorbance value by 50% in the dark in 5 hrs. There is no change to a lower λ band.

Compound	Solvent	Remarks on Behavior
$\text{ISnMn}_3(\text{CO})_{15}$	T.H.F.	- There is a shift of the 4100 \AA band to 3970 \AA . There is a shoulder in 3000 \AA region which becomes well defined after 6 hrs but there is no isobestic point. The compound is very soluble.
$\text{ClSnMn}_3(\text{CO})_{15}$	MeOH	- The 3875 \AA band converts to a band at 3290 \AA with accompanying isobestic point. The product band is not stable indefinitely but long enough to isolate small quantities of the product.
	MeOH - 1% HCl	- The acidification of the MeOH does not appear to speed the conversion from that of pure MeOH. An isobestic point can still be observed but the product λ_{max} now appears at 3375 \AA . The product is stable indefinitely in the dark and may be separated. It has been shown to be $\text{Cl}_2\text{SnMn}_2(\text{CO})_{10}$.
	CH_3CN	- 3880 \AA band appears to be reasonably stable but over a 24 hr period there is a 15% decrease in the λ_{max} value. There is a hint of a shoulder in the 3100 \AA region but no isobestic point appears.
	C_6H_{12} Dimethyl- formamide	- Stable in the dark. - 3860 \AA band disappears rapidly but no stable intermediate is evident nor is there any trace of an isobestic point.
	Water	- The solubility in water is limited but is sufficient to observe the immediate appearance of a 3220 \AA band similar to the conversion which takes place in MeOH.

APPENDIX II

Symmetry Analysis of the Bonding in the Tetracarbonyl Dimers

A group theoretical approach to the classification of bonding orbitals in the tetracarbonyl dimer compounds $(X_2M_2(CO)_8)$ uses D_{2h} symmetry with the axes representation shown below.



The combination of metal valence orbitals under D_{2h} symmetry transform as follows:

Metal Orbitals	Symmetry Operations								Orbital Symmetries	
	E	$C_2(z)$	$C_2(y)$	$C_2(x)$	i	$\sigma(xy)$	$\sigma(xz)$	$\sigma(yz)$		
s	2	0	2	0	0	2	0	2	a_g	b_{2u}
p_z	2	0	-2	0	0	-2	0	2	b_{3g}	b_{1u}
p_x	2	0	-2	0	0	2	0	-2	b_{1g}	b_{3u}
p_y	2	0	2	0	0	2	0	2	a_g	b_{2u}
d_{z^2}	2	0	2	0	0	2	0	2	a_g	b_{2u}
$d_{x^2-y^2}$	2	0	2	0	0	2	0	2	a_g	b_{2u}
d_{xy}	2	0	-2	0	0	2	0	-2	b_{1g}	b_{3u}
d_{xz}	2	0	2	0	0	-2	0	-2	a_u	b_{2g}
d_{yz}	2	0	-2	0	0	-2	0	2	b_{3g}	b_{1u}

There are 12 σ -bonds in the molecule and they transform under D_{2h} symmetry to give the following reducible representation.

	E	$C_2(z)$	$C_2(x)$	$C_2(y)$	i	$\sigma(xy)$	$\sigma(xz)$	$\sigma(yz)$
Γ_{σ}	12	0	0	0	0	8	0	4

The reducible representation gives the irreducible representations

$$\Gamma_{\sigma} \longrightarrow 3a_g, 2b_{1g}, b_{3g}, b_{1u}, 3b_{2u}, 2b_{3u}$$

There are 2 π^* orbitals on each CO and a total of 8 CO's so that

	E	$C_2(z)$	$C_2(x)$	$C_2(y)$	i	$\sigma(xy)$	$\sigma(xz)$	$\sigma(yz)$
Γ_{π^*CO}	16	0	0	0	0	0	0	0

This representation reduces to give the appropriate symmetry labels

$$\Gamma_{\pi^*CO} \longrightarrow 2a_g, 2b_{1g}, 2b_{2g}, 2b_{3g}, 2a_u, 2b_{1u}, 2b_{2u}, 2b_{3u}$$

for the $\pi^*(CO)$ orbitals. Since each CO also has 2 filled π orbitals the symmetry labels for $\pi(CO)$ orbitals are the same as those for the π^*CO .

There is one filled π orbital on each X atom giving

	E	$C_2(z)$	$C_2(x)$	$C_2(y)$	i	$\sigma(xy)$	$\sigma(xz)$	$\sigma(yz)$
$\Gamma_{\pi(X)}$	2	0	0	-2	0	-2	2	0

which reduces to $b_{2g} + b_{1u}$.

The symmetry representations for ligand orbitals are combined with the appropriate metal orbital representations to give the σ and π bonding interactions. It is assumed that σ bonding has priority over π bonding where symmetry allows a choice and that p orbitals

geometrically favor σ bonding over π bonding as in the treatment for C_{4v} molecules given in Chapter 2.

σ Interactions

Metal Orbital Representations.

Ligand Orbital Representations

s	-	a_g	}		
d_z^2	-	a_g			
p_y	-	a_g			
					$3a_g$
p_x	-	b_{1g}	}		
d_{xy}	-	b_{1g}			
					$2b_{1g}$
p_z	-	b_{3g}	}		
					b_{3g}
p_z	-	b_{1u}	}		
					b_{1u}
s	-	b_{2u}	}		
p_y	-	b_{2u}			
d_z^2	-	b_{2u}			
					$3b_{2u}$
p_x	-	b_{3u}	}		
d_{xy}	-	b_{3u}			
					$2b_{3u}$

This indicates that 12 metal orbitals ($2s$, $2p_x$, $2p_y$, $2p_z$, $2d_z^2$, $2d_{xy}$) are involved in the 12 σ bonds. There remain for $d - \pi^*(CO)$ interactions the metal $d_{x^2-y^2}$, d_{xz} and d_{yz} orbitals and the 16 $\pi^*(CO)$ representations.

π Interactions

Metal Orbital	Representation	Ligand $\pi^*(\text{CO})$ Representation
$d_{x^2-y^2}$	$a_g + b_{2u}$	a_g, b_{2u}
d_{xz}	$a_u + b_{2g}$	a_u, b_{2g}
d_{yz}	$b_{3g} + b_{1u}$	b_{3g}, b_{1u}

Of the 16 possible $\pi^*(\text{CO})$ states only 6 interact with the metal orbitals. The remaining 10 $\pi^*(\text{CO})$ states are labelled $\pi^*(\text{CO})\text{N.I.}$ in Figure 5.07. The filled π orbitals on the X atoms may interact with the $\pi^*(\text{CO})$ levels of the same symmetry through the metal b_{2g} and b_{1u} levels as shown in the qualitative energy level diagram in Chapter 5 (Figure 5.07). The filled π orbitals of the CO's are expected to lie low enough in energy to neglect possible $\pi(\text{CO}) - \text{M}(\pi)$ interactions to a first approximation.

B29981